Studying water-wedging as a cause for short term overheating in the boiler of a coal-fired power plant

Prepared by:

Nicol Basson

RSSNIC014

Department of Mechanical Engineering

University of Cape Town

Supervisor:

A/Prof. Wim Fuls

August 2017

Submitted to the Department of Mechanical Engineering at the University of Cape Town in partial fulfilment of the academic requirements for a Master's of Science degree in Mechanical Engineering

Key Words: Flownex®, short term overheating, spraywater, superheater, transient.

Abstract

A common failure occurrence on fossil fuel power plant boiler systems is referred to as short term overheating (STO). This phenomenon occurs when the tube is heated to higher than its design temperature in a short period of time, causing a ductile failure of the tube material. The superheaters are particularly susceptible to STO. Such a failure can be caused by various conditions, where most of these are condition-based, i.e. based on the physical condition of the pipes or boiler. However, there are some cases which are process-related, i.e. based on the thermo-physical process occurring inside the pipe.

Very often a water blockage or water wedge is recorded to be the root cause of the short term overheating in superheaters when no condition-based indicators can be found. It then is claimed to be the result of over-attemperation spray by the operator. This type of failure tends to happen at the outlet of vertical (pendant-type) superheaters.

This study aims to find thermo-physical conditions where such a conclusion is valid by studying the transient behaviour of a representative superheater segment under postulated conditions. The specific geometry chosen is one for which short term overheating due to water wedging has been recorded in the past.

A transient flow model was constructed and verified by comparing its results with plant data, as well as some results from a numerical model developed from fundamental principles. Once the simulation modelling methodology was confirmed, the model was modified to resemble the geometry of the final superheater outlet leg to facilitate direct comparison with a pendant boiler component as found on a power plant. A number of scenarios were executed in transient state on the model at different boiler loads. The temperature evolution of the pipe wall was tracked over time, and together with calculated equivalent stresses, was compared to the yield strength of the material. A temperature vs yield strength curve was obtained from material testing using new and aged tube material.

The results showed that short term overheating at the superheater outlet tubes due to water blockages alone is unlikely to occur, even at low loads and substantial over firing. The stresses exerted over the tube wall and throughout the tube length is not enough to overcome the yield stress of the superheater tube material, even for aged material. Thus, the claim of over-attemperation as the root cause of a short term overheating failure is improbable, and other explanations for the failure must be observed. Even though it is possible for water-wedging to occur, the phenomenon alone is unlikely to be the root cause for the occurrence of short term overheating.

Declaration

I, Nicol Basson, hereby declare the work contained in this dissertation to be my own. All information which has been gained from various journal articles, text books or other sources has been referenced accordingly. I have not allowed, and will not allow, anyone to copy my work with the intention of passing it off as their own work or part thereof.

I know the meaning of plagiarism and declare that all the work in the document, save for that which is properly acknowledged, is my own. This thesis/dissertation has been submitted to the Turnitin module (or equivalent similarity and originality checking software) and I confirm that my supervisor has seen my report and any concerns revealed by such have been resolved with my supervisor.

Signed by candidate

Signature

2018-08-17

Date

Acknowledgements

I would like to express my deepest appreciation to my study leader, A/Prof. Wim Fuls, for his intellectual contribution and constant availability during the course of this project. Without his guidance and patience, this report would not have materialized.

I am very thankful for Mr. Russell Tarr, Mr. Jan Pretorius and Mr. Marthinus Bezuidenhout, for lending their technical skills to the completion of this project. A special thank you goes out to Johann Venter for providing the topic that put this project into motion.

I want to thank all of my fellow students that have crossed my path over the past two years, as well as our Research Manager, Mr. Priyesh Gosai, for their contributions and suggestions during my visits to campus.

I would like to acknowledge Mr. Werner Smit and Mr. JB Jansen van Rensburg for providing me with boiler tube materials from their plants, Prof. Robert Knutsen for organizing the testing and experimental data from these samples and Mr. Richard Curry along with his team for the final lab results.

My deepest gratitude goes to my husband, Marco, whose patient, loving and kind nature encouraged me throughout the past three years. Also, a very special thank you to my parents, Pieter and Amanda and my sister, Michelle: their care and support always gave me comfort.

Above all, to my Father in Heaven, whose favour rests on us, and who establishes the work of our hands for us (Ps. 90:17).

Table of Contents

List of Figures

List of Tables

List of Nomenclature

General symbols

A	Area / Variable	$[m^2]$ / [-]
C	Variable	[-]
c_p	Constant pressure specific heat capacity	[kJ/kg]
D	Diameter	[m]
E	Elastic modulus	[MPa]
F	Variable	[-]
f	Friction factor	[-]
G	Mass flux	$[kg/m^2.s]$
g	Gravitational constant	$[m/s^2]$
h	Heat transfer coefficient	$[W/m^2.K]$
H	Height	[m]
K	Loss factor	[-]
k	Conductivity	[W/m.K]
L	Length	[m]
m	Mass	[kg]
$\dot{m}$	Mass flow rate	[kg/s]
n	Variable	[-]
Pr	Prandtl number	[-]
Δp	Pressure drop	[kPa]
p	Pressure	[kPa]
$\dot{Q}$	Rate of heat transfer	[kW]
Re	Reynolds number	[-]
r	Cylindrical coordinate, radius	[m]
T	Temperature / Variable	[°C, K] / [-]
t	Time / Wall thickness	[s] / [mm]
v	Velocity	[m/s]
x	Vapour quality	[-]

Greek symbols

σ	Stress [MPa]	[MPa]
α	Thermal expansion	[K^{-1}]
Δ	Difference	
ε	Surface roughness/ Emissivity	[µm] / [-]
Λ	Variable	[-]
$\hbar$	Enthalpy	[kJ/kg]
μ	Dynamic viscosity	[kg/m.s]
ρ	Density	[kg/m^2]
ν	Specific volume / Poisson's ratio	[m^3/kg] / [-]

Subscripts

2Φ	Two phase flow
a	Axial
avg	Average values
B	Boiler properties
c	Cross sectional / Circumferential
e	Evaporation conditions
f	Fluid in tube properties
fg	Flue gas properties
g	Gas phase
H	Hydraulic
h	Hoop
i	Initial / Inlet / Inner
l	Liquid phase
o	Final / Outlet / Outer
p	Plugged conditions
r	Radial
st	Steam conditions
t	Tangential / Tube property
th	Thermal
tot	Total
v	Variable
VM	Von Mises
w	Water wedge properties

Acronyms and Abbreviations

ASME	American Society of Mechanical Engineers
ASTM	American Section of the International Association for Testing and Materials
BL	Boiler Load
BTL	Boiler Tube Leak
EPPEI	Eskom Power Plant Engineering Institute
FD	Forced Draught
FG	Flue Gas
GO	General Overhaul
HP	High Pressure
HV	Vickers Scale Hardness
ID	Inner Diameter / Induced Draft
LHS	Left Hand Side
LTO	Long Term Overheating
LP	Low Pressure
MS	Main Steam
OD	Outer Diameter
OF	Overfiring
PF	Pulverized Fuel
RH	Reheater
RHS	Right Hand Side
SH	Superheater
SS	Steady State
STO	Short Term Overheating
UCT	University of Cape Town

1. Introduction

1.1 The role of coal-fired power plants

Coal is currently the primary fuel source for generating electricity worldwide. In South Africa, 77% of the country's energy requirements are provided by Eskom's coal-fired power stations, followed by hydro, solar, wind and nuclear power.

Coal-fired power stations work on the principle of energy conversions. The process starts with the coal, which contains chemical energy. Once the pulverised coal is sent to the burners, the chemical energy is released as heat in the furnace of the boiler. This heat transferred to the water in the water-walls of the boiler. The water evaporates into steam, creating a steam flow in the boiler tubes. The steam is further superheated in a series of heat exchangers, called superheaters. The steam exits the boiler and is received by the high pressure (HP) turbine, which uses the heat from the steam to drive the turbine blades, thus converting the thermal energy to kinetic energy.

In re-heat plants, the steam is sent back to the boiler for reheating after the HP turbine, and then enters the intermediate pressure (IP) turbine and then the low pressure (LP) turbine. The rotating turbine drives a generator which converts the mechanical energy into electrical energy. This energy is that which is used by the Eskom grid to supply homes and businesses with electricity. [1]

1.2 Boiler tube leaks

The purpose of the boiler is to convert the chemical energy extracted from the coal into thermal energy, which is transferred from the flue gas in the furnace to the steam inside the boiler tubes. These tubes make up various heat exchangers, namely the economiser, evaporator, superheaters and reheater. The total length of all the boiler tubes joined together can be as long as 650 km [2].

Boiler tubes need to be regularly monitored and cleaned to ensure the lifetime of the entire boiler, which, in turn, ensures the lifetime of the entire plant itself. Because of the high-pressure steam that flows in these tubes, a leak or failure of any kind can be hazardous to the station and personnel.

In 2011, 70% of Eskom's boiler tube failures occur during a unit's start-up procedure following a forced outage. A total of 152 tube failures transpired on Eskom's 79 various boilers [2] at that time.

Some of the most common causes of boiler tube failures include, but is not limited to, the following:

- Short term overheating
- Long term overheating
- Fly ash erosion
- Welding defects
- Corrosion (steam side and/or fire side)

For the purpose of this study, the focus will be on short term overheating. Long term overheating will also be briefly discussed to clarify the difference between these two causes.

1.3 Long and short term overheating

The typcal design lifetime of a boiler tube is 200 000 to 300 000 operational hours, or about 23 to 34 years, depending on the material's composition and quality [2]. Long term overheating takes place when a tube has reached the end of this lifetime. Because of the high-temperature high-pressure steam transported in these tubes, the material will eventually degrade and fail due to creep. An illustration of this type of overheating is shown in Figure 1.1.

Figure 1.1 Damages as a result of long term overheating [2]

Short term overheating, on the other hand, is a premature tube failure. It is essential to determine if a failure occurred prematurely or not, so that the root cause can be identified. Preventative actions may then be studied and implemented in order to prevent future failures.

Short term overheating occurs when the tube is exposed to a heat higher than its design temperature, reducing the material's strength drastically until it ruptures. When the tube material is allowed to exceed its design temperature, it will, depending on the temperature reached, fail in the short term. This can be caused either by a lack of cooling or due to a high firing temperature. The rupture can occur instantaneously, or it may take up to a few days, depending on the temperature reached. The most likely causes of this type of overheating include:

- Tube blockages and partial blockages;
- Steam starvation;
- Excessive firing;
- Maldistribution of flue gas due to slagging.

As a result of hoop stresses [3], the damages of this sort imitate that of a fish mouth, illustrated in Figure 1.2.

Figure 1.2 "Fish mouth" damage as a result of short term overheating [2]

Any tube in the boiler can become a susceptible to short term overheating [2], which predominantly occurs in the water walls, the final stage superheater or the final reheater. Short term overheating is much less likely to occur in colder sections of the boiler, such as the economiser. In section 2.6 of this report, occurrence investigations are discussed of short term overheating that took place at Eskom in the final superheater.

Eskom's most common means of detecting a tube leak is the use of microphones at the boiler's manhole entrances. The microphones are able to record the distinct hissing sound of a tube leak. The recording is fed through a processor and is displayed as a bar chart. Normal conditions are indicated in a green colour, as shown in Figure 1.3. A high noise level triggers an audible alarm, and introduces an orange column to the bar chart, illustrated in Figure 1.4.

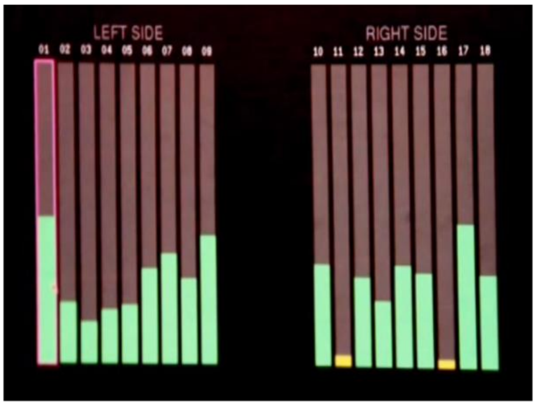

Figure 1.3 Display of normal conditions [2]

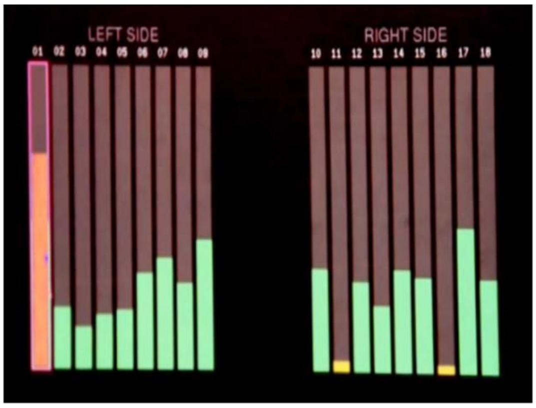

Figure 1.4 Orange column indicates a tube leak [2]

The earlier a tube failure is detected, the better the chances are of minimising the repair time and damages that is to follow. Once a leak is detected, it is necessary to shut down that specific unit. Once the unit is shut down, the components are force-cooled by means of the plant forced draft (FD) fans and induced draft (ID) fans, according to safety regulations. Once cooled and cleared of all possible harmful boiler gasses, a physical investigation of the tubes can be carried out.

A piece of the tube containing the failure is cut out and examined by a metallurgist to determine the failure mechanism. Tubes that may have been exposed to secondary damages are identified through ultrasonic tube thickness measurements. All of these tubes would require replacement.

The entire process, shutting down the unit up to the point when the unit is safely returned to service, takes approximately 63 hours, depending on the extent of the damage.

1.4 Problem statement

Of the various caused for STO listed previously, steam starvation is one which is difficult to identify from physical evidence extracted from the failed tube or boiler region. This is because this cause is process-related, i.e. something in the thermo-physical conditions inside the tube results in insufficient cooling of the material. Such short term overheating often occurs at low load or start-up. In these operating modes, the steam temperatures are not always stable, and can rise beyond the allowed limits. In an attempt to reduce the possibility of STO when steam temperatures do rise, the plant operator may increase the spraywater flow of the attemperation system [4], hence over-spraying occurs. This has been suspected to cause water blockages, which decreases the steam flow in the superheater tubes. When the flow is insufficient, the tubes are exposed to the high metal temperatures heated by the furnace since cooling from the steam flow is absent, also causing short term overheating.

A commonly given cause of STO is thus complete or partial water blockage, which is caused by water wedging [3]. This means that when condensate forms in the superheater tubes, the pressure between the inlet and outlet is not great enough to transport the water through the tubes, causing a blockage. This statement, however, may be untrue for two main reasons:

1. Firstly, the steam in the superheater operates at a temperature in the range of 550°C, whereas condensate can only occur below ±350°C for the typical boiler pressure (±18 MPa) of sub-critical Eskom plants. For this to occur, the temperature of the superheater should be drastically decreased.
2. Secondly, if water should start to form, it would form at such a high temperature that it would not take a long period of time to once again evaporate, since the water would be hot to begin with. Thus, the water would not exist in the tubes long enough to cause short term overheating.

The purpose of this project is to investigate the thermo-physical ability of overspraying to cause water blockages in superheater tubes which would lead to a failure.

1.5 Hypothesis

The study in this dissertation aims to answer the following questions:

1. Is it possible for water to form in a boiler tube to create a plug when the boiler operates above saturation conditions?
2. If such a possibility exists, under what process conditions will short term overheating take place?

This study will specifically focus on short term overheating caused by a water wedge due to over-attemperation in pendant-type pipes. This causes the boiler tube to be starved of steam, depriving the boiler tube material of a cooling medium. The failure occurrences that were investigated took place at the outlet of the tube during low boiler load conditions. It is hypothesized that, if a water plug should form at low load, the pressure difference over the tube inlet and outlet will not be great enough to force the plug out of the tube.

If the water plug should remain in the tube and cannot be evaporated within a specified time, the outlet of the tube will be starved of steam. This will cause the temperature from the furnace to rapidly increase the tube material. Due to the stresses then placed upon the tube, coupled with the weakening of the material at high temperatrues, short term overheating may occur.

The following assumptions were made in the analysis:

- The model only simulates short term overheating as a result of water-wedging specifically;
- The simulation is modelled after the final superheater as explained in section 4.2;
- The short term overheating occurrence only takes place on a single superheater tube;
- The short term overheating occurrence takes place at the outlet of the superheater tube (as was found to be the case based the data collected);
- The external heat transfer remains constant for the full duration of the transient, and can be determined from the plant operating conditions just before the event. (This assumption will be motivated / elaborated on in section 3.2.3).
- The short term overheating events in this dissertation focuses on those which are referred to as sudden onset events. The transient simulation was therefore limited to 10 minutes;
- The short term overheating event takes place at low load conditions;
- The water-wedge that would exist is assumed to be still-standing, being replenished by a continuous flow of spraywater such that it does not evaporate for the full duration of the transient. (If the water-wedge does evaporate, the pressure difference will push the water out, and thus end the steam starvation);
- The plant operated properly before the event, i.e. there were not any existing blockages or other defects. However, the boiler firing system may not be stable, and could be over-firing before the event.

1.6 Objectives

To accurately study the above-mentioned hypothesis and finally predict the circumstances for the failure mechanism of short term overheating, the following objectives had to be met:

- Understanding the phenomena of short term overheating;
- Study short term overheating scenarios and causes;
- Obtain the process conditions under which short term overheating takes place according to literature;
- Develop a mathematical process model to determine the thermodynamic properties of short term overheating events;

- Develop a transient model to simulate short term overheating events;
- Obtain data of boiler material temperature versus material stresses;
- Determine the stresses of a boiler tube where short term overheating takes place for different scenarios;
- Identify the conditions for short term overheating to occur.

1.7 Structure of this report

The document consists of the following main points:

- A literature study establishes a theoretical framework for the topic on the short term overheating, outlining similar studies conducted and models created.
- A chapter on theory defines the key terms and terminology, as well as the necessary scientific formulae that were used throughout this project.
- The methodology for acquiring the relevant data for this project is explained, as well as the setup of transient simulation and the numerical model.
- The final results for both the transient simulation and numerical are made available while also being verified with actual plant data, and conclusions are drawn.
- Recommendations are given to assist with any future studies to be performed.

2. Literature review

2.1 Introduction

In the chapter to follow, a literature study was conducted to better understand the causes of short term overheating, and how it is distinguished from long term overheating or creep. The study includes the design of the boiler unit, specifically focusing on the final superheater specifications. The study also focuses on previous works and projects conducted by experts in the industry. This chapter discusses some of these methodologies and their results. The relevancy of these studies can then be used as a basis for the project discussed in this dissertation.

2.2 Understanding the design of a boiler

The boiler considered for this project has a front side and a rear side which is known as a twin-pass boiler (previously called a Carolina boiler) as shown in Figure 2.1. The boiler makes use of natural circulation to transport steam from the boiler drum through the water-walls to the boiler components.

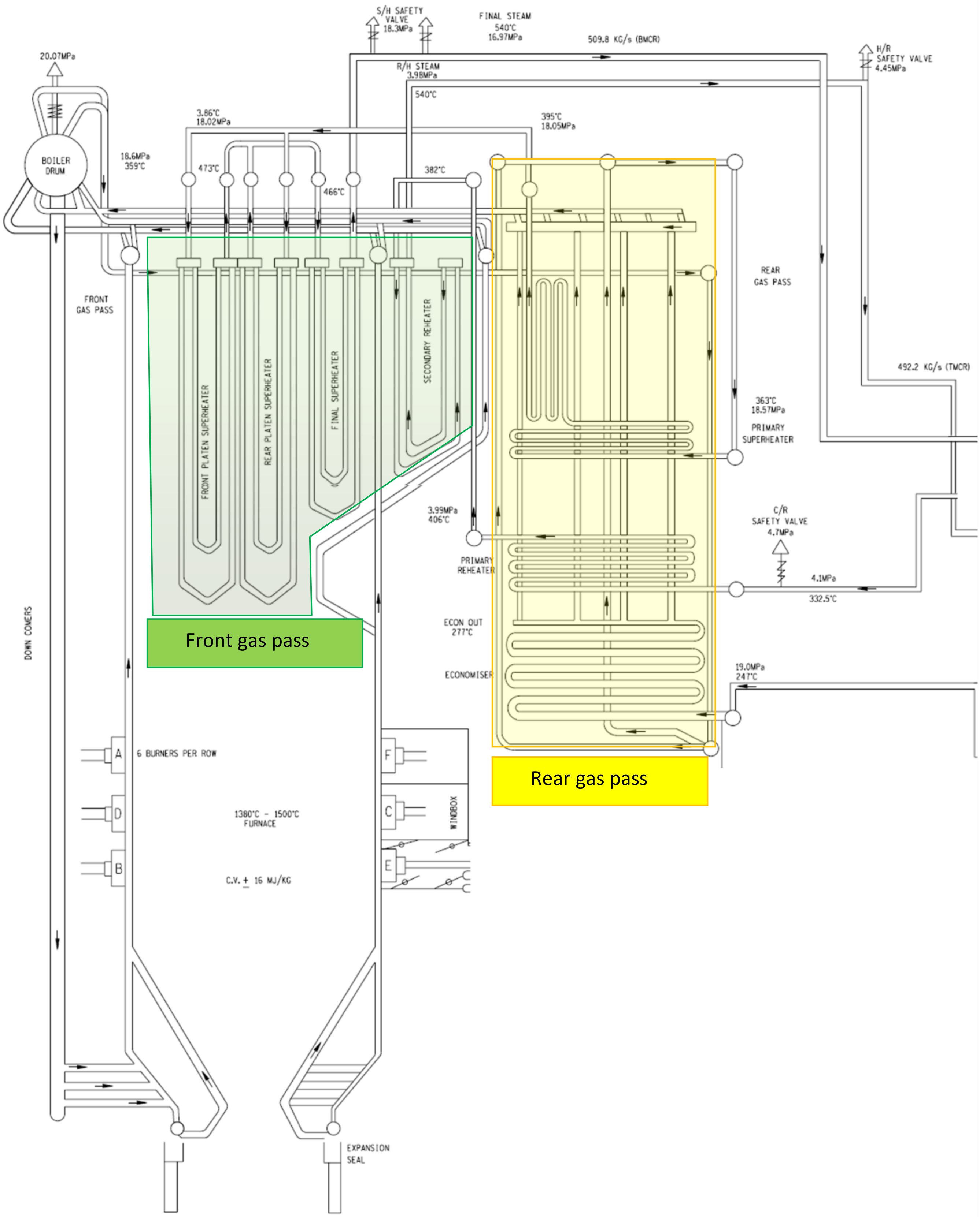

Figure 2.1 Twin pass boiler design [1]

The boiler system, particularly the steam system, consists of the high pressure (HP) and low pressure (LP) steam cycles. The HP steam refers to that part of the cycle where the steam is being superheated, while the LP steam refers to the reheated steam. The saturated HP steam is fed to the boiler from the boiler drum. Through a number of tubes, the primary superheater is the first component in the boiler to receive this steam. Here the steam is heated to a specific temperature. The steam exits through a vertical outlet bank to the primary superheater outlet headers.

The first stage attemperation then takes place between the primary superheater outlet headers and the platen superheater inlet headers. Attemperation is achieved via a high-pressure spraywater system supplied by the line from the feedwater system to the economizer. The steam is heated at the inlet of the platen superheaters. The platen superheater consists of two groups of pipe elements that are suspended above the furnace in the form of loops. The front loop acts as a parallel flow heat exchanger, while the loop at the rear is counter-flow. After the steam completes its progression through these loops to the outlet headers, it is attemperated (second stage attemperation) before being transported to the final superheater inlet manifolds. This concept is simply explained with the illustration in Figure 2.2.

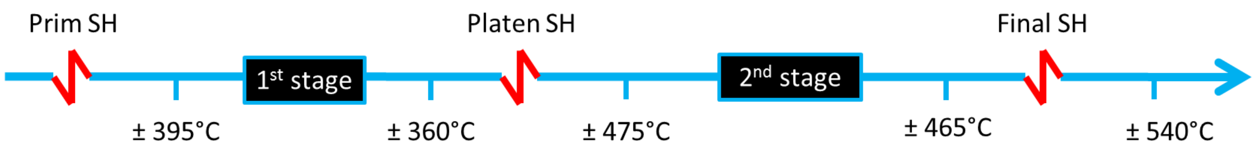

Figure 2.2 Superheater attemperation system

2.3 Causes of short term overheating

The greatest cause of forced outages on power plants is boiler tube failures, of which short term overheating contributes 8.8% as the failure mechanism [5]. According to Babcock & Wilcox, an international company that is partly responsible for Eskom's high pressure boiler parts, short term overheating most commonly takes place during a unit start-up [6]. This occurs mainly due to condensation formed in the boiler tube when the unit was being force cooled. During the start-up procedure, the condensate that is still present in the bends of the tubes obstructs the steam flow, causing the tubes to overheat. This is known as steam starvation.

An example of a short term overheating occurrence took place on the water walls of a fossil fire power plant, according to an investigation done by Ahmad et al. [7]. The water wall tubes were constructed out of SA210-A1 material, with a wall thickness measuring at 7.9 mm. The average operating steam pressure and metal temperature is 14.2 MPa and 360°C, respectively.

The failure occurred upon boiler start-up following a forced outage due to another tube leak in the front gas pass. Figure 2.3 indicates where the water wall tube failure took place.

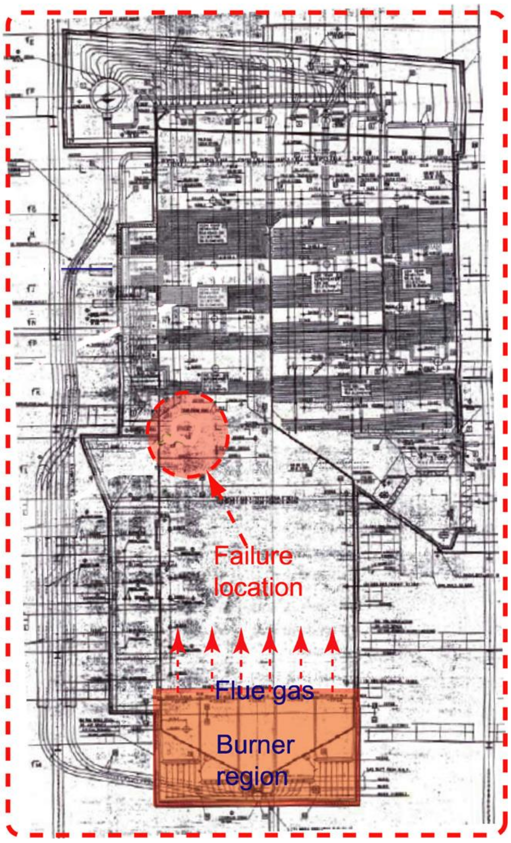

Figure 2.3 Location of water wall tube failure [7]

Upon investigating the event, it was discovered that the tube operated at a higher temperature than its design temperature. Visually, the tube was still in a good condition, with just some discolouration on the outer surface. However, the microstructures indicated spheroidization of the ferrite and pearlite structures. This led to the conclusion that the tube experienced steam and water flow restrictions, leading to overheating at a temperature higher than 600°C. This caused the strength of the material to decrease and the operational stresses became too great to be managed by the tube, which caused the eventual rupture.

Chaudhuri [8] conducted a metallurgical assessment of various boiler tube failures, one of which was a rupture that took place on one of the final superheater tubes of a 500MW boiler. The failure took place during a trial run after the tubes had reached an operating life of 100 hours. The metallurgical findings are furthered discussed in section 2.4 of this document. The direct cause was assumed to be a partial choking of the tube, resulting in steam starvation.

A failure may also occur in such a manner that long term overheating is discovered to be the failure mechanism, where short term overheating becomes a contributing component. This was found to be the case in a study conducted by Perdomo and Spry [9].

Another cause that often leads to short term overheating is the thinning of the boiler tube wall thickness due to scale build-up. This was found to be the case during a root cause analysis conducted by Purbolaksono et al. [10]. The occurrence involved the primary superheater which was refitted with SA213-T12 tubes with a wall thickness of 5 mm. A new type of coal was introduced to the boiler some time later together with a new firing pattern to accommodate for this new coal. Less than 10 days later, the failure took place on the tubes which had only been in service for 28 194 hours. Upon investigating the tube failure, it was found that enormous clinkers had formed on the top bank of the primary superheater, as shown in Figure 2.4.

Figure 2.4 Clinker formation on top bank of primary superheater [10]

The new coal had an ash fusion temperature of 1210°C, which is low compared to the average boiler's furnace flame temperature at approximately 1400°C. As a result, some of the exposed tubes experienced a more concentrated gas flow in the tubes due to the new firing patterns, causing a build-up of oxide scaling on the inner tube wall. Because of this build-up, the tube wall becomes thinner, making it insufficient for handling the high flue gas temperatures. This occurrence is illustrated in Figure 2.5.

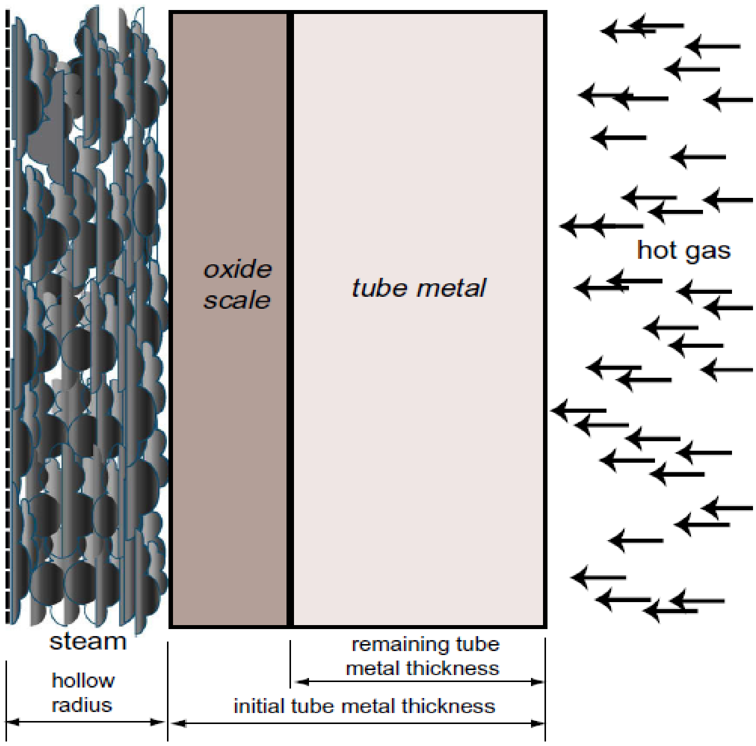

Figure 2.5 Oxide scaling in superheater tube [10]

The series of events eventually led to the failure of the primary superheater tube, with the direct cause identified as short term overheating. The root cause was discovered to be localized flue gas flow. This was preceded by the heavy development of clinkers on the top bank tubes due to a low ash fusion temperature. Proper heat transfer is then restricted in the areas of the tubes where the clinkers form. This causes some areas to heat up more than others. The localized overheating is then caused due to a maldistribution of temperatures.

A similar occurrence took place on the water wall tubes near the superheater at Sultan Shalahuddin Abdul Aziz Shah Power Station, which was investigated by Rahman et al. [5]. The boiler was introduced to a new type of coal when a failure occurred a few weeks later due to heavy clinker formation, as shown in Figure 2.6. The SA213-T 22 tube had only been in operation for 394 hours at 12.25 MPa.

Figure 2.6 Clinker formation in superheater region [5]

2.4 Visual and metallurgical assessment

Any tube from any boiler component transporting water or steam can be subjected to short term overheating. These boiler tubes are designed to operate within the ASME oxidation limits [11]. Short term overheating occurs when the boiler tubes are exposed to temperatures higher than design temperatures, or above the eutectoid transformation temperature, which is typically 727°C [12].

A selection of creep-resistant steels is used in the large-scale power industry to ensure the longest possible life for components. Table 2-1 lists the most commonly used of these steels and their compositions. The elements in these steels are arranged in such a way to tolerate high pressures and temperatures to create the highest possible resistance against creep and ruptures.

Table 2-1 Selection of creep-resistant steels [8]

Steel type	C	Cr	Mo	Other elements
Group 1: carbon steels				
Tubes SA-192	0.06–0.18			Mn: 0.27–0.63, Si: 0.25
Pipe SA-106	0.35			Mn: 0.29–1.06, Si: 0.10 minimun
Group 2: low alloy steels and 9Cr–Mo steels				
1Cr–0.5Mo	0.11	1.0	0.5	Mn: 0.5, Si: 0.25
2.25Cr–1Mo	0.12	2.25	1.0	Mn: 0.5, Si: 0.25
0.5Cr–0.5Mo–0.25V	0.11	0.5	0.5	Mn: 0.5, Si: 0.25, V: 0.25
9Cr–1Mo	0.10	9.0	1.0	Mn: 0.5, Si: 0.60
Group 3: 12Cr steels				
12Cr–Mo–V	0.12	12.0	0.6	V: 0.2, Ni: 0.80
12Cr–Mo–V–Nb	0.11	11.0	0.6	V: 0.2, Ni: 0.8, Nb: 0.35
Group 4: austenitic steels				
Type 304	0.05	18.5		Mn: 1.3, Ni: 10
Type 316	0.05	18.0	2.5	Mn: 1.4, Si: 0.4, Ni: 10
Esshete 1250	0.10	15.0	1.0	Mn: 6, Si: 0.5, Ni:10, V: 0.3, Nb: 1

.

When a tube failure occurs within a boiler, a visual examination can be done to estimate the possible failure mechanism. Visual examinations can then be verified by means of metallurgical examinations.

Short term overheating can be estimated by inspecting the failed tube visually. The first visible indication of short term overheating is the tube rupture itself, which would have a thin-lipped fish-mouth appearance, as illustrated in Figure 2.7. This type of rupture is a result of the longitudinal fracture that occurs during failure. The tube will also show some discoloration due to localized heating [7].

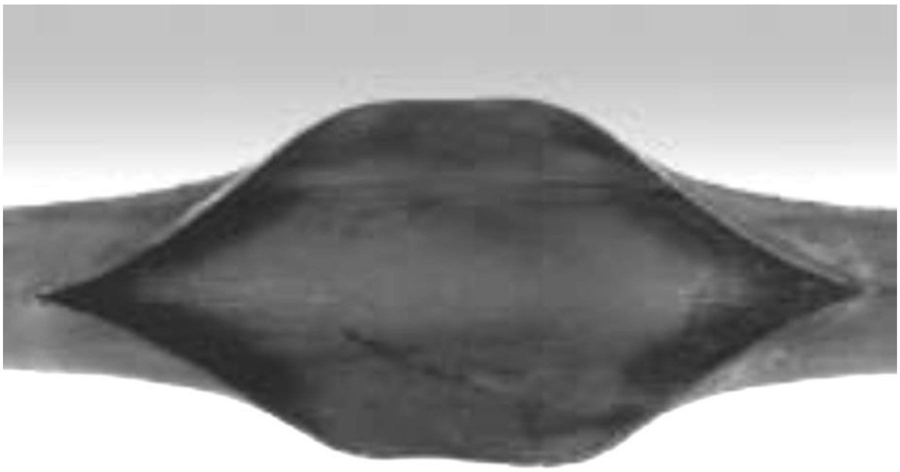

Figure 2.7 Thin-lip fish-mouth rupture due to STO [6]

The first metallurgical examination to be carried out on the tube is a life assessment to determine if the failure occurred prematurely. There are three metallurgical methods of determining the life of a failed tube, namely by examining the:

- Material microstructure;

- Oxide scale thickness;
- Material hardness.

To determine if tubes were operating above the eutectoid temperature, the microstructure of the material is studied during a metallurgical assessment following a tube failure [12]. More specifically, the amount of martensite (also known as bainite) mixed with ferrite is examined. When the formation of bainite is shown to have increased, the microstructure will show an elongation of the grains, causing a decrease in yield strength. The increase of bainite is a result of the quenching effect that takes place when water or steam suddenly escapes from the semi-austenitic tubes during the failure [13].

Oxide scaling is formed on the inner wall of a superheater tube when the material is operating at a higher than design temperature. These high temperatures cause the steam particles to react with the iron in the tube material. This reaction results in a mixture of hydrogen and magnetite, as given in the chemical reaction formula below. If the metal temperature increases, the rate at which the reaction takes place will also increase.

$$3Fe + 4H_2O \Rightarrow Fe_3O_4 + 4H_2$$

Because the boiler tubes are constantly exposed to high pressures and temperatures, the strength of the material decreases over time. Changes in the material's hardness are indicative of the material's remaining operating life. The Larsen-Miller parameter is often used to establish these changes.

During the study done by Ahmad et al. [7], a scanning electron microscope was used to inspect the microstructure of the failed tube. After comparing their findings to those of a tube with a normal microstructure, it was concluded that the failed tube was exposed to higher than design temperatures. These findings are shown in Figure 2.8 and Figure 2.9. These differences indicate spheroidization, leading to the conclusion of short term overheating.

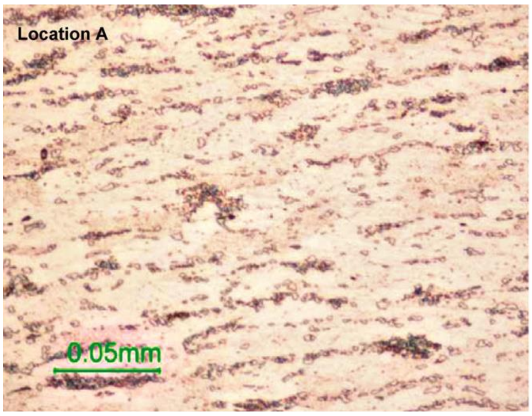

Figure 2.8 Microstructure of failed tube [7]

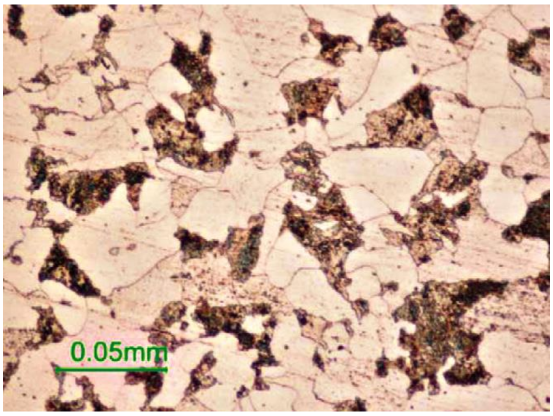

Figure 2.9 Normal microstructure [7]

The metallurgical assessment conducted by Chaudhuri [8] begins with a collection of three samples. The first sample is taken from the failed tube, which is to be compared with a sample of one of the undamaged adjacent tubes of the final superheater. All of the results gathered from these two samples can then finally be compared to a piece of virgin tube with a similar chemical composition as those tubes of the final superheater. All of these samples meet the requirements as determined by ASTM specifications.

The first finding was that the outer diameter of the failed tube, compared to the undamaged adjacent tube, had expanded with 19% from 44.5 mm to 49.2 mm. This clearly indicates that the tube operated under abnormal conditions. The hardness measurements, shown in Table 2-2, support this claim by displaying a considerable increase in hardness.

Table 2-2 Hardness values of virgin, undamaged and failed tube [8]

Tubes	Hardness, HV20		
	Inner	Middle	Outer
Virgin	145	149	151
Undamaged	143	143	145
Failed	179	178	180

The microstructure comparisons are given in Table 2-2. Both the hardness and structure of the virgin and adjacent tubes are almost similar, whereas the failed tube clearly suggests a recent formation of bainite. Also, the scale thickness of the failed tube was measured at 0.25 mm, which was several times thicker than that measured for the virgin and adjacent tubes.

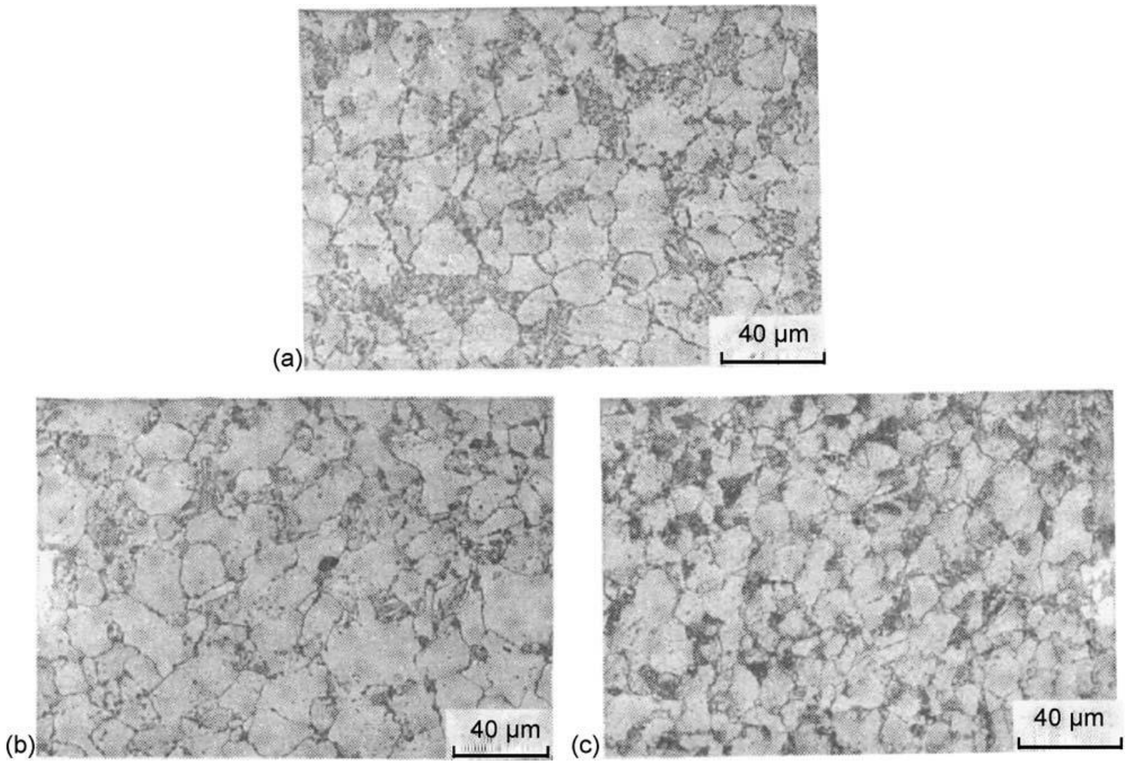

Figure 2.10 Microstructures of (a) virgin tube; (b) adjacent tube; (c) failed tube [8]

All of these assessments lead to the conclusions that short term overheating took place on the failed tube of the final superheater.

2.5 Possible solutions

As the demand for electricity is increasing world-wide, a reduction in forced outages becomes vital. Since boiler tube leaks are the leading cause of forced outages [14], a greater effort should be made to decrease such failures. These outages also result in major economic implications due to a loss in generation and sizeable repair costs.

The safe operation of boiler tubes can be ensured by using a suitable material [5]. A selection of such materials was previously given in Table 2-1. These materials safeguard the use of the boiler tubes under high temperatures and pressures over a lengthy period of time. However, this alone cannot guarantee a 0% chance of boiler tube failures.

The temperature and time it takes for overheating to occur depends on the tube material. A tube may fail at a very high temperature over a short period of time, or a relatively lower temperature over a longer period of time. By studying the grain of the tube after failure, the temperature and time of failure can be determined.

Also, regular maintenance ensuring that the tubes are in good condition can assist in preventing future incidents.

2.6 Eskom BTL occurrence reports

One of the most prominent incidents in Eskom occurred at one of their power station's in 2000 due to short term overheating [15]. A unit was taken off load for a boiler tube inspection that was to last for five days. After the unit was returned to service, it ran for 7.5 hours before a boiler tube leak was detected. Upon inspection of the final stage superheater, six tubes were found to have burst along with multiple other damaged tubes. A collection of such images is shown in Figure 2.11, Figure 2.12 and Figure 2.13.

All six of the bursts were attributed to short term overheating. Visual inspections of the tubes indicated a thin-lipped burst with a fish-mouth appearance. Metallurgical investigations found a substantial measure of oxide in the tube exit bends. The failure was owed to a rapid decrease in cooling steam flow in the tubes.

Further investigations revealed that the steam inside the final superheater tube reached saturation temperatures shortly after the light-up of the unit, which could have caused the possible blockage, cutting off steam supply. Two possible reasons for this was given as water plugging of the tubes or exfoliated oxide settling in the bends.

It was suggested that longer light-up times be enforced when it is known that oxide scaling is present in the tubes [15].

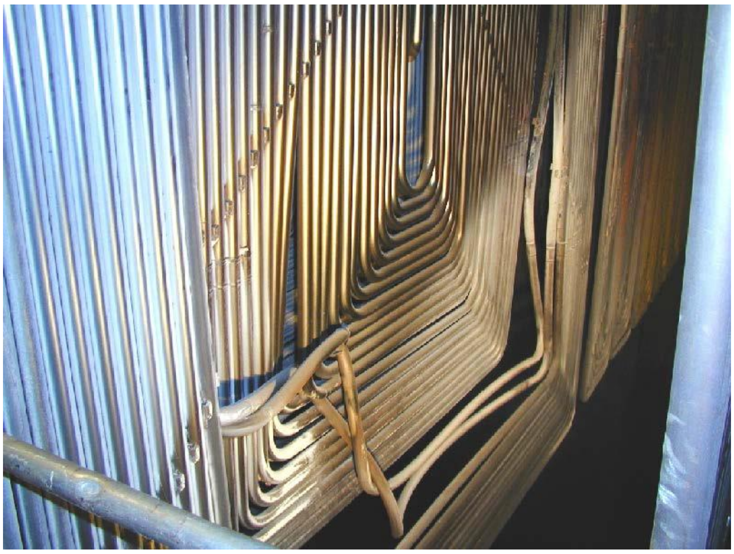

Figure 2.11 STO damages on power station 2000 (a) [15]

Figure 2.12 STO damages on power station 2000 (b) [15]

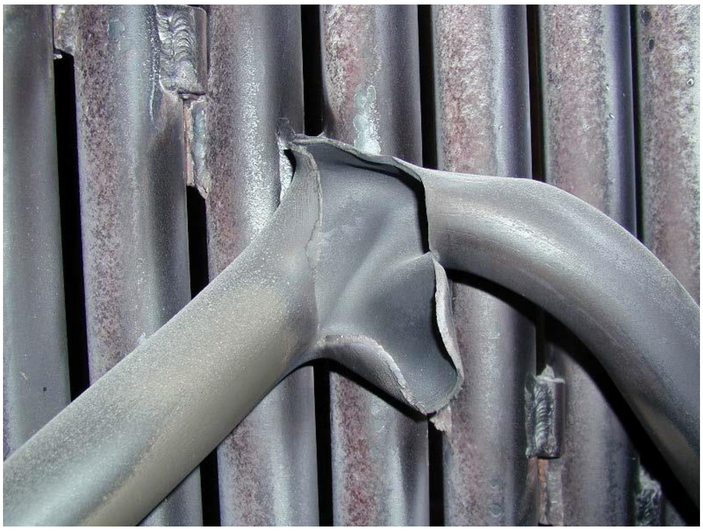

Figure 2.13 STO damages on power station 2000 (c) [15]

Boiler failures in Eskom can be contributed to many factors. The five most common causes of these failures are (in order):

1. Fly-ash Erosion (FE)
2. Thermal Fatigue (TF)
3. Sootblower Erosion (SE)
4. Short Term Overheating (STO)
5. Long Term Overheating & Creep (LTOC)

Statistics (years 2003 to 2016) from all of the tube leak reports throughout Eskom shows that short term overheating is the fourth leading failure mechanism of boiler failures, following fly ash erosion, thermal fatigue and sootblower erosion, and is closely followed by long term overheating and creep (see Figure 2.14 [16] and Table 2-3 for an explanation of the acronyms).

April 2003 to December 2016									
2003/04/01 00:00:00	1	2	3	4	5	6	7	8	
Leading Mechanisms	Mech 1	Mech 2	Mech 3	Mech 4	Mech 5	Mech 6	Mech 7		
	FE - -	TMF TFW CF	SE - -	STO - -	LTOC - -	WRD - -	UNK - -	Other	Total
Total failures/mechanism	642	355	218	181	170	170	63	407	2206
% of total failures	29%	16%	10%	8%	8%	8%	3%	18%	100%

Figure 2.14 Failure mechanism statistics throughout Eskom from 2003 to 2016 [16]

Table 2-3 Acronyms - Boiler failure mechanisms

Acronym	Description
FE	Fly-ash Erosion
TMF	Thermo-Mechanical Fatigue
TFW	Thermal Fatigue
CF	Corrosion Fatigue
SE	Sootblower Erosion
STO	Short Term Overheating
LTOC	Long Term Overheating & Creep
WRD	Weld Defect
UNK	Unknown

From April 2003 to December 2016, Eskom has recorded a total of 2206 boiler tube failures throughout its various fossil fuel power stations. The failure mechanism for 181 of these events is short term overheating. That is to say, short term overheating has caused approximately 8% of Eskom's boiler tube failures over the past thirteen years [16].

Of all the short term overheating events, 45% of the root causes have been attributed to "water-wedging". The amount of boiler tube failures overall (and especially examining STO) seemed to increase over the years. Figure 2.15 and Figure 2.16 depicts these increasing failures.

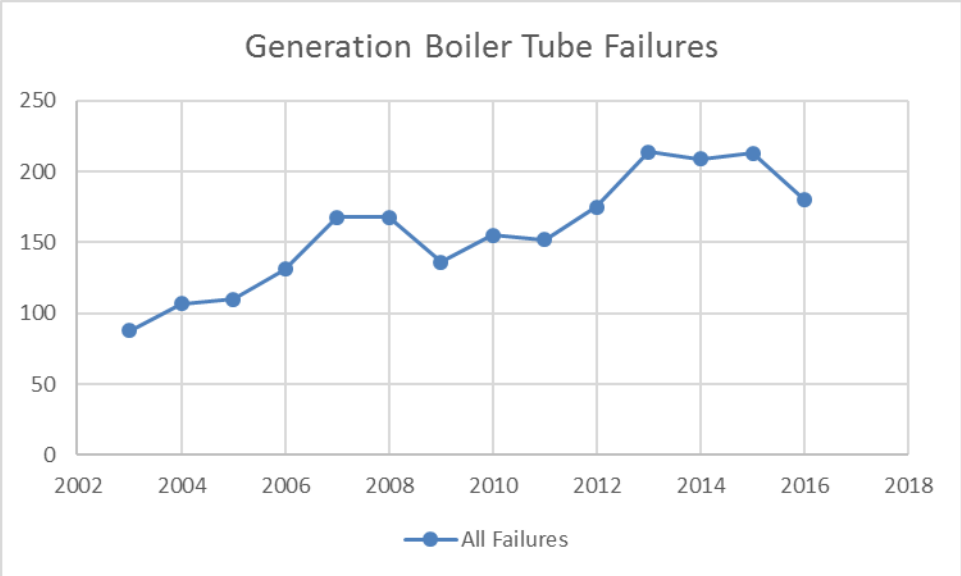

Figure 2.15 Eskom overall boiler tube failures

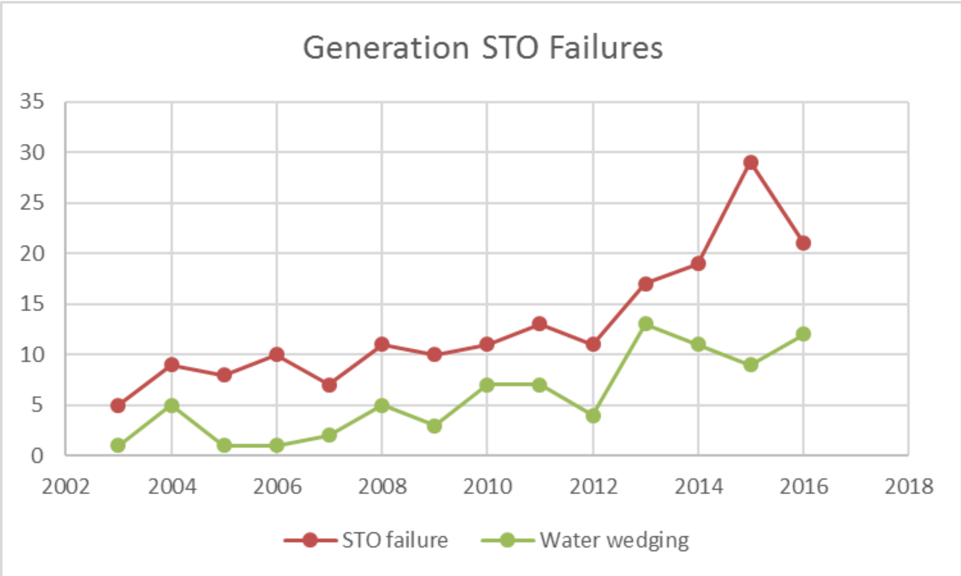

Figure 2.16 Eskom STO and water-wedging events

From Figure 2.16, it can be seen that a great number of short term overheating events that take place in Eskom is attributed to water-wedging.

By individually examining all of these investigative reports, a pattern was discovered: In a twin pass type boiler, short term overheating due to water wedging only occurs in the front gas pass, where the pendant-type superheaters are situated. An extract from this pattern data is displayed in Figure 2.17 (station names have been removed for confidentiality purposes). It is postulated that condensate formation occurs at the bottom bends of these tubes, causing the water blockage leading to the final rupture due to steam starvation.

Date	Component failure	Pass	SH type	Root cause
15 July 2004	Platen SH	FGP	Pendant	PO
04 March 2010	SH2	FGP	Pendant	Poor operating during unit start-up. Hot and cold light up procedures are to be use during light up to make sure no condensate are present. The outlet temperatures have to exceed the inlet temperatures.
25 August 2010	Platen SH outlet	FGP	Pendant	Water wedging due to overspraying
05 November 2010	Platen SH	FGP	Pendant	The failure is related to reported regular trips and thermal excursions caused upon start-ups resulting in high heat fluxes in this area of the boiler, which over relatively short periods of time result in accelerated weakening of material.
15 January 2011	SH3	FGP	Pendant	
22 January 2011	SH3	FGP	Pendant	
17 June 2011	Platen SH	FGP	Pendant	Procedural deficiency resulting in ineffective boil out of the Platen and Secondary Superheaters.
03 November 2011	Final SH outlet	FGP	Pendant	Water wedging due to overspraying
12 November 2011	Final SH inlet?	FGP	Pendant	Water wedging
04 May 2012	Platen SH	FGP	Pendant	Tube Blockages, source of blockage still under investigation.
08 May 2012	Platen SH	FGP	Pendant	Blockage inside the tubes, root cause still under investigation.
19 May 2012	SH2	FGP	Pendant	Blockage on the tubes, still under investigation.
10 February 2013	Final SH	FGP	Pendant	Water wedging
20 August 2013	SH2	FGP	Pendant	Under investigation
31 August 2013	RH2	FGP	Pendant	To be investigtaed
05 September 2013	Platen SH	FGP	Pendant	To be investigated
19 November 2013	Final SH outlet	FGP	Pendant	Water wedging due to overspraying
31 December 2013	Platen SH outlet	FGP	Pendant	To be investigated
16 March 2014	Platen SH	FGP	Pendant	To be investigated
05 May 2014	SH4	FGP	Pendant	Water carry over into SH elements
23 June 2014	SH4	FGP	Pendant	Condensate accumulation in bottom bends
15 June 2014	Final SH inlet?	FGP	Pendant	Overspraying of 2nd stage attemperation
01 January 2015	SH2	FGP	Pendant	Non adherence of light up procedure by introducing mills quickly
04 January 2015	Platen SH	FGP	Pendant	Non compliance of light up procedure, OMOP 3488 and 3508
03 February 2015	Platen SH outlet	FGP	Pendant	Overspraying
05 April 2015	SH1	FGP	Pendant	Suspected tube blockage
15 April 2015	SH4	FGP	Pendant	Procedure for boilout during lightup not followed
03 August 2015	Platen SH outlet	FGP	Pendant	Drum water carry-over causing water wedging
08 October 2015	Final SH inlet?	FGP	Pendant	Under investigation
20 January 2016	RH2	FGP	Pendant	Under investigation.
31 January 2016	Platen SH outlet	FGP	Pendant	Under investigation
05 February 2016	RH2	FGP	Pendant	Under investigation
13 February 2016	Platen SH	FGP	Pendant	Under investigation. Probable root cause could be, operating related whereby a tube experienced high temperatures resulting a tube to failed due to short term overheating.
20 February 2016	Platen SH outlet	FGP	Pendant	Drum water carry-over causing water wedging

Figure 2.17 Investigation report data of twin pass boiler patterns [16]

For the specific superheater covered in this study, the above-mentioned data revealed that most of the short term overheating events occurred at upper portion of the tube outlet. The locations for the failures are illustrated in Figure 2.18.

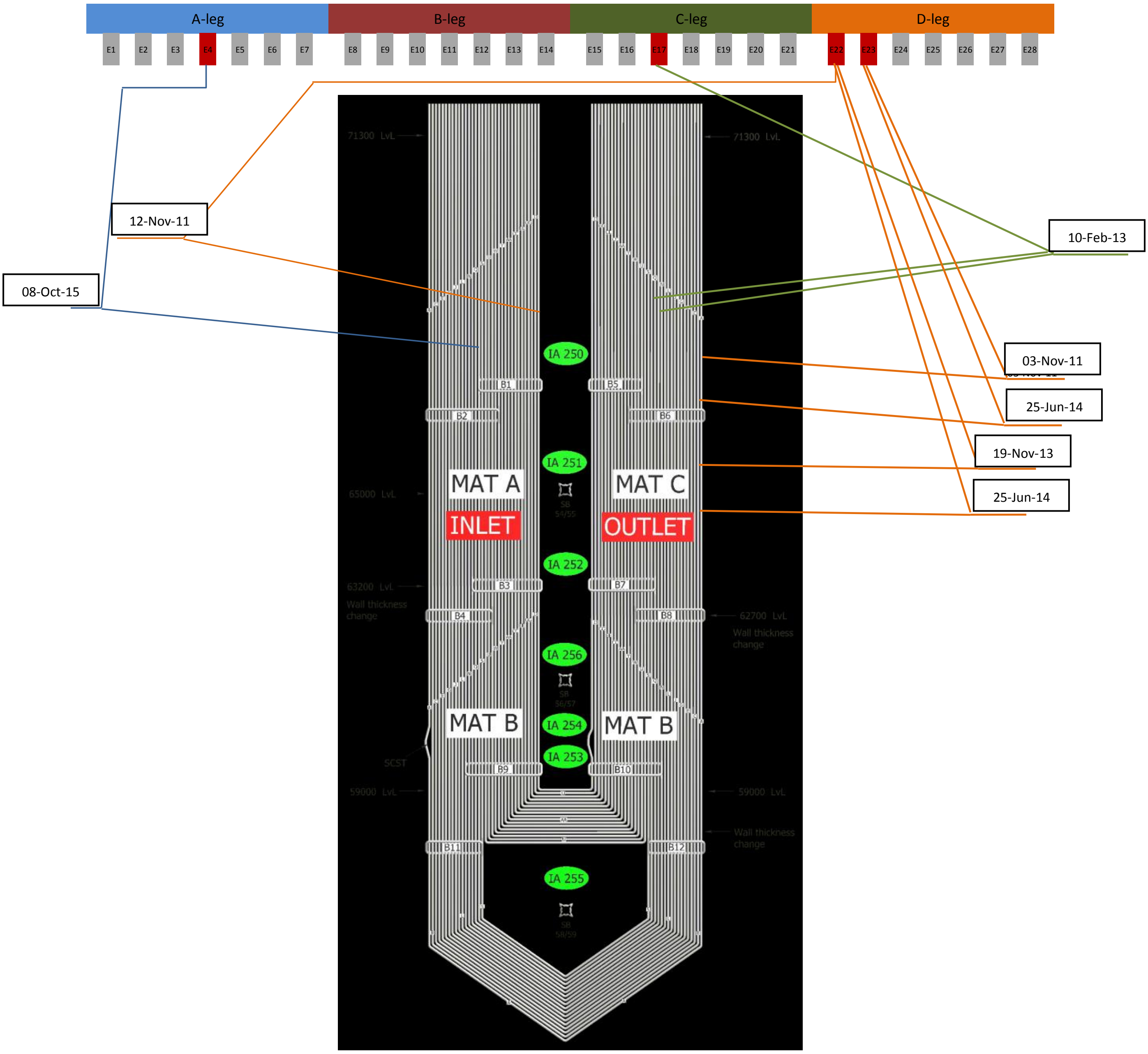

Figure 2.18 Failure locations for STO events on final superheater

The failures shown in the above figure can be associated with the events explained in Figure 2.17. The tube bundles of the superheater are divided into four sections, namely A-leg, B-leg, C-leg and D-leg. Each tube bundle is identical in geometry. Figure 2.18 illustrates which tube bundle experienced the burst, which tube in the bundle failed and at what position of the tube. Although it is not impossible for a short term overheating failure to occur at the inlet of the tube, Figure

2.18 clearly shows that the majority of the bursts occurred at the outlet. Thus, the focus of this study will be at the outlet of the tube.

Further investigating water-wedging events showed that the sling-type tubes of tower-type boilers (once-through boilers) were primarily affected, as shown in the data of Figure 2.19.

Date	Component failure	Pass	SH type	Root cause
25 August 2009	SH2	TTB	Sling	Poor Operating
28 December 2009	SH 2	TTB	Sling	Inadequate test and inspection plan
07 March 2010	SH3	TTB	Sling	Operations failure to notice that the check sheets for the panel and actual plant conditions did not correspond, resulting in MSSV 4 being closed during the unit light up.
20 March 2014	SH3	TTB	Sling	Unknown, suspected blockage that escapped when tube ruptured

Figure 2.19 Investigation report data of tower-type boiler patterns [16]

Operating procedures have been revised in the past to reduce the risk of a short term overheating occurrence by constantly monitoring saturation temperatures within the boiler and ensuring that steam temperatures remain above these saturation temperatures. The purpose of this solution is to prevent the condensation of steam within the boiler tubes, which could result in liquid collection causing water blockages [17]. Some of these occurrence investigations, however, show that even though the steam temperatures never dropped below saturation temperatures, STO still occurs (see the extract from one of Eskom's occurrence investigations in Figure 2.20). The root causes for these occurrences are then attributed to over-attemperation by plant operators [17].

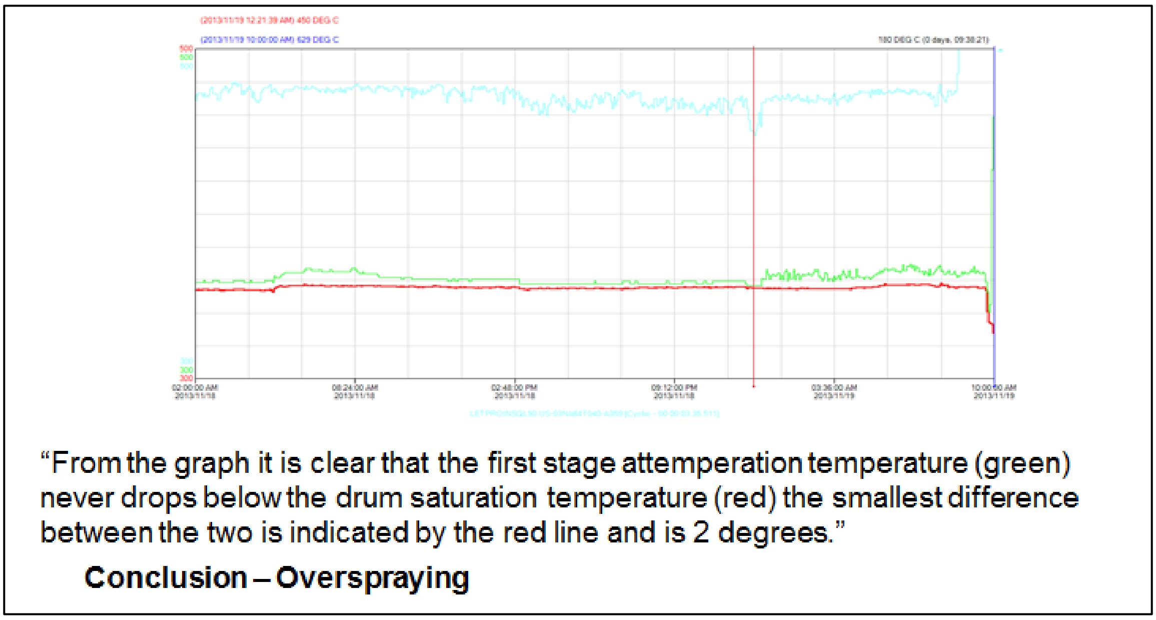

Figure 2.20 Extract from STO occurrence investigation of 2013 [17]

The question as to how a water blockage could occur, even though the temperatures in the superheater tubes are high enough to evaporate the water spray due to attemperation, remains unanswered. It is precisely this contradiction which this study aims to address.

2.7 Boiler tube material properties

According to the EPRI 2011 Technical Report (Volume 2: Water-Touched Tubes) [18], three classes of short term overheating exists, namely:

- Upper-critical short term overheating;
- Inter-critical short term overheating;
- Subcritical short term overheating.

These three classes can be identified by making use of the phase equilibrium diagram for iron-carbide as given in Figure 2.21 (a). From the diagram, it is explained that the degree to which short term overheating occurs is highly dependent on the temperature experienced by the tube material and resulting carbon formation.

Figure 2.21 (b) illustrates that upper-critical short term overheating occurs when the tube material exceeds the A3 temperature and austenitic formation takes place. Inter-critical short term overheating results when ferrite along with austenite forms prior to the tube failure and when temperatures are between the A1 and A3 temperatures. Finally, if the failure should occur when the tube material is just below the A1 temperature, subcritical short term overheating is likely to transpire. Table 2-4 gives a good explanation of the distinguishing features between the three classes of short term overheating.

Long term overheating will occur when the tube material is operated just above its normal allowable design temperature for longer periods of time.

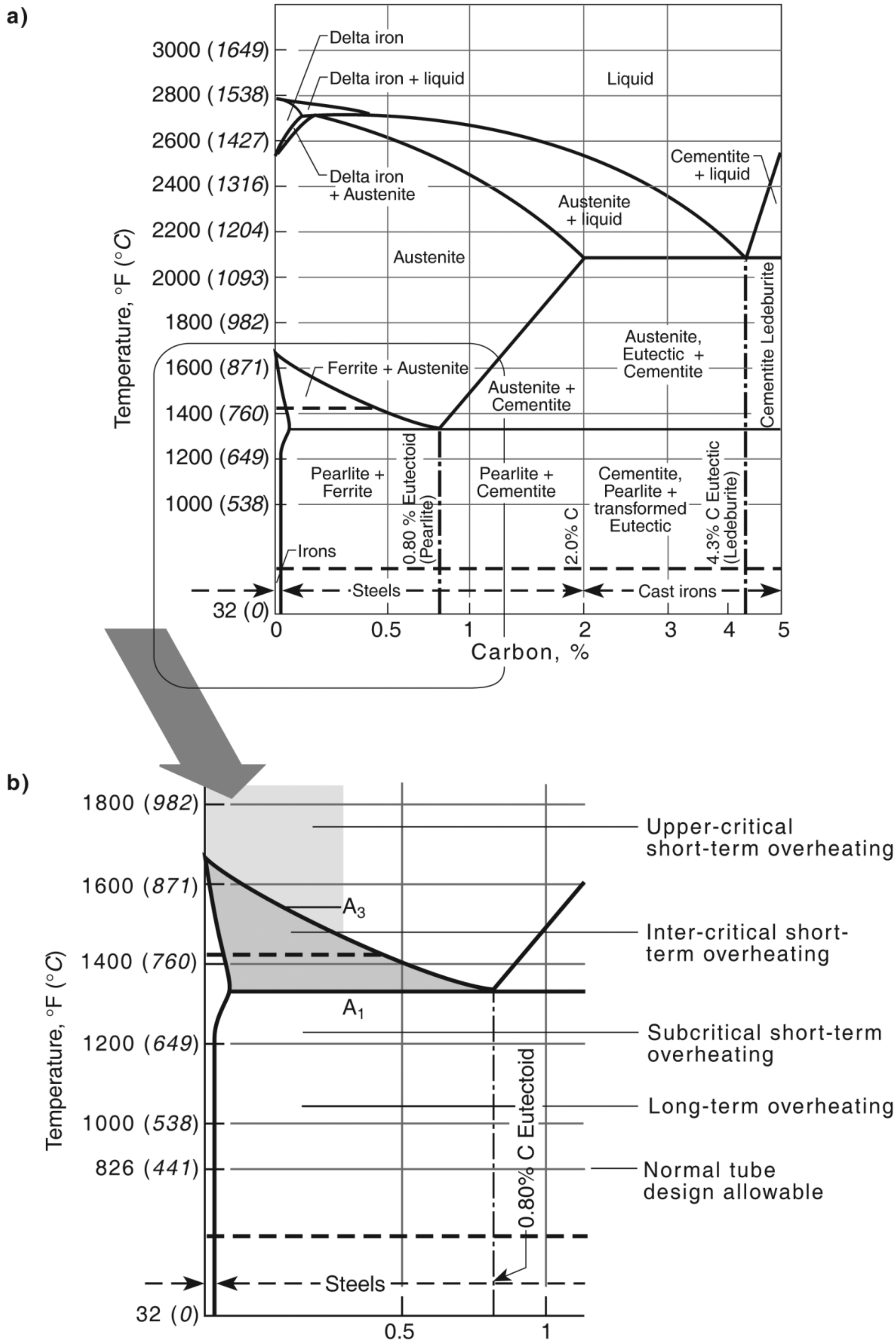

Figure 2.21 (a) Phase equilibrium diagram for iron-carbide. (b) Detail of equilibrium diagram, showing short term overheating and long term overheating regimes along with the normal tube design allowable. [18]

Table 2-4 Distinguishing Features of the Three Levels of Short Term Overheating [18]

Type of Overheating	Temperature Range	Fracture Surface	Extent of Tube Swelling	Fracture Mechanism	Microstructure (for ferritic tubing)	Hardness Characteristics
Subcritical short term overheating	> Design < Lower critical temperature, A_1	Thin-lipped, "fish-mouth"	Considerable	Transgranular void formation by power law creep.	Ferrite and spheroidized pearlite or bainite.	Near that of original hardness.
Intercritical short term overheating	Between the lower critical temperature, A_1 and the upper critical temperature, A_3	Thin-lipped, "fish-mouth"	Considerable	Transgranular or mixed inter- and transgranular void formation by power law creep.	Ferrite, transformational products (pearlite, bainite, and/or martensite). Some spheroidized pearlite or bainite may also be present.	Variable, with hardness near transformation products being above the original.
Upper critical short term overheating	Upper critical temperature, A_3	Thick-lipped, "fish-mouth"	Little	Inter- or transgranular creep fracture.	Near rupture, transformational products (pearlite, bainite, and/or martensite). Some ferrite may also be present.	Above original.

All of the above-mentioned failures occur due to the higher-than-design temperatures at which the tubes are operated. Depending on the extent of the abnormal operating conditions, the tube material's design life is significantly shortened. Table 2-5 provides a sample indication of the remaining lifetime assigned to the typical boiler tube material after high temperature operation. For the purposes of this project, which focuses on the sudden onset of short term overheating during a boiler start-up, a rupture time of ten minutes or less will be considered.

Table 2-5 Sample Minimum Rupture Times as a Function of Tube Temperature [18]

Temperature, °C (°F)	Minimum Time to Rupture at 55 MPa (8 ksi)
Design Allowable 441°C (826°)	288,000 hrs. (33 yrs.)
455°C (~850°F)	100,000 hrs. (11 yrs.)
510°C (~950°F)	1686 hrs. (70 days)
565°C (~1050°F)	49 hrs. (2 days)
620°C (~1150°F)	2 hrs.
675°C (~1250°F)	0.14 hrs (8.5 minutes)
Lower critical temperature 737°C (1358°F)	0.01 hrs. (36 seconds)
> 737°C (1358°F)	< 30 seconds

For SA-210 Grade A-1.

In a study conducted by Mertens et al. [19], the design impact of frequent natural-circulation boiler start-ups were investigated and the temperature gradients in terms of thermal stresses of critical components were analysed. Thermal stresses were determined using a general thermal stress calculation,

$$\sigma_{th} = \alpha_t \frac{\beta_{lin} E}{1 - \nu} \Delta T$$

where β_{lin} = linear expansion coefficient;

E = modulus of elasticity;

ν = Poisson's ratio (approximately 0.3 for steel);

ΔT = difference in outer wall temperature and inner wall temperature.

The variable α_t is a factor of stress concentration, which takes into account the connected piping's geometry and welding joint specifications and how these weaken the tube wall. This stress concentration was not relevant to this study, since the pipe studied had no discontinuities, and can thus be approached as having a value equal to 1. The modulus of elasticity is calculated at the average wall temperature.

The paper by Mertens do not cite the source of the equation, nor does it elaborate on the origin or fundamental assumptions used. Other sourced using this equation could not be found, nor is there any better/credible method described in the ASME Boiler and Pressure Vessel Code. To gain confidence in using this equation, it was compared with a Finite Element Method case study. This validation will be discussed in section 4.8.

2.8 Simulation and Analytical Software

To further study the subject of short term overheating, software packages can be utilised to simulate and analytically calculate various boiler scenarios, respectively.

In order to simulate events of short term overheating, a simulation software known as Flownex® was used. Flownex® is a thermal-fluid simulation package that can be used to design and optimize thermal fluid systems. Some of the applicable systems include air, water and steam networks and refrigeration cycles. The code provides the user with system elements such as piping, valves, heat exchangers, tanks and pumps. These elements can be connected to form complex fluid networks which represents the system to be analysed. The elements are specified by the user by inserting certain property values, sizing of the elements and indicating the boundary conditions of the network. Boundary condition properties may include pressure, temperature and/or mass flow rate. The fluid medium should also be specified.

Flownex® is based on fundamental principles – thermodynamics, fluid flow dynamics and heat exchange. It solves the set of one-dimensional conservation equations for mass, energy and momentum using an implicit pressure correction method. It is possible to represent a system with very detail and highly simplified elements, and solve during steady and transient conditions.

Mathcad is a tool used to compile analytical models using fundamental mathematics. It is essentially a mathematical word processor which performs live mathematics, and is used to develop and understand the fundamental principles underlying the process. Mathcad is used to verify the model implementation in Flownex, and in some cases gain confidence that the numerical tool and model produces valid answers. It is also used to develop boundary conditions or inputs needed in the Flownex model.

2.9 Summary

From the literature discussed in section 2.3, a pattern can be observed: It appears as if failures occurring in the higher heat boiler areas, such as the final superheater [8] and front gas water wall tubes [7], are more likely to experience short term overheating as a result of steam starvation. This phenomenon was verified to occur in the Eskom fleet by capturing data from investigations for short term overheating events due to water-wedging. The most common tubes to be affected were pendant-type and sling-type superheater tubes, i.e. no failures occur in horizontally oriented tubes.

At the rear gas pass, or lower heat regions, components like the primary superheater [10] and division wall superheater tubes [5] are more susceptible to short term overheating due to clinker formations on the tubes according to the study performed by Purbolaksono et al [10]

Focusing on the metallurgical aspect of the literature, it was shown that short term overheating can occur at several temperatures over various time periods. This study will focus on short term overheating occurring in no more than ten minutes' time, and the thermal stresses over the tube wall will be taken into consideration during stress calculations. The reason for choosing these short duration events, is because some failures are attributed to water wedging caused by operator over-attemperation. This is therefore an event which happens quickly in response to an operator action, and not due to prolonged overheating. It is questionable if over-attemperation can in fact cause steam starvation to the extent that STO will occur.

3. Theory

3.1 Introduction

This section discusses the applicable theory for the numerical modelling of fluid dynamics and heat transfer relevant to this project, as well as the appropriate load and thermal calculations.

For the purpose of this study, two scenarios will be considered, namely:

Scenario A. An unblocked tube – this scenario will be simulated and confirmed with analytical calculations to determine the boundary conditions of the superheater tube under low-load conditions. These conditions include the pressure drop over the superheater, which in turn defines the minimum height of a water column that cannot be pushed out of the U-tube pipe. It also defines the steam and pipe initial temperatures at the start of a blocking event. The analysis assumes a quasi-steady operation before the blockage.

Scenario B. A water-wedged (blocked) tube – various scenarios will be simulated for a blocked tube for a range of boiler load conditions. These are transient analyses, where the temperature evolution of the pipe wall is followed. Specific transient conditions are needed to simulate the heat up of the water column, as well as the rate of evaporation, which would have to be replenished by attemperation spray in order for the water column to remain for at least 10 minutes.

3.2 Scenario A: Unblocked tube

3.2.1 Pressure drop through tube

In order to determine the pressure drop through the boiler tube, the geometric structure of the tube must be taken into consideration. For the case study selected, the superheater leg is made up of three sections as shown in Figure 3.1. The inlet section (section A) is the tube consisting of the thinnest tube wall. When section A intersects with section B, the tube wall thickness is increased. The same concept is applied between section B and section C. The length for each section also differs.

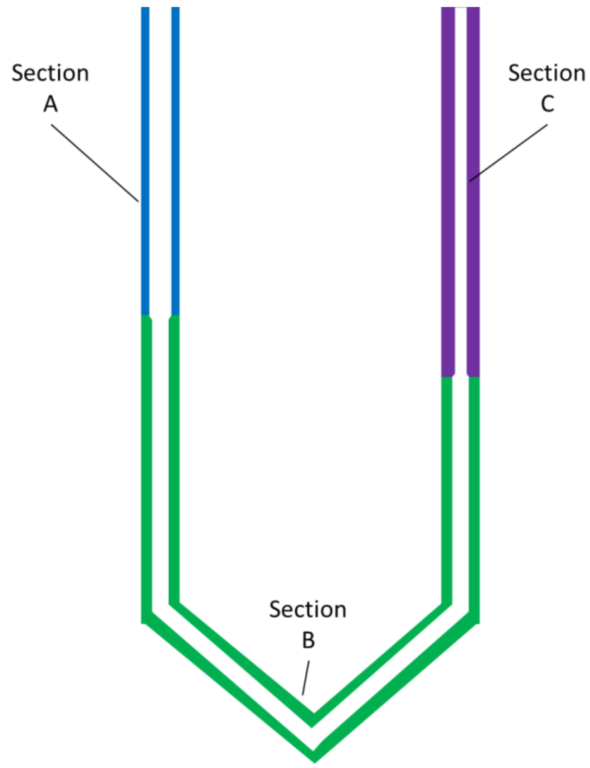

Figure 3.1 Boiler tube sections

For each section of tubing described in Figure 3.1, the Reynolds number can be calculated as

$$Re = \frac{\rho_f \, v_f \, D_i}{\mu_f} \tag{3-1}$$

or else

$$Re = \frac{4\dot{m}_f}{\pi D_i \mu_f} \tag{3-2}$$

where D_i is the inner diameter;

$\dot{m}_f$ is the mass flow rate of the fluid within the tube;

A is the cross-sectional area of the tube, which differs for each tube section;

ρ_f is the fluid density;

v_f is the fluid velocity;

μ_f is the dynamic viscosity.

Note that the fluid properties are approximated as staying constant throughout the tube element. The assumption is reasonably valid for highly superheated steam. This assumption is not valid in Scenario B where water is gradually heated from saturated steam, hence the pipe will be discretised into small sections to track the fluid property change for Scenario B.

In the same way, the frictional factor can be determined through each tube section. The frictional factor is calculated using the Swamee-Jain equation [20]:

$$f = 0.25\left[log\left(0.27\frac{\varepsilon}{D_H} + \frac{5.74}{Re^{0.9}}\right)\right]^{-2} \tag{3-3}$$

This equation is only valid for $5000 < Re < 10^8$ (which implies that the flow is turbulent) and $10^{-6} \leq \frac{\varepsilon}{D_H} \leq 10^{-2}$, where

ε is the tube roughness;

D_H is the hydraulic diameter;

Re is the Reynolds number of the gas flow.

The typical roughness value for boiler tubes is approximately 60 µm.

If the Reynolds number of the gas flow should be lower than 5000, the friction factor can be calculated as in eq. (3-4) which is used for laminar flow.

$$f = \frac{64}{Re} \tag{3-4}$$

In the unlikely event that the Reynolds number is larger than 10^8 the friction factor will be limited to that at $Re = 10^8$.

The pressure drop for each section is then calculated as

$$\Delta p = \left(\frac{fL}{D_i} + \sum K\right)\frac{\rho_f\, {v_f}^2}{2} \tag{3-5}$$

where L is the length of the tube section;

D_i is the internal tube diameter;

$\sum K$ is the sum of the secondary frictional losses through the tube section.

Secondary frictional losses occur due to tube bends, entrances and exits, as well as an increase or decrease of the tube wall. These losses may also occur where valves are present, which is not applicable to this project.

The loss coefficient associated with each tube bend is dependent on its angle as well as the sharpness. Figure 3.2 gives a good indication of the coefficient values associated for each loss.

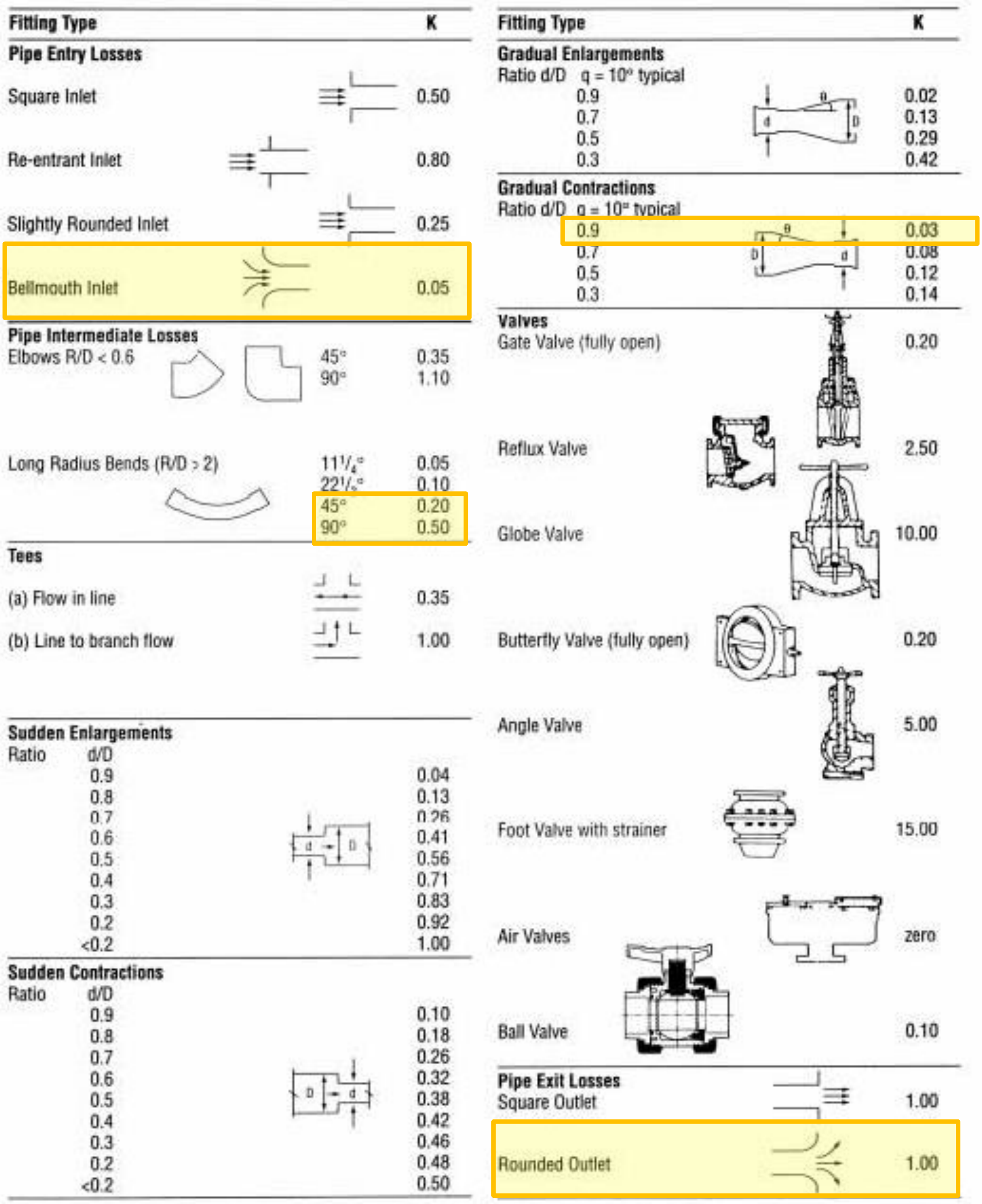

Fitting Type		K
Pipe Entry Losses		
Square Inlet		0.50
Re-entrant Inlet		0.80
Slightly Rounded Inlet		0.25
Bellmouth Inlet		0.05
Pipe Intermediate Losses		
Elbows R/D < 0.6	45°	0.35
	90°	1.10
Long Radius Bends (R/D > 2)	11¼°	0.05
	22½°	0.10
	45°	0.20
	90°	0.50
Tees		
(a) Flow in line		0.35
(b) Line to branch flow		1.00
Sudden Enlargements		
Ratio	d/D	
	0.9	0.04
	0.8	0.13
	0.7	0.26
	0.6	0.41
	0.5	0.56
	0.4	0.71
	0.3	0.83
	0.2	0.92
	<0.2	1.00
Sudden Contractions		
Ratio	d/D	
	0.9	0.10
	0.8	0.18
	0.7	0.26
	0.6	0.32
	0.5	0.38
	0.4	0.42
	0.3	0.46
	0.2	0.48
	<0.2	0.50

Fitting Type		K
Gradual Enlargements		
Ratio d/D q = 10° typical		
	0.9	0.02
	0.7	0.13
	0.5	0.29
	0.3	0.42
Gradual Contractions		
Ratio d/D q = 10° typical		
	0.9	0.03
	0.7	0.08
	0.5	0.12
	0.3	0.14
Valves		
Gate Valve (fully open)		0.20
Reflux Valve		2.50
Globe Valve		10.00
Butterfly Valve (fully open)		0.20
Angle Valve		5.00
Foot Valve with strainer		15.00
Air Valves		zero
Ball Valve		0.10
Pipe Exit Losses		
Square Outlet		1.00
Rounded Outlet		1.00

Figure 3.2 Secondary frictional loss coefficients [21]

Referring back to Figure 3.1 and making use of some interpolation calculations, the secondary frictional losses for each section can be calculated as follow:

<u>Section A</u>

- Bellmouth inlet → 0.5
- Gradual contraction ratio ${D_{iA}}/{D_{iB}} \approx 0.9$ → 0.03

<u>Section B</u>

- Long radius 55^o bend → 0.267 (interpolated)
- Long radius 70^o bend → 0.367 (interpolated)
- Long radius 55^o bend → 0.267 (interpolated)
- Gradual contraction ratio ${D_{iB}}/{D_{iC}} \approx 0.9$ → 0.03

<u>Section C</u>

- Rounded outlet → 1

The total pressure drop through the entire tube will then be the sum of the pressure drops through each tube section.

3.2.2 Energy balance

Consider the diagram illustrated in Figure 3.3 representing a control volume of a single boiler tube. The tube receives an amount of steam from the preceding superheaters as well as a spray of attemperating water. This will mix together and gets heated by the flue gas passing on the outside of the tube before exiting into the outlet header.

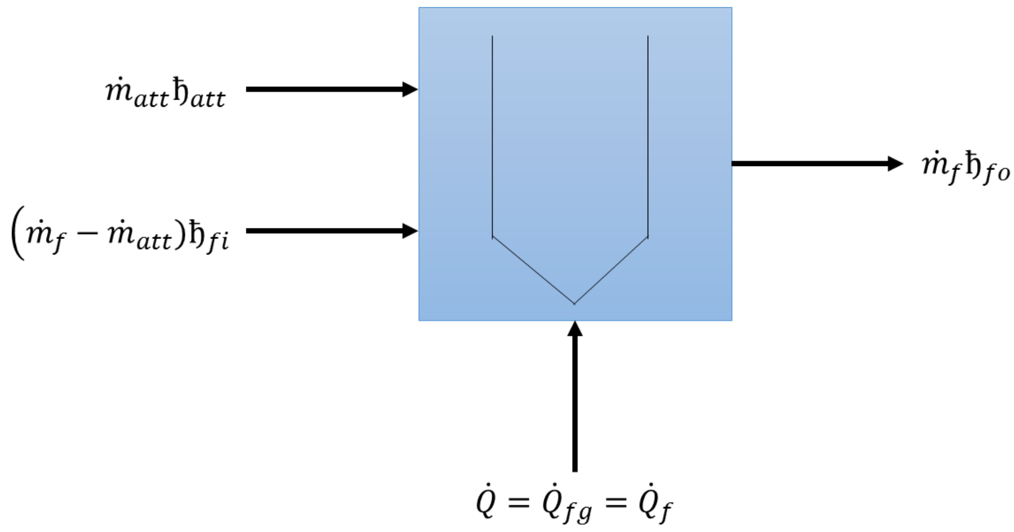

Figure 3.3 Element diagram representing energy and mass balance

In Figure 3.3 $\dot{m}_f$ is the mass flow rate of the final steam;

$\dot{m}_{att}$ is the attemperating spray which is known according to the boiler load;

$\dot{m}_f - \dot{m}_{att}$ is the calculated mass flow rate of the inlet steam, assuming a uniform distribution of the total mass flow rate into each tube;

$\hbar_{fi}$ is the enthalpy for the inlet steam;

$\hbar_{att}$ is the enthalpy for the attemperating spray;

$\hbar_{fo}$ is the enthalpy for the outlet steam;

The enthalpies are functions of the pressures and temperatures under the specific operating condition of each stream. Normally only the steam at the exit of the pipe is known, as well as the attemperation mass flow.

From the energy balance, one can determine the heat transfer to the tube as

$$\dot{Q}_f = \dot{m}_f \hbar_{fo} - (m_f - \dot{m}_{att})\hbar_{fi} - \dot{m}_{att}\hbar_{att} \qquad (3\text{-}6)$$

3.2.3 Heat transfer

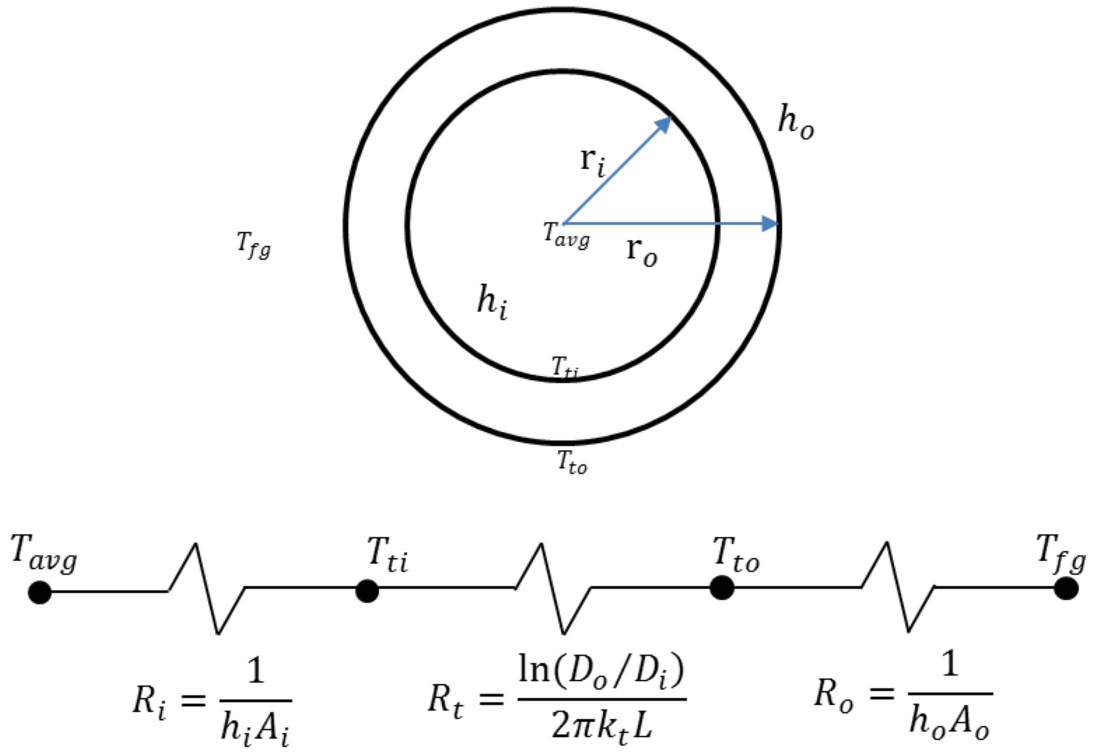

Figure 3.4 Heat transfer resistances through tube

Considering the diagram of Figure 3.4 and using Fourier's Law, the total conductive heat transfer through the tube wall can be calculated as

$$\dot{Q}_f = \frac{T_{to} - T_{avg}}{R_i + R_t} \quad \text{(3-7)}$$

where T_{to} is the temperature on the outer surface of the tube;

T_{avg} is the average steam temperature in the tube;

R_i is the thermal resistance due the inner convection and is calculated as

$$R_i = \frac{1}{h_i A_i} \quad \text{(3-8)}$$

with A_i the inner tube area;

h_i the inner convection heat transfer coefficient.

The variable R_t is the thermal resistance through the tube material due to its wall thickness and can be calculated as

$$R_t = \frac{\ln\left(D_o/D_i\right)}{2\pi k_t L} \tag{3-9}$$

where L is the tube length;

k_t is the thermal conductivity of the tube material;

D_o and D_i represents the outer and inner diameters of the tube, respectively.

The heat transfer coefficient on the inside of the tube is calculated as

$$h_i = \frac{Nu \cdot k_f}{D_i} \tag{3-10}$$

where the Nusselt number will be $Nu = 3.66$ if the steam flow in the tube is laminar and $Nu = 0.023Re^{4/5}Pr^n$ if the flow is turbulent [22].

Furthermore, k_f is the thermal conductivity of the steam;

Pr is the Prandtl number of the steam;

$n = 0.4$, since the steam is being heated [22].

The tube inner area is calculated as

$$A_i = \sum \pi D_i L \tag{3-11}$$

The total resistance of the system can also be calculated as

$$R_{tot} = \frac{T_{fg} - T_{avg}}{\dot{Q}_f} \tag{3-12}$$

It is then possible to the find the value of the outer resistance

$$R_o = R_{tot} - R_i - R_t \tag{3-13}$$

Next, the heat transfer coefficient on the flue gas side can be determined as

$$h_o = \frac{1}{R_o A_o} \tag{3-14}$$

In this study, the reference tube is assumed to be exposed to cross-flow heat transfer. This assumption will be explained in more detail in section 4.4. The convective heat transfer coefficient associated with a boiler tube as part of a boiler tube bundle is determined by its position within that bundle. The tube specific to this study is the first tube exposed to convective heat transfer from the flue gas. For cross-flow scenarios, the convection coefficient for a tube in the first row of the tube bundle is approximately equal to that for a single tube in cross-flow, whereas larger heat transfer coefficients are associated with tubes of the inner rows.

Thus, the convective heat transfer coefficient for cross-flow over a tube bundle can be determined as

$$h_{con} = \frac{Nu \cdot k_f}{D_H} \qquad (3\text{-}15)$$

For cross flow over a single tube, the following Nusselt number correlations (known as Churchill & Bernstein [22]) are applicable:

For $Re < 10\,000$

$$Nu = 0.3 + \frac{0.62 \cdot Re^{1/2} \cdot Pr^{1/3}}{\left[1 + \left(\frac{0.4}{Pr}\right)^{2/3}\right]^{1/4}} \qquad (3\text{-}16)$$

For $10\,000 < Re < 400\,000$

$$Nu = 0.3 + \frac{0.62 \cdot Re^{1/2} \cdot Pr^{1/3}}{\left[1 + \left(\frac{0.4}{Pr}\right)^{2/3}\right]^{1/4}} \cdot \left[1 + \left(\frac{Re}{282\,000}\right)^{1/2}\right] \qquad (3\text{-}17)$$

For $Re > 400\,000$

$$Nu = 0.3 + \frac{0.62 \cdot Re^{1/2} \cdot Pr^{1/3}}{\left[1 + \left(\frac{0.4}{Pr}\right)^{2/3}\right]^{1/4}} \cdot \left[1 + \left(\frac{Re}{282\,000}\right)^{5/8}\right]^{4/5} \qquad (3\text{-}18)$$

So, for a transient study conducted over the short period of ten minutes, the value of h_o is assumed to remain unchanged. This is due to the fact that the flue gas velocity used to calculate the Reynolds number in eq. (3-1) stays constant during this time period. The Reynolds number calculated is then used to determine the appropriate Nusselt number, which in turn is used to calculate h_o.

Due to the high gas temperatures, radiation also takes place between the flue gas and the boiler tubes. The heat transfer coefficient for radiation in the convective pass of a boiler can be determined as a functional equation:

$$h_{rad} = \varepsilon_{rad}\sigma\left(T_{fg}^2 + T_t^2\right)\left(T_{fg} + T_t\right) \quad (3\text{-}19)$$

where ε_{rad} is the relevant emissivity factor;

σ is the Stefan-Boltzmann constant;

T_{fg} is the temperature of the flue gas;

T_t is the temperature of the surface of the tube wall.

As explained in a study by Rossouw [23], the contribution of radiation could be accounted for by calculating a heat transfer coefficient for radiation similar to the convective coefficient. If this radiative coefficient should be added to the convective coefficient, the result would be the total heat transfer coefficient of the external fluid over the tube. In this case, the coefficient for the flue gas over the boiler tube. It can thus be assumed that

$$h_o = h_{con} + h_{rad} \quad (3\text{-}20)$$

It is then concluded that the value for h_o as calculated eq. (3-14) considers both the convection and radiation heat transfer emitted from the furnace. Also, since the radiative coefficient (h_{rad}) is a function of the flue gas temperature, which remains constant during the transient, it can be assumed that the heat transfer coefficient of the flue gas over the boiler tube remains constant for a specific boiler load.

In other words, the value for h_o changes subject to the boiler load, but is unaffected by the possibility of a water blockage in a tube during the transient. Thus, the value calculated from eq. (3-14) can also be applied if a blockage should occur.

3.3 Scenario B: blocked tube

3.3.1 Heat transfer

Water from the attemperation spray enters the tube at saturated conditions. If heating of the tube is not sufficient to evaporate the water and be carried through the tube with the superheated steam, a water column can temporarily form in the outlet leg of the tube. If the pressure difference over the tube inlet and outlet is not large enough to force the plug of water out through the tube, and excessive spray water is continually introduced, then it is possible for a still-standing column of water to plug the tube. It should also be noted that, in a transient simulation, the water need not be in thermal equilibrium with the surrounding steam, i.e. it is possible to have liquid in a system which operates at temperatures above the saturation temperature.

Should the tube now be plugged with saturated water, the heat transfer to the water plug will be

$$\dot{Q}_p = \frac{T_{fg} - T_{sat}}{R_o + R_t} \tag{3-21}$$

The temperature of the saturated water is represented by T_{sat}, and it is assumed that the thermal resistance between the pipe and average water temperature is insignificant. Note that the length L used to calculate R_o and R_i is now only the length of the water column, and not the total pipe length. Given that the transient is reasonably short (10 minutes as chosen for this study), one may assume that the outer heat transfer coefficient h_o (calculated in eq. (3-14)) remains unchanged, as was argued previously.

From the above, the mass flow rate of evaporation can be determined. This is the rate at which the water evaporates from the water column. The evaporation rate is calculated as

$$\dot{m}_e = \frac{\dot{Q}_p}{\hbar_{fg}} \tag{3-22}$$

The variable $\hbar_{fg}$ represents the difference between the enthalpies for saturated steam and saturated water at the pressure inside the boiler tube element.

As long as the spraywater mass flow rate is equal or more than this calculated amount, the water column will remain. A lower spraywater flow will result in a drop in the column height, which would then be pushed out by the prevailing pressure difference between the inlet and outlet header. On the other hand, a higher mass flow rate will increase the water column height, thus reducing the length of “starved” tube.

The mass flow of evaporated steam will flow along the pipe towards the outlet, and this would be the only “cooling” flow to protect the pipe from overheating. A lower mass flow (lower evaporation rate), could thus result in a larger temperature excursion of the outlet tube, where the top-most part would be the hottest (assuming uniform fluegas heating all along the length).

While the water column remains, the spray water entering the tube will result in an improved cooling on the inlet side, because of the much colder conditions of the water compared to the tube wall conditions before the event.

The most extreme case is therefore when the water column is at a minimal height, and remains there for the full 10 min duration.

3.3.2 Water column length and evaporation

For this study, a single tube from an actual Eskom power plant was selected to simulate a short term overheating event. The tube selection was based on the data collected and analysed in section 2.6 of this dissertation. Since it was concluded that short term overheating most commonly occurs in pendant-type superheaters at the outlet, a single final superheater tube was chosen. This specific tube is situated in the front gas pass of the boiler and is the longest (most outer) tube of the superheater bundle. The selection was made to cater for a “worst-case” scenario. The longer the tube, the more cause there will be for short term overheating. This is because there is a greater area of tubing that will be exposed to high temperature if cooling through the tube should decrease. The small amount of evaporation steam will also heat up more the longer the tube would be. Thus, it can be concluded that if the type of short term overheating studied cannot occur in this chosen tube geometry, it is unlikely to occur in the shorter tubes. The selected tube is also comparable to tubes of other Eskom boilers, making this study applicable to other stations in terms of methodology and conclusions.

As was argued before, the most severe case exists with the shortest water column. This would be when the water column starts at the lowest part of the superheater tube. If the water column should start at any point on the left side of the tube, the level at the right side will increase by the same height so that the hydraulic pressure between the levels remains the same as the pressure difference over the headers.

The illustration in Figure 3.5 shows the actual measurements of the reference tube used throughout this project, as well as the probable water column.

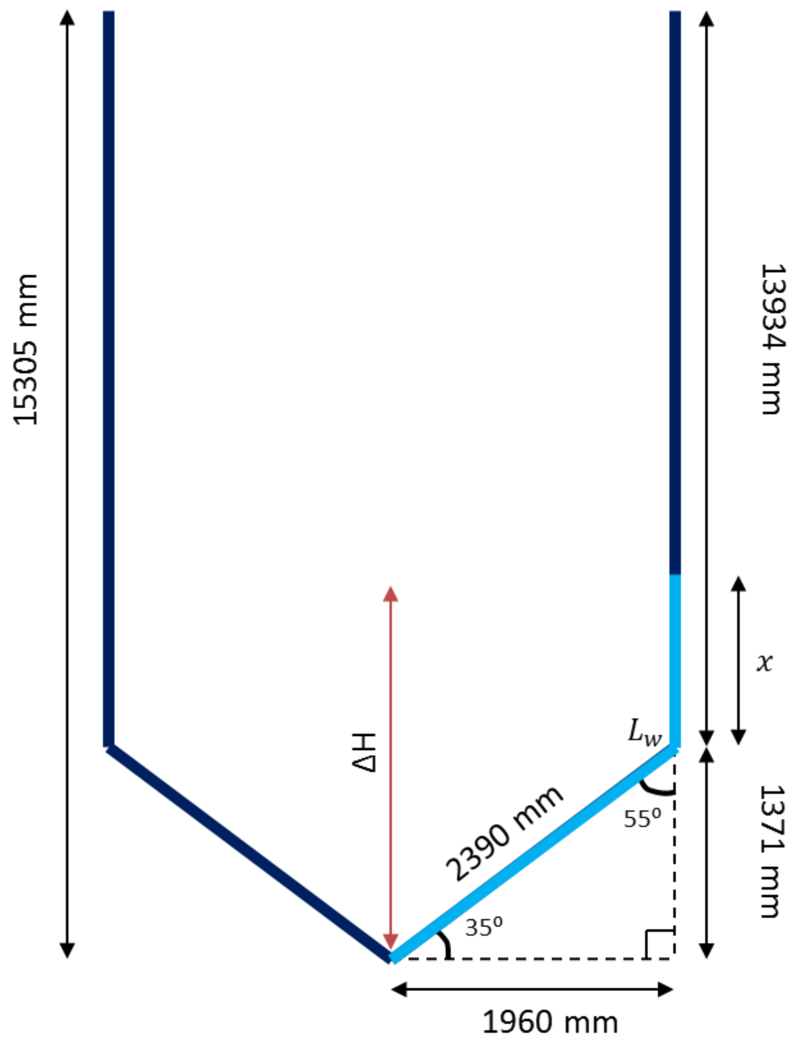

Figure 3.5 Boiler tube element measurements, $\Delta H > 1371\ mm$

The total height of the tube is H_t = 15305 mm. The diagonal piece of tubing is identified as 2390 mm and its associated vertical height is 1371 mm. The total vertical height of the water column is given as ΔH. The value ΔH is the longest possible water column that will form under specific boiler load conditions. Thus, this value will vary for each scenario. In order to determine the total length of the water column lying in the tube, simple geometric calculations can be used.

If the total water column height (ΔH) is more than 1371 mm (as shown in Figure 3.5), then the total length of the water column lying within the tube will be calculated as

$$L_w = 2390 + x \tag{3-23}$$

$$L_w = 2390 + \Delta\mathrm{H} - 1371 \tag{3-24}$$

$$L_w = \Delta H + 1019 \tag{3-25}$$

However, if the column height (ΔH) is less than 1371 mm (see Figure 3.6), the total length of the water column is determined as

$$L_w = \frac{\Delta H}{sin35°} \tag{3-26}$$

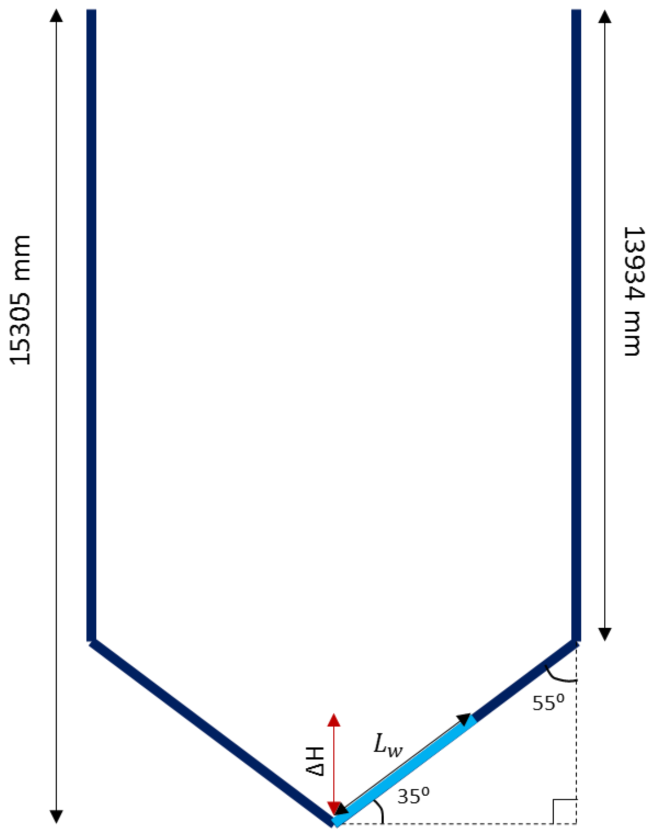

Figure 3.6 Boiler tube element measurements, $\Delta H < 1371\ mm$

The water column height itself is calculated as

$$\Delta H = \frac{\Delta p}{(\rho_w - \rho_{st})g} \tag{3-27}$$

where Δp is the pressure difference between the inlet and outlet of the tube;

ρ_w is the density of the spraywater creating the water column;

ρ_{st} is the density of steam at the tube outlet;

g is the gravitational constant.

If a water column should exist, the exposed tube length above the water column is determined as

$$H_{st} = H_t - \Delta H \tag{3-28}$$

Also, since the length of the water column can be calculated, the volume of water can be determined, which, in turn, can provide the mass of water (m_w). The time required for the water column to heat up from original attemperation spray conditions to saturated steam conditions (in order to begin evaporating) is calculated as

$$t_e = \frac{m_w(\hbar_l - \hbar_{att})}{\dot{Q}_p} \tag{3-29}$$

Here, $\hbar_l$ is the enthalpy of the fluid in the superheater tube at saturated liquid conditions.

The aim of these calculations is to simulate a still-standing water column in a single superheater tube and then to determine if the rate of evaporation is enough to cool the tube to prevent short term overheating from occurring. The purpose of the time calculated here is to gradually increase the rate of evaporation, in order to emulate the delay caused by the heat-up process. The time is used in the transient model as discussed in section 4.4.

3.4 Thick-walled cylinder stress calculations[1]

Thick wall cylinder calculations are used to determine the axial (σ_a), circumferential (σ_c) and radial stresses (σ_r) exercised upon a vessel (see Figure 3.7). These thick wall cylinder stress calculations apply when the ratio of $\frac{r_m}{t}$ has a value smaller than 10, where r_m is the mean radius of the vessel and t is the wall thickness, that is the inner radius (r_i) subtracted from the outer radius (r_o). The ratio for the tube at the outlet segment used for this specific project has a value of 1.523.

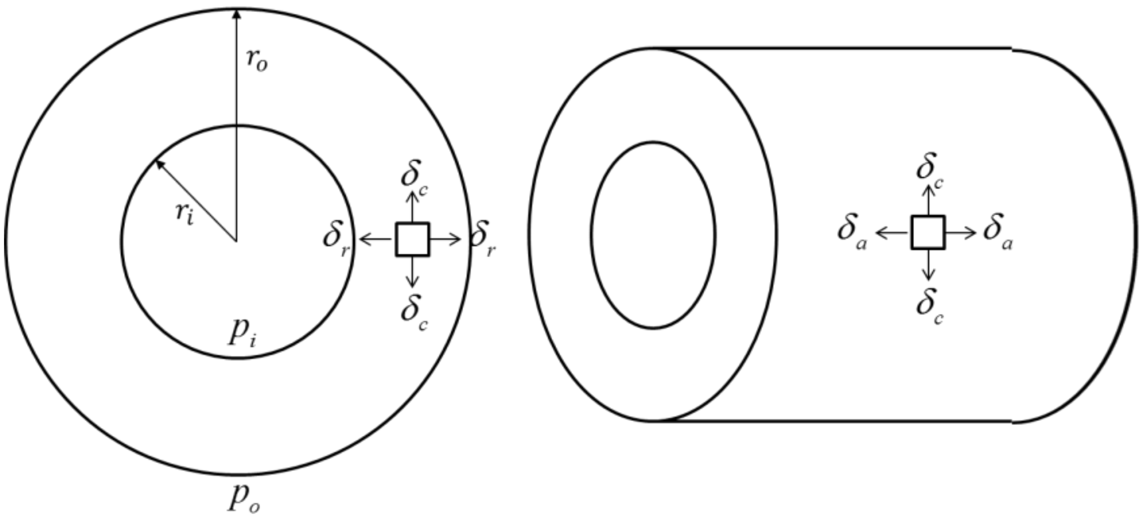

Figure 3.7 Thick wall cylinder stress illustration

The equations associated with thick wall vessels are as follow:

[1] Information in this section is sourced from Hibbeler [30] and Zhu [31].

The stresses in the axial direction are calculated as

$$\sigma_a = \frac{p_1 r_i^2 - p_2 r_o^2}{r_o^2 - r_i^2} \tag{3-30}$$

where p_1 is the pressure exerted on the inside of the tube;

p_2 is the pressure exerted upon the outside of the tube.

These stresses ignore the axial load exerted by the tube mass being suspended from the roof of the boiler.

The stresses exercised around the circumference of the tube are called circumferential or hoop stresses and are calculated as

$$\sigma_c = \frac{p_1 r_i^2 - p_2 r_o^2}{r_o^2 - r_i^2} - r_i^2 r_o^2 \frac{p_2 - p_1}{r_i^2 \left(r_o^2 - r_i^2\right)} \tag{3-31}$$

A tube may also experience stresses in its radial direction at the inside and the outside of the tube. The inner and outer radial stress calculations are given below respectively.

$$\sigma_{ri} = \frac{p_1 r_i^2 - p_2 r_o^2}{r_o^2 - r_i^2} + r_i^2 r_o^2 \frac{p_2 - p_1}{r_i^2 \left(r_o^2 - r_i^2\right)} \tag{3-32}$$

$$\sigma_{ro} = \frac{p_1 r_i^2 - p_2 r_o^2}{r_o^2 - r_i^2} + r_i^2 r_o^2 \frac{p_2 - p_1}{r_o^2 \left(r_o^2 - r_i^2\right)} \tag{3-33}$$

One would simply use the larger of the two in further stress combination calculations as σ_r.

Additionally, due to the high temperature gradients experienced by the tube, circumferential thermal stresses should also be taken into consideration. Taking into consideration the study conducted by Mertens et al [19], as discussed in section 2.7 of this document, together with its formulation for the calculation of thermal stress, the circumferential thermal stress for the application of this project can be determined by

$$\sigma_{th} = \frac{\beta_{lin} E}{1 - \nu} \Delta T \tag{3-34}$$

The stress concentration factor as mentioned in the study is assumed to have a value equal to one, based upon the MacGregor and Crossman study [24].

The final hoop stress can now be calculated as

$$\sigma_h = \sigma_c + \sigma_{th} \tag{3-35}$$

The Von Mises yield criterion can now be used to combine the stresses as follows:

Say that

$$\sigma_x = \sigma_a \tag{3-36}$$

$$\sigma_y = \sigma_h \tag{3-37}$$

$$\sigma_z = \sigma_r \tag{3-38}$$

The stresses determined in order to calculate the final combined stress are

$$\sigma_1 = \max(\sigma_x, \sigma_y, \sigma_z) \tag{3-39}$$

$$\sigma_2 = A - \sigma_y - \sigma_z \tag{3-40}$$

where

$$A = \sigma_x + \sigma_y + \sigma_z \tag{3-41}$$

$$\sigma_3 = \min(\sigma_x, \sigma_y, \sigma_z) \tag{3-42}$$

The final Von Mises combined stress is then calculated as

$$\sigma_{vm} = \sqrt{\frac{(\sigma_1 - \sigma_2)^2 + (\sigma_2 - \sigma_3)^2 + (\sigma_3 - \sigma_1)^2}{2}} \tag{3-43}$$

This will be used as failure criteria relative to the material's yield strength at actual temperatures during the transient.

4. Methodology

4.1 Introduction

The following section aims to explain the methods utilized to determine if a water column existing in a boiler tube alone can be the cause of short term overheating.

This section discusses the boiler design of the specific Eskom power station as selected for this project and the numerical models to be used for comparison to actual plant data. The Flownex® setup is explained, followed by verification of the model. Finally, the stress calculations done in Mathcad are discussed.

4.2 Boiler design

In section 2.2 of the literature review in this document, the component layout within a twin-pass boiler was briefly discussed. The HP steam is transported through the boiler by means of three superheaters, where attemperation takes place between each of these components. For the specific purposes of this project, the final superheater's design will briefly be explained.

The third and final superheater is located in the front gas pass after the platen superheater. The final superheater is a hanging (pendant) boiler component consisting of 28 elements, of which each element is made up of 34 tubes in a U-shape. Element tubes are stacked next to one another via a common inlet and outlet header, respectively. The material used to construct these tubes is specified as 10CrMo910 and is simply referred to as grade 22 steel.

For the purpose of this study, the longest (outer-most) tube element from the final superheater tube bundle was chosen to be modelled. As briefly discussed in section 3.3.2, the geometry for the tube model was chosen for the following reasons:

- The geometry specified is from the actual superheater tube on an Eskom power plant, and is thus a practical approach to establishing of short term overheating is possible on such a tube;
- The geometry is comparable with those found in other Eskom boilers;
- As shown in Figure 2.18 earlier in this document, this specific tube has undergone multiple failures due to short term overheating in the past;

- The longer the tube, the greater the chance is for short term overheating to occur, since the outlet leg has a longer section exposed to the heat of the furnace as the water-wedge evaporates.

Each element is made up of three sections, namely the inlet section, the intermediate section and the outlet section. The inlet section is connected to the inlet header which receives the steam from the platen superheaters. The first part of the inlet section is inside a dead space, referring to the tube areas located in the boiler roof which receives minimal exposure to the heat emitted from the furnace. These tubes have a length of 339 mm with an outer diameter (OD) of 44.5 mm and wall thickness 6.3 mm. Following are the inlet tubes with a length of 7761 mm which are exposed to the flue gas. Some tubes are an exception to this tube length, as some of them are extended in order to wrap around some of the other tubes for alignment purposes. This is also true for the outlet section.

The outlet section feeds to the outlet header. This segment also includes an outlet dead space of tube length 339 mm, OD of 44.5 mm and wall thickness of 11 mm. The exposed outlet section length is 8261 mm, with the exception of wrap-around tubes.

The intermediate section is where the bends are located, connecting the inlet and outlet sections. This segment also contains wrap-around tubes and each tube differs in length with an OD of 44.5 mm and a wall thickness of 8.8 mm. The total length of the intermediate section is 16626 mm.

Notice how, at each section, the inner diameter (ID) decreases. This was so designed in order to increase the wall thickness of the tube as the steam flows through the component, thus protecting the material as the heat increases through the component. An illustration of the entire final superheater (created in Solidworks®) is shown in Figure 4.1 and Figure 4.2.

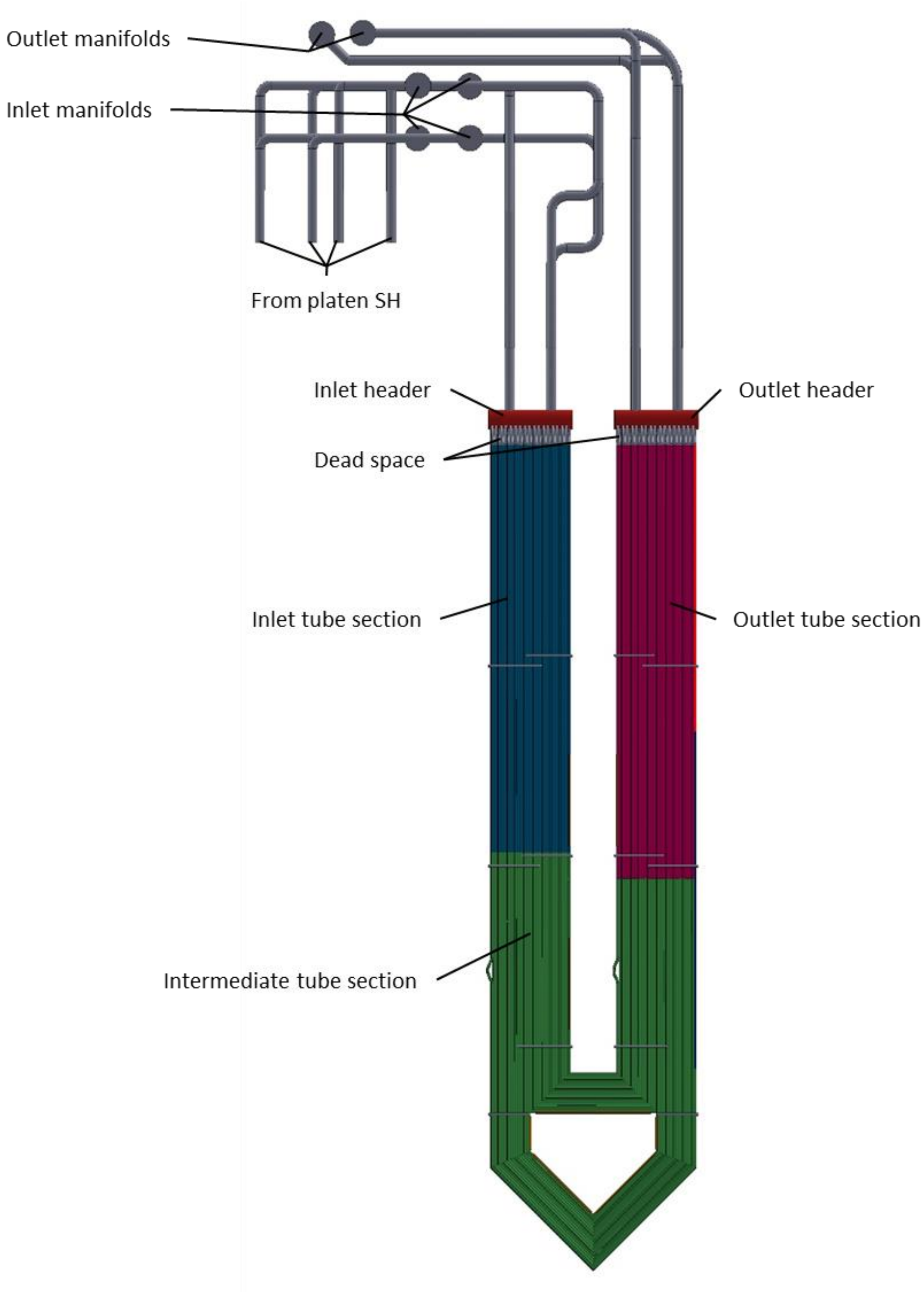

Figure 4.1 Front view of final superheater tube bundle

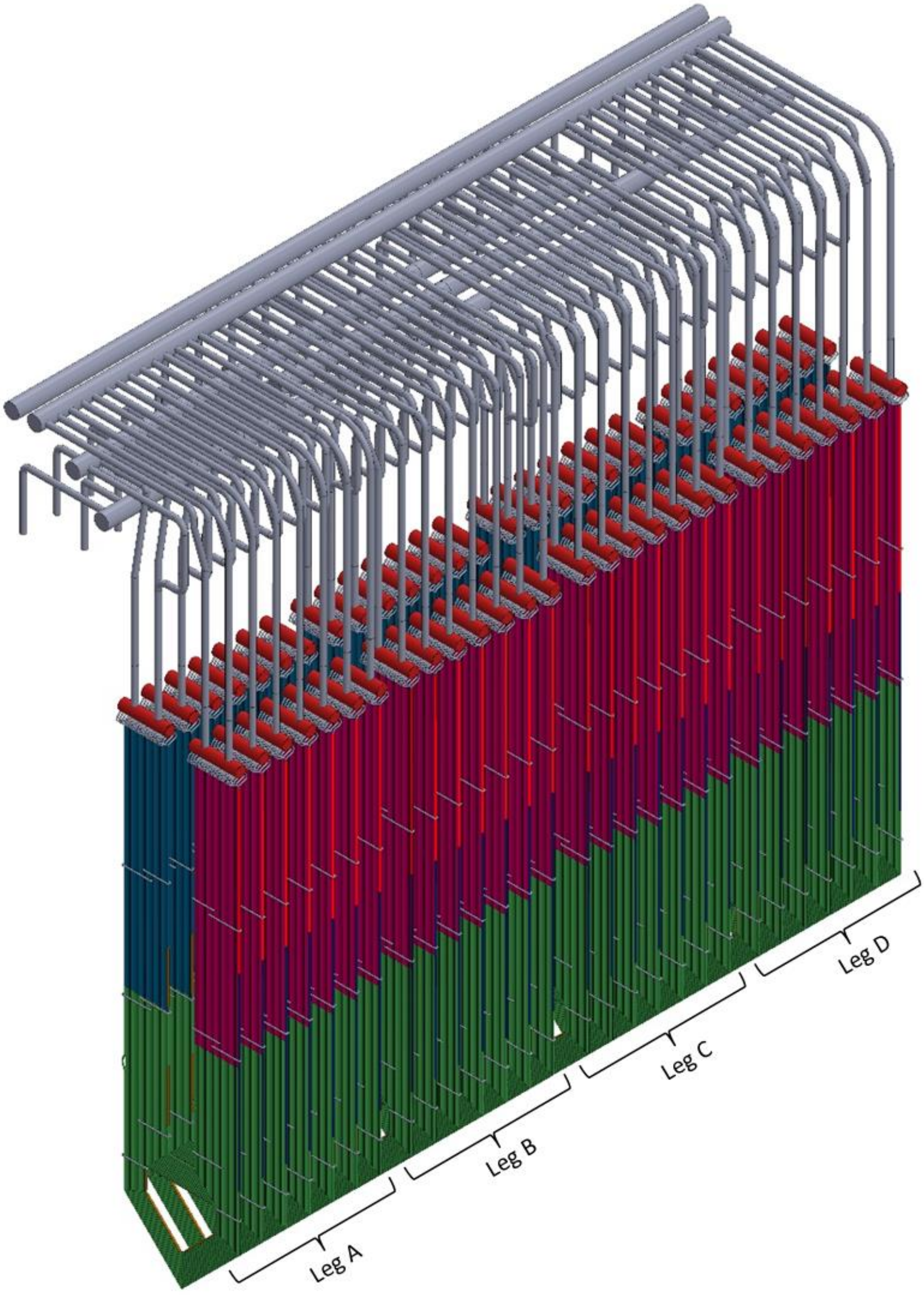

Figure 4.2 Isometric view of final superheater

In Figure 4.2, the isometric view of the final superheater is given. The superheater is divided into four sections, namely A-leg, B-leg, C-leg and D-leg. For each section, attemperating spraywater is introduced into the manifold and distributed throughout the various tubes for cooling.

4.3 Load cases

The load conditions chosen for this project is at 4%, 12%, 20% and 32% of full Boiler Load (BL) at 618 MW. These loads were chosen since short term overheating was identified likely to occur at low boiler loads. As the boiler load increases (and hence the steam flow), the pressure difference across the tube increases. The consequence is that a longer water column is needed if it were to remain in the tube, and hence a shorter exposed outlet section. The worst case would be for the shortest possible water column. At a load typically above 50% the pressure difference is so large that the full height of the pipe will be filled with water, and can actually not remain inside the pipe. This is another reason why STO due to water wedging could only occur at low loads.

As was alluded to in the introduction, it is postulated that at the low load / start-up conditions, the firing is not fully stable, and overfiring may occur. The resulting excess steam temperatures might prompt the operator to over-attemperate which in turn may result in water wedging. The larger the overfiring, the higher would the tube wall temperatures be at the start of the water wedge, which may result in a shorter time before STO would occur. Overfiring scenarios were simulated at 0%, 25%, 50%, 100% and 200% of the set boiler load. This is defined as flue gas mass flow and temperature for a load that is a given percentage above the operating load case. For example, if the boiler's steam flow and pressure is set to levels which corresponds to 20% load (124MW), an overfiring of 25% would thus be flue gas mass flow and temperatures corresponding to 155MW load.

The various load and overfiring conditions have been combined into 20 load case scenarios. For each scenario, the boiler and furnace properties, as well as the water column length, would be different, resulting in different boundary conditions for the transient simulation. Making use of the chosen power plant's available boiler C-schedules [25], the various properties for the superheater steam, furnace flue gas and attemperation spray could be determined as it relates to mass flow rates, pressures and temperatures. These design properties were inserted into Mathcad as shown in Appendix A, which is then used to extrapolate data for lower load conditions. The linear extrapolation may not be 100% correct at very low loads, but this was the most credible method to determine low load conditions in the absence of plant data.

4.4 Establishing the boundaries

The water column length can be calculated as described in section 3.3.2 of this document, making use of the figures below.

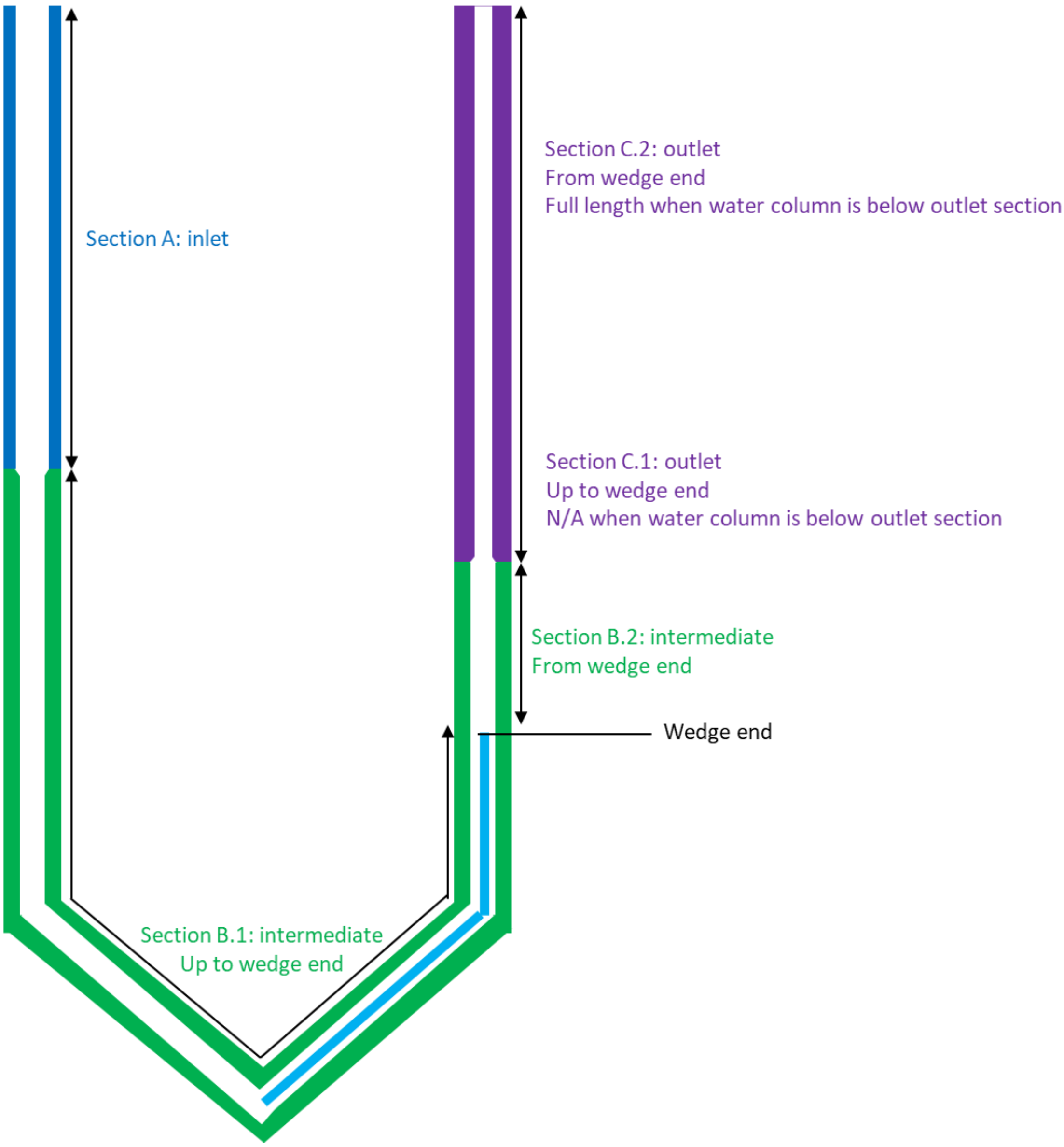

Figure 4.3 Superheater tube illustration with water column end below outlet section

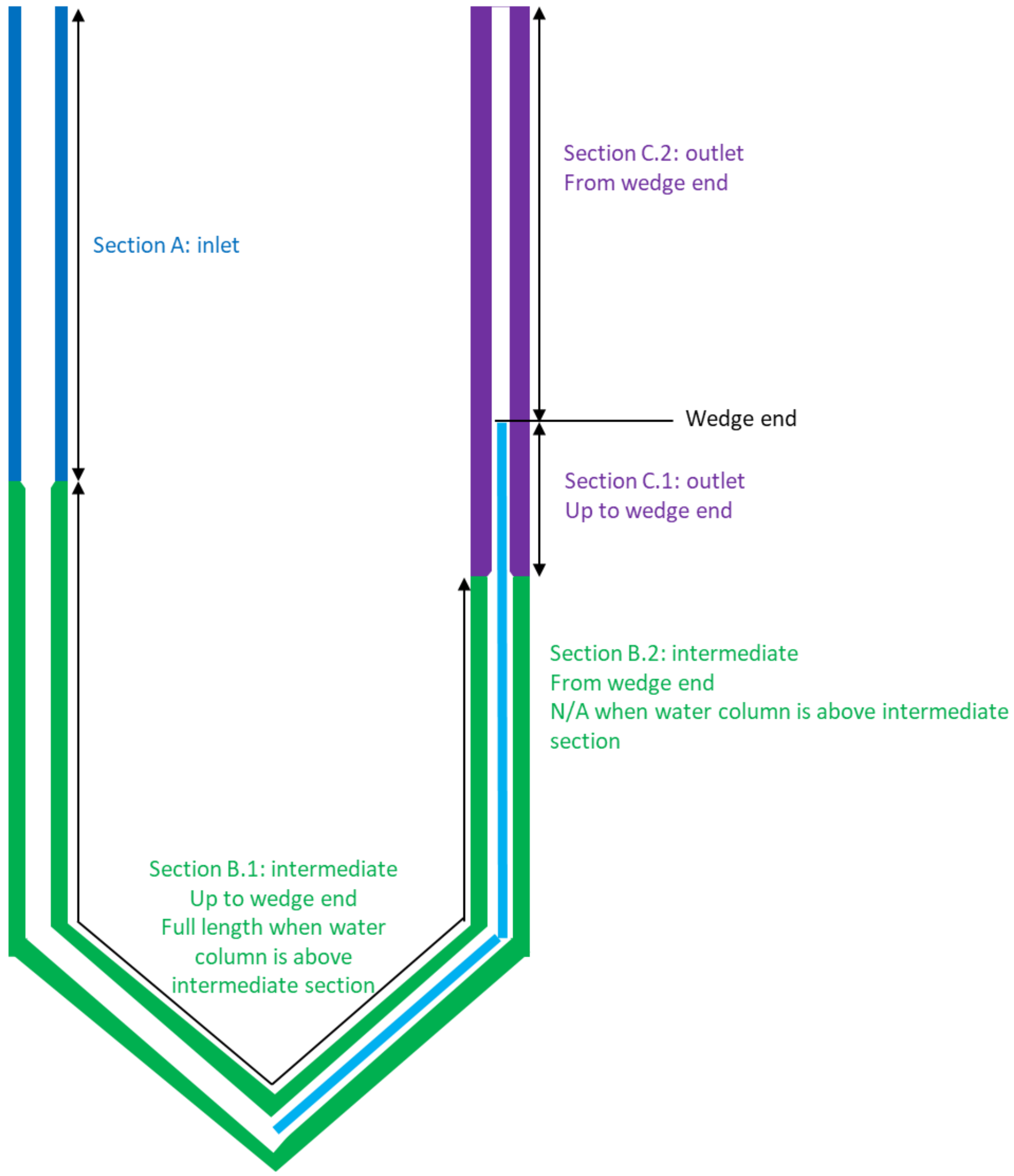

Figure 4.4 Superheater tube illustration with water column end above intermediate section

The distribution of the water column throughout the superheater tube can then be determined with the assistance of the illustrations as shown in Figure 4.3 and Figure 4.4. The following key is applicable to these figures:

Key:

Section A:	Inlet section with 6.3 mm wall thickness
Section B.1:	Intermediate section with 8.8 mm wall thickness up to end of water column
Section B.2:	Intermediate section with 8.8 mm wall thickness from end of water column
Section C.1	Outlet section with 11 mm wall thickness filled with water
Section C.2:	Outlet section with 11 mm wall thickness filled with steam

The intermediate and outlet sections are each divided into two separate sections. This is done to distinguish between the section with water in it and the section exposed to overheating. The Flownex® models to follow only simulate the section of pipe that is being overheated to determine when and where a failure will occur. Thus, the correct geometry for each model must be established.

The length of section A, which is the inlet section shown in blue, would stay constant at 7761 mm, since the model caters for a worst-case scenario only allowing for a still-standing water column to start forming at the lowest point in the superheater tube.

The total length of the intermediate section (green) is 16626 mm. This section is divided into two parts – section B.1 and section B.2. section B.1 represents that part of the intermediate tube from where it connects at the inlet section to the point where the water column ends. This is done in order to determine the boundary conditions just where the water-wedge ends and the final length of the tube being starved of steam. Section B.2 represents the part of the intermediate tube remaining should the water column not fill up the whole of the intermediate section. If section B.2 is calculated to be 0 mm (or not applicable), then the entire intermediate section is filled up with the water column.

The final purple section is the outlet section of the tube with a total length of 8261 mm. Section C.1 is that part of the outlet tube that is filled with water if the water column extends past the intermediate section. If section C.1 shows to be 0 mm (N/A), then there is no water in the outlet part of the tube. Section C.2 is the remaining pat of the tube being starved of its cooling medium.

A Flownex® model was created with the boundary conditions as it relates to the set boiler load and applicable overfiring scenario. (This is Scenario A as described in the Theory chapter). This model was used to determine the boundary conditions of the exposed tube length at the outlet of the superheater. The information gathered here can then be utilised in another Flownex® model (Scenario B), which will be explained in section 4.5. The model to determine the boundary conditions is shown in Figure 4.5.

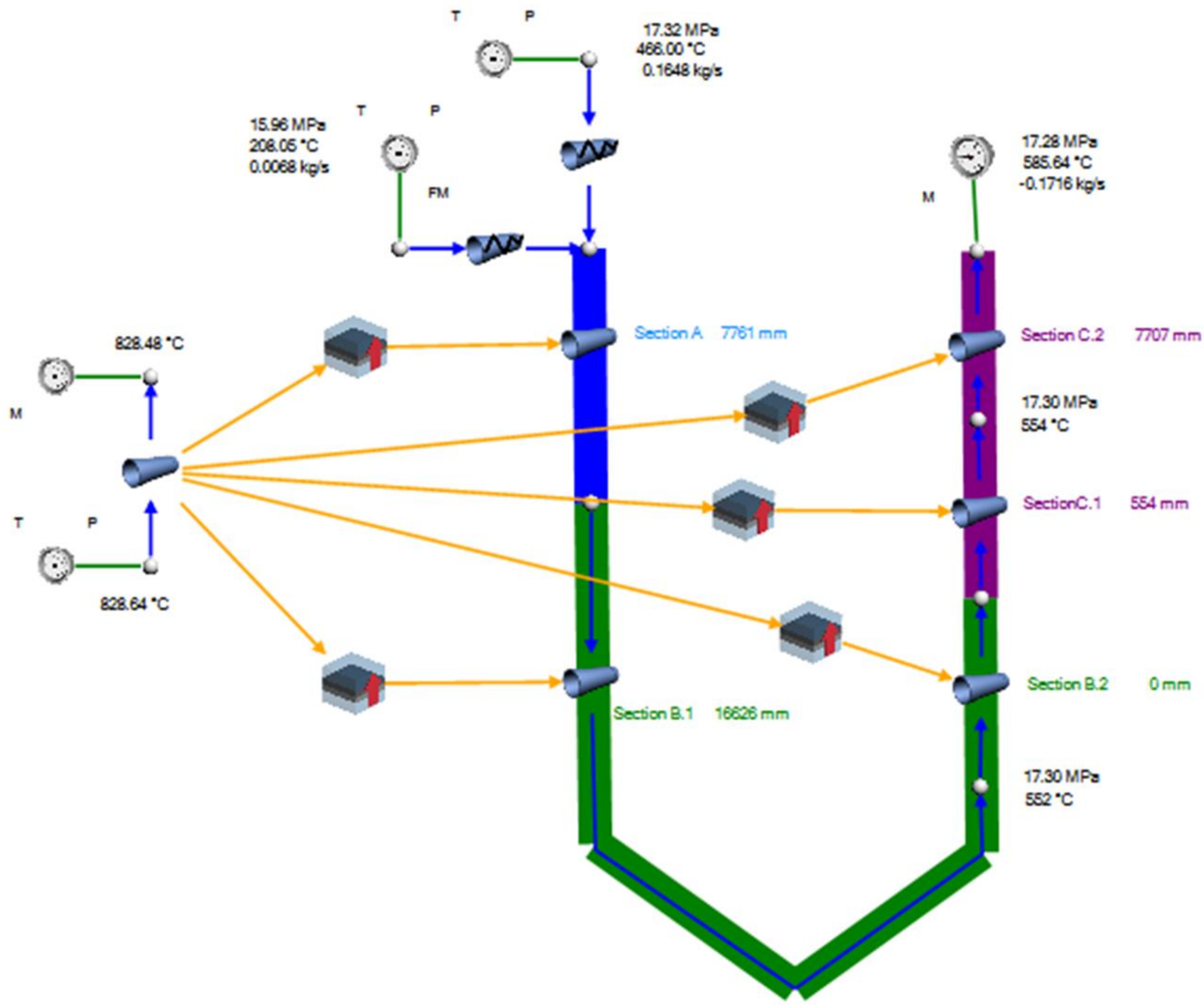

Figure 4.5 Initial Flownex® model establishing boundary condition at water-wedge end

The model applies the same principle as explained for Figure 4.3 and Figure 4.4 in terms of the exposed pipe lengths, which changes according to various scenarios. There are two nodes on the outlet side, which are merely there to extract the pipe temperatures at exactly the correct position as determined by the level calculation. The length of the tubes are therefore adjusted for each load case to ensure that the node is at the height of the potential water level.

The superheater inlet conditions are divided into two parts – steam from the preceding platen superheater and attemperation spray. The condition of the steam flow is determined by the incoming steam pressure and temperature for the chosen load case. The spray is also determined by these same conditions. The superheater outlet condition requires a mass flow rate property.

The furnace is also represented by a pipe element with inlet conditions using properties of pressure and temperature and an outlet condition of flue gas mass flow rate for the chosen firing condition. The furnace and superheater pipe elements are connected by means of heat exchanger elements. These elements represented the heat transfer taking place between the flue gas and the steam through the boiler tube. The heat transfer is defined by its relevant heat transfer coefficient. The heat transfer is approached as being cross-flow due its natural movement throughout the boiler, as illustrated in Figure 4.6. By the time the flue gas reaches the final superheater, the flow of the flue gas is approximately at a 90° angle in relation to the tubes.

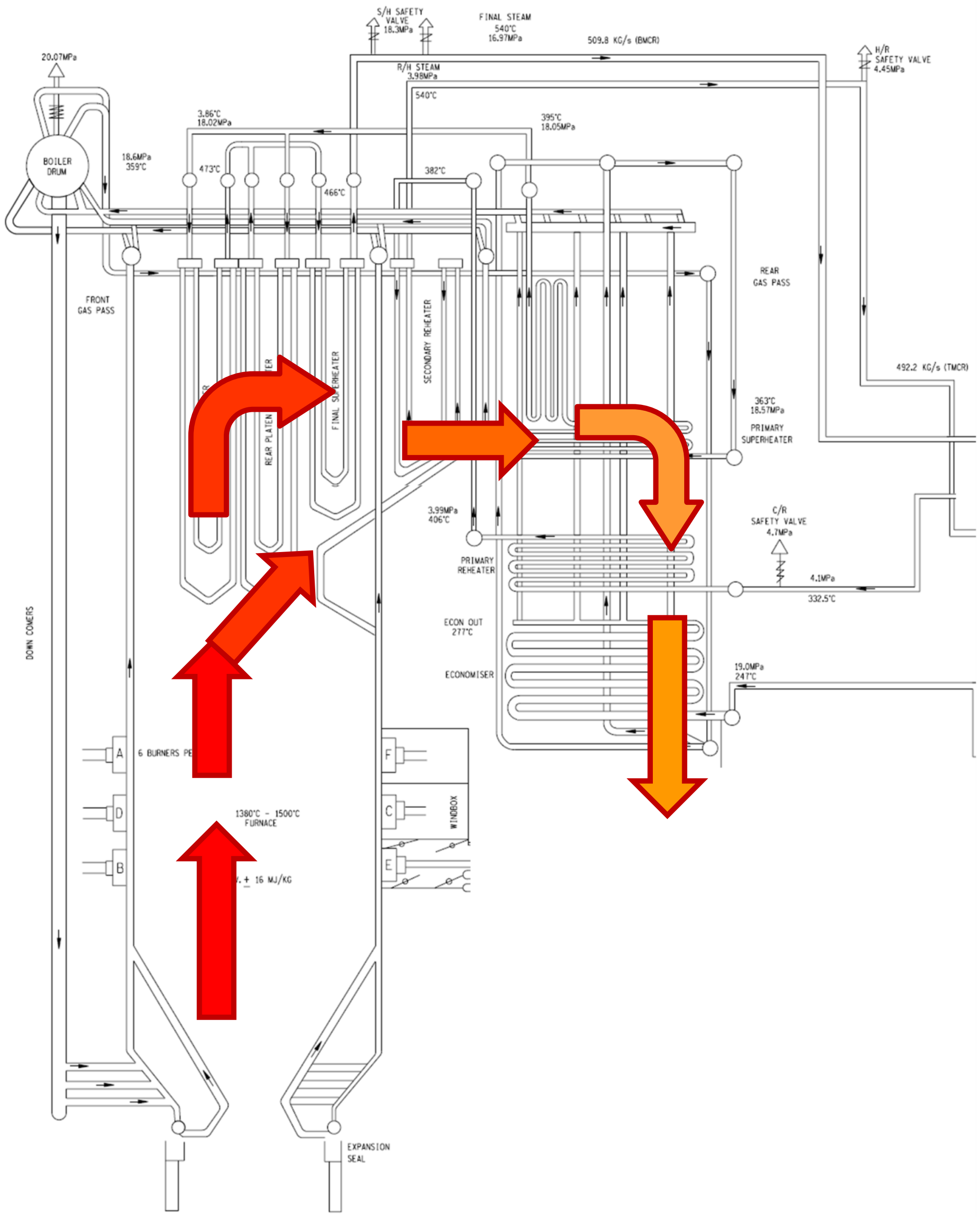

Figure 4.6 Flue gas flow through boiler

For each scenario stipulated, the input property values would be as indicated in Table 4-1, Table 4-2, Table 4-3 and Table 4-4.

Table 4-1 Input properties for scenarios set at 4% boiler load

Scenario	4% BL, 0% OF	4% BL, 25% OF	4% BL, 50% OF	4% BL, 100% OF	4% BL, 200% OF
Full boiler load %	**4%**	**4%**	**4%**	**4%**	**4%**
Overfiring % on running boiler load	**0%**	**25%**	**50%**	**100%**	**200%**
FG temperature [°C]	691.86	694.88	698.40	704.43	717.00
FG mass flow rate [kg/s]	158.24	163.75	170.18	181.19	204.14
Heat transfer coefficient [W/m^2.K]	8.165	9.657	11.398	14.383	20.602
Fluid mass flow rate [kg/s]	0.0217	0.0217	0.0217	0.0217	0.0217
Attemperating pressure [MPa]	15.29	15.29	15.29	15.29	15.29
Attemperating temperature [°C]	191.24	191.24	191.24	191.24	191.24
Attemperating mass flow rate [kg/s]	0.00082	0.00082	0.00082	0.00082	0.00082
Water column length [mm]	238	238	238	238	238
Steam length at outlet [mm]	16086	16086	16086	16086	16086

Table 4-2 Input properties for scenarios at 12% boiler load

Scenario	12% BL, 0% OF	12% BL, 25% OF	12% BL, 50% OF	12% BL, 100% OF	12% BL, 200% OF
Full boiler load %	12%	12%	12%	12%	12%
Overfiring % on running boiler load	0%	25%	50%	100%	200%
FG temperature [°C]	716.50	726.05	735.11	753.71	790.92
FG mass flow rate [kg/s]	203.22	220.66	237.18	271.14	339.07
Heat transfer coefficient [W/m^2.K]	20.35	25.08	29.56	37.29	48.42
Fluid mass flow rate [kg/s]	0.0641	0.0641	0.0641	0.0641	0.0641
Attemperating pressure [MPa]	15.48	15.48	15.48	15.48	15.48
Attemperating temperature [°C]	196.00	196.00	196.00	196.00	196.00
Attemperating mass flow rate [kg/s]	0.00252	0.00252	0.00252	0.00252	0.00252
Water column length [mm]	1918	1918	1918	1918	1918
Steam length at outlet [mm]	14406	14406	14406	14406	14406

Table 4-3 Input properties for scenarios at 20% boiler load

Scenario	20% BL, 0% OF	20% BL, 25% OF	20% BL, 50% OF	20% BL, 100% OF	20% BL, 200% OF
Full boiler load %	**20%**	**20%**	**20%**	**20%**	**20%**
Overfiring % on running boiler load	**0%**	**25%**	**50%**	**100%**	**200%**
FG temperature [°C]	741.64	757.23	772.82	804.00	866.35
FG mass flow rate [kg/s]	249.11	277.57	306.02	362.93	476.75
Heat transfer coefficient [W/m^2.K]	32.789	38.582	43.519	51.579	64.120
Fluid mass flow rate [kg/s]	0.1074	0.1074	0.1074	0.1074	0.1074
Attemperating pressure [MPa]	15.67	15.67	15.67	15.67	15.67
Attemperating temperature [°C]	200.86	200.86	200.86	200.86	200.86
Attemperating mass flow rate [kg/s]	0.00426	0.00426	0.00426	0.00426	0.00426
Water column length [mm]	4039	4039	4039	4039	4039
Steam length at outlet [mm]	12285	12285	12285	12285	12285

Table 4-4 Input properties for scenarios at 32% boiler load

Scenario	32% BL, 0% OF	32% BL, 25% OF	32% BL, 50% OF	32% BL, 100% OF	32% BL, 200% OF
Full boiler load %	**32%**	**32%**	**32%**	**32%**	**32%**
Overfiring % on running boiler load	**0%**	**25%**	**50%**	**100%**	**200%**
FG temperature [°C]	778.85	804.00	828.64	878.42	977.99
FG mass flow rate [kg/s]	317.04	362.93	407.91	498.78	680.52
Heat transfer coefficient [W/m^2.K]	45.430	51.579	57.530	66.076	78.727
Fluid mass flow rate [kg/s]	0.1716	0.1716	0.1716	0.1716	0.1716
Attemperating pressure [MPa]	15.96	15.96	15.96	15.96	15.96
Attemperating temperature [°C]	208.05	208.05	208.05	208.05	208.05
Attemperating mass flow rate [kg/s]	0.00684	0.00684	0.00684	0.00684	0.00684
Water column length [mm]	8617	8617	8617	8617	8617
Steam length at outlet [mm]	7707	7707	7707	7707	7707

4.5 Transient simulation setup

This section describes Scenario B as defined in the Theory section. The tube model is set up according to the geometric specifications of the chosen Eskom superheater tube, for which the methodology can then be applied to other boiler components as well.

The need for a transient model, specifically, is to determine how temperatures and pressures change as time passes while a tube is blocked. The Flownex® Simulation Environment package was used to perform the transient analyses.

The Flownex® model required for this project was constructed as illustrated in Figure 4.7. Only the portion of exposed tube above the water wedge need to be modelled, as STO is assumed to happen in this segment of the pipe.

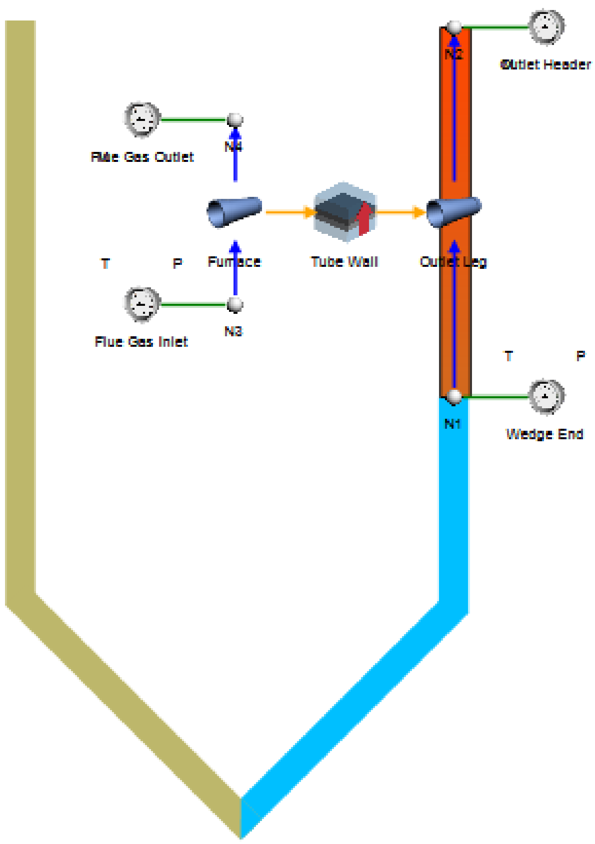

Figure 4.7 Constructed Flownex® model

A Flownex® pipe element was used to represent the outlet leg and contains the geometry for the chosen superheater component. The top boundary condition attached to the pipe element is for the outlet header of the leg, which would then allow the steam to flow into a manifold before it enters the main steam line going to the turbine. The boundary condition at the bottom simulates flow conditions at the point in the tube where the standing water-wedge ends, as determined and explained in section 4.4. This point would depend upon the length of the water-wedge column that would be formed should the pressure difference over the tube be insufficient to transport the water through to the outlet.

The flue gas flow is also represented using a pipe element, for which the flue gas inlet and outlet boundaries are set. The flue gas and superheater outlet leg elements are connected by means of a heat transfer element, representing the tube wall where heat transfer takes place between the steam in the tube and the flue gas, and also represents the tube internal convection. It is at this element where the tube is divided into increments throughout the tube length and wall thickness. The sensitivity analysis performed in order to determine the number of these increments can be found in Appendix F. Figure 4.8 represents a section of the Flownex® Outlet Leg component, which visually illustrates how the tube is discretised into thirty increments through the tube length as well as the tube wall thickness, with the nomenclature used to identify a specific element.

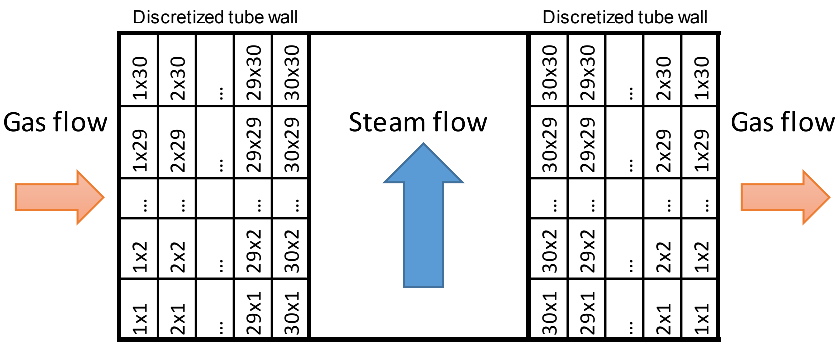

Figure 4.8 Discretization of tube outlet leg over length and wall

The inputs for each element are as given in Table 4-5 and differ with load.

Table 4-5 Flownex® model element input properties

Element	Input properties
Outlet leg	Inner diameter, Length, Wall thickness, Roughness
Wedge end	Temperature, Pressure
Outlet header	Mass flow rate
Furnace	Inner diameter, Length
FG1	Temperature, Pressure
FG2	Mass flow rate
Tube Wall	Wall thickness, Tube material, Heat transfer coefficient

Various input properties were identified in creating the Flownex® simulation model. Table 4-6 gives the input properties that would stay constant. That is, the properties that will remain unchanged as several different scenarios are simulated.

Table 4-6 Flownex® model input properties unchanging

Property	Value	Unit
	Furnace	
Fluid	Air| Gases (Pure Fluids)	-
Number of increments	30	-
	Outlet Leg	
Fluid	Water| General (Two Phase Fluids)	-
Wall thickness	11	mm
Diameter	22.5	mm
Roughness	60	µm
K forward	0	-
Number of increments	30	
	Tube Wall	
Thickness	11	mm
Number of nodes	31	
Material	Chromium (low) Steel - (1Cr-0.5Mo)| Metals (Solids)	-
	Scheduler Setup	
Time step size	1	s
End time	60	min

For each simulation scenario that is set up, the inputs, as shown in Table 4-7, are different. It is with these initial properties that the Flownex® model is run under steady-state conditions to obtain the initial wall temperature of the tube just before the wedge occurs.

Table 4-7 Initial Flownex® component inputs

Input property	Unit
Flue Gas Inlet	
Pressure	kPa
Temperature	^{o}C
Flue Gas Outlet	
Mass Source	kg/s
Wedge End	
Pressure	MPa
Temperature	^{o}C
Outlet Header	
Mass Source	kg/s
Outlet Leg	
Length	m
Tube Wall	
Convection coefficient (h)	W/m^{2}K

After the steady state solution is found, the Flownex® simulation is run in transient mode, meaning that the scenarios are analysed over a period of time. During this transient simulation, various events take place to mimic the happenings during and after the water wedge formation.

For each scenario, the transient starts by simulating the low load steam flow through a single boiler tube as-if no blockage occurs. This is similar to the steady state initial condition. After 60 seconds, the steam mass flow rate is reduced to 0 kg/s and the fluid conditions at the tube inlet changes from normal superheated steam at the specific load, to saturated vapour at the specific load pressure. Following this, the evaporation rate starts to increase until it eventually reaches the rate associated with the boiler load as explained in section 3. This is done to imitate the effect of a sudden blockage in the tubes and the water blockage slowly starting to evaporate through the tube due to the heat from the furnace.

The boundary condition labelled as "Wedge End", which is where the water blockage would occur in the outlet pipe of the boiler superheater tube, is initially set up with an input for a temperature value. When the simulation creates the water wedge (after 60 seconds), the temperature property is changed to a quality property, which is then set to a value of 1. This indicates that the water being evaporated has now reached its boiling point, and saturated steam is moving along the tube.

Figure 4.9 attempts to explain this action setup in a more visual manner. A timeline of zero to ten minutes (as set for the transient simulation) is given, and the changes made to the components during the transient simulation are explained according to each component.

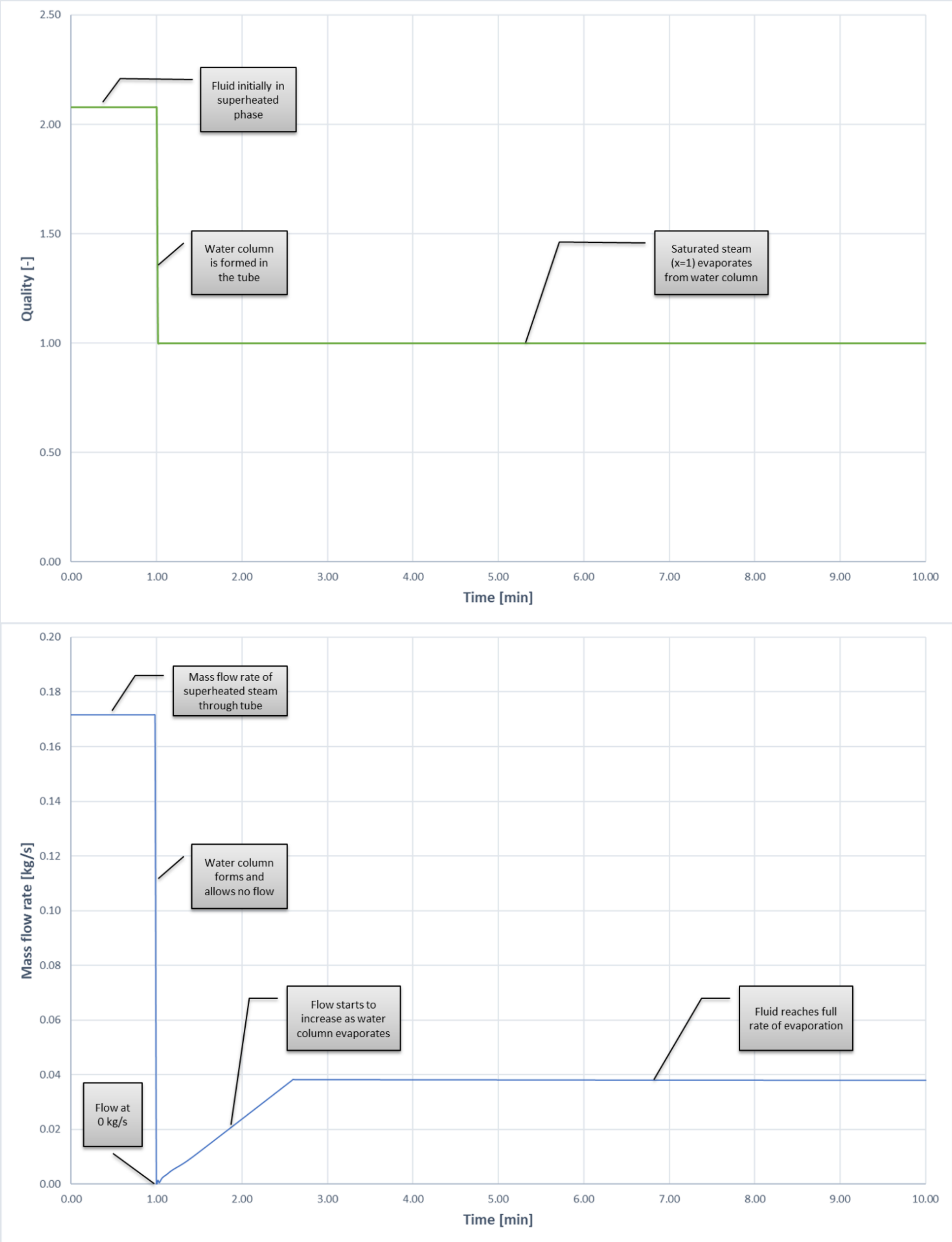

Figure 4.9 Illustration of property changes taking place during simulated Flownex® scenarios

Finally, when all of the above activities have occurred and the rate of final evaporation is reached, the mass flow rate is set to constantly run at these values until the end of the transient simulation. The assumption here is that that the water column remains at the current height, being replenished with spray water which is nominally already at saturation conditions. The desired output properties are given in Table 4-8. Refer to Figure 4.8 for an explanation on the inner and outer tube wall temperatures.

Table 4-8 Flownex® scenario outputs

Output property	Unit
Wedge End	
Pressure	MPa
Temperature	^oC
Quality	-
Outlet Header	
Pressure	MPa
Temperature	^oC
Mass source	kg/s
Tube Wall	
Outer temperature [1x30]	^oC
Inner temperature [30x30]	^oC

The tube wall temperatures chosen are the top-most increments (inside and outside) at the outlet of the tube. These were specifically chosen, since it can be assumed that if a failure does not occur at these points, where the tube is the hottest, it will not occur anywhere further down the tube.

4.6 Validation of Flownex® model

In order to verify that the steady-state Flownex® model was valid, the results were compared with that of an analytical Mathcad model. The model can be seen in Appendix B and Appendix C. Table 4-9 shows these comparisons and the error percentage between the values, which were executed at design conditions (100% boiler load).

Table 4-9 Result comparison between Flownex® model and Mathcad calculations (618 MW load conditions)

Property @ 618 MW	Flownex	MathCAD	Error %
Final SH outlet temperature [^{o}C]	542.3	540.0	0.4%
Pressure @ final SH outlet [MPa]	16.99	17.00	0.1%
Steam flow Reynolds number [-]	868455	883142	1.7%
Average frictional factor [-]	0.024	0.024	0.0%
Average pressure in tube [MPa]	17.13	17.20	0.4%
Pressure drop in final SH [MPa]	0.327	0.317	3.2%

From the table, it can be concluded that the Flownex® model was confirmed. The percentage errors are small enough to verify the applicability of the Flownex® model, with the largest percentage error being only 3.2%.

The differences observed above could be a result of small differences in the built-in fluid property and component characteristic relationships used in the Flownex® and Mathcad simulation packages. Where the Reynolds number was directly calculated in Mathcad, Flownex® takes a correction factor into account based upon the amount of bends throughout the pipe, leading to a minor error of 1.7%. In turn, the pressure drop over the superheater is calculated using the calculated Reynolds number, resulting in the slightly larger error percentage of 3.2%, which is still acceptable.

4.7 Material properties

The Flownex results provide the tube wall temperatures at various locations, but do not specify the yield strength of the material at certain points while operating at different temperatures. In order to determine if the material will fail under certain conditions, the combined yield strength for the various scenarios was calculated using the thick wall cylinder theory (see calculations explained in section 3.4 and Appendix D).

Figure 4.10 and Figure 4.11 gives the characteristics of the material regarding modulus of elasticity and thermal expansion, respectively, which was used to calculate the thermal hoop stress as explained in section 3.4.

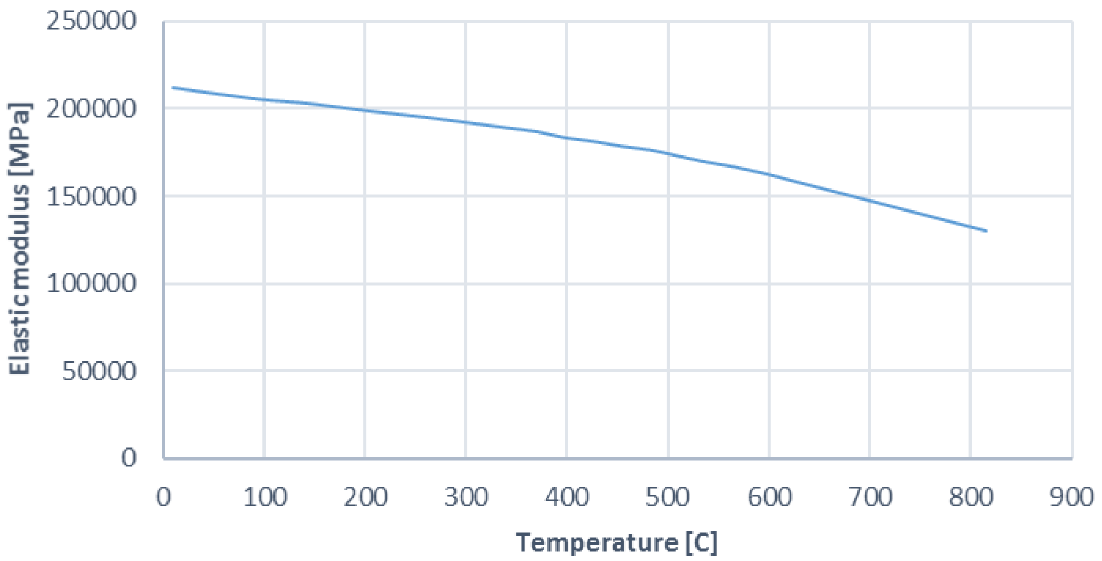

Figure 4.10 Elastic modulus of Grade 22 steel (derived from Gandy [26])

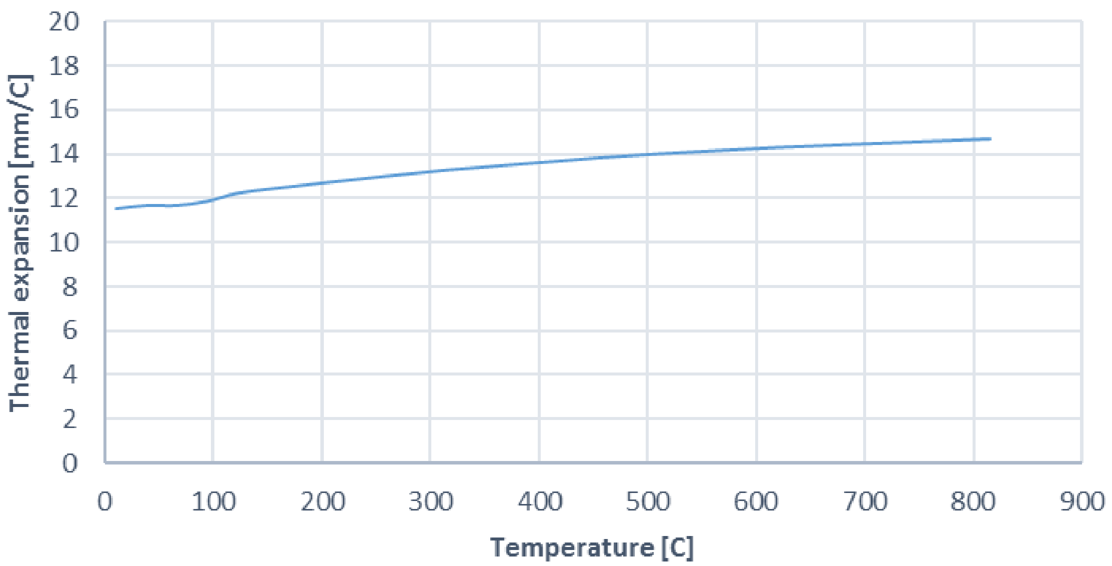

Figure 4.11 Thermal conductivity of Grade 22 steel (derived from Gandy [26])

Tube material from the actual power station simulated in this project was provided to a team in the EPPEI Specialization Centre in Materials Management at The University of Cape Town to test the samples' yield strength at elevated temperatures.

The high temperature tests were conducted by means of an integrated thermomechanical system known as the Gleeble 3800, shown in Figure 4.12. The system contains a servo-hydraulic mechanism which has the ability to load the specimen up to 100 kN and is also capable of heating a material sample through feedback control from thermocouples at 10 000°C/s. For this, direct resistance heating is applied, which involves conducting heat at a low frequency current (approximately 50 Hz) through the sample. This approach utilizes the Joule effect and allows uniform heating throughout the sample due to constant current density.

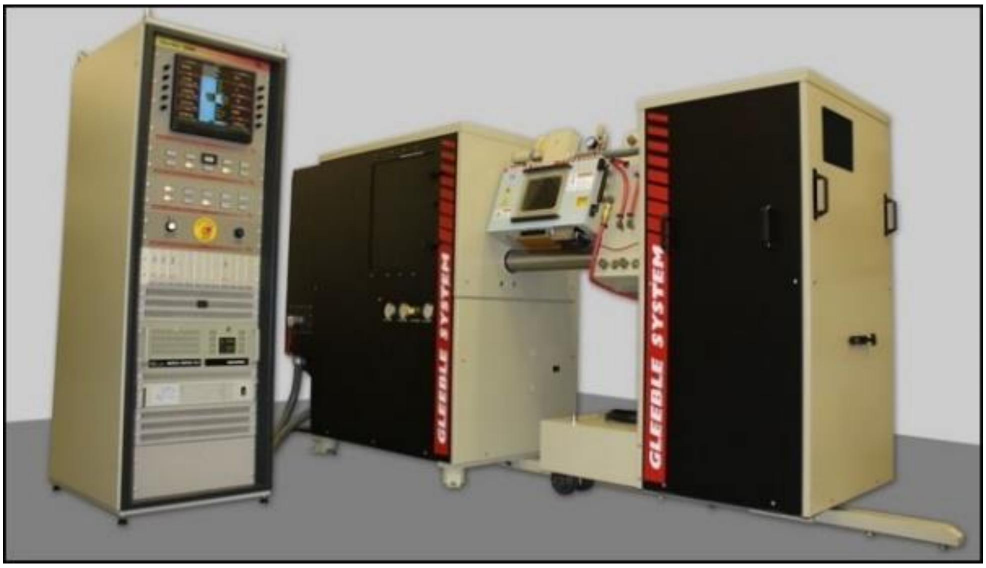

Figure 4.12 Gleeble 3800

The sample is heated and conducts heat away from the central heated section towards the water-cooled grips (see Figure 4.13 and Figure 4.14). This creates a temperature gradient over the material sample. By altering the various resistive elements within the conduction path, such as the specimen geometry, chamber atmosphere, the type of grip material and the free span distance between grips, the hot zone[2] length and consequently the entire temperature profile can be closely controlled.

[2] The area known as the hot zone is the region where the temperature falls within certain limits near the centre of the specimen length.

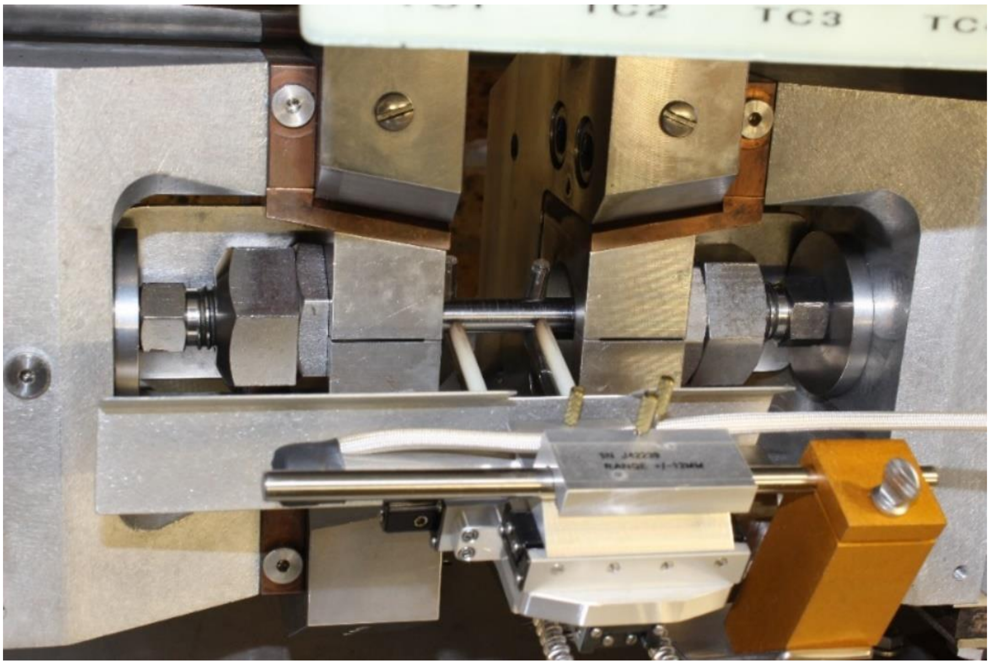

Figure 4.13 Centralized heating of sample

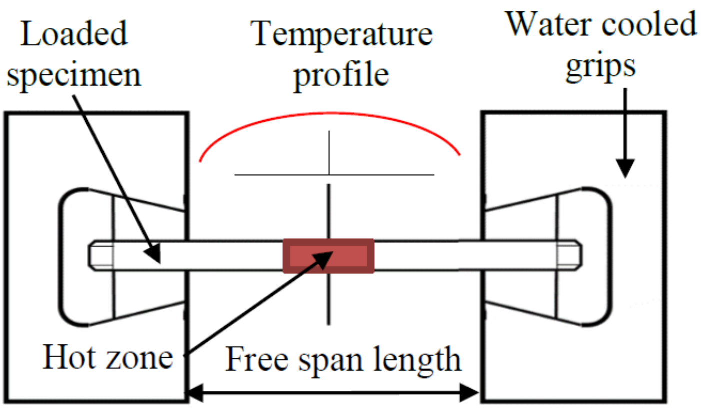

Figure 4.14 Temperature profile of sample

The material sample used for the study as described in this project were 10 mm in diameter and 124 mm long, with a 10 mm long M10 threaded section at each end. The specimen strain was measured with an extensometer that was connected to the sample with an initial gauge length of 24 mm, as illustrated in Figure 4.15.

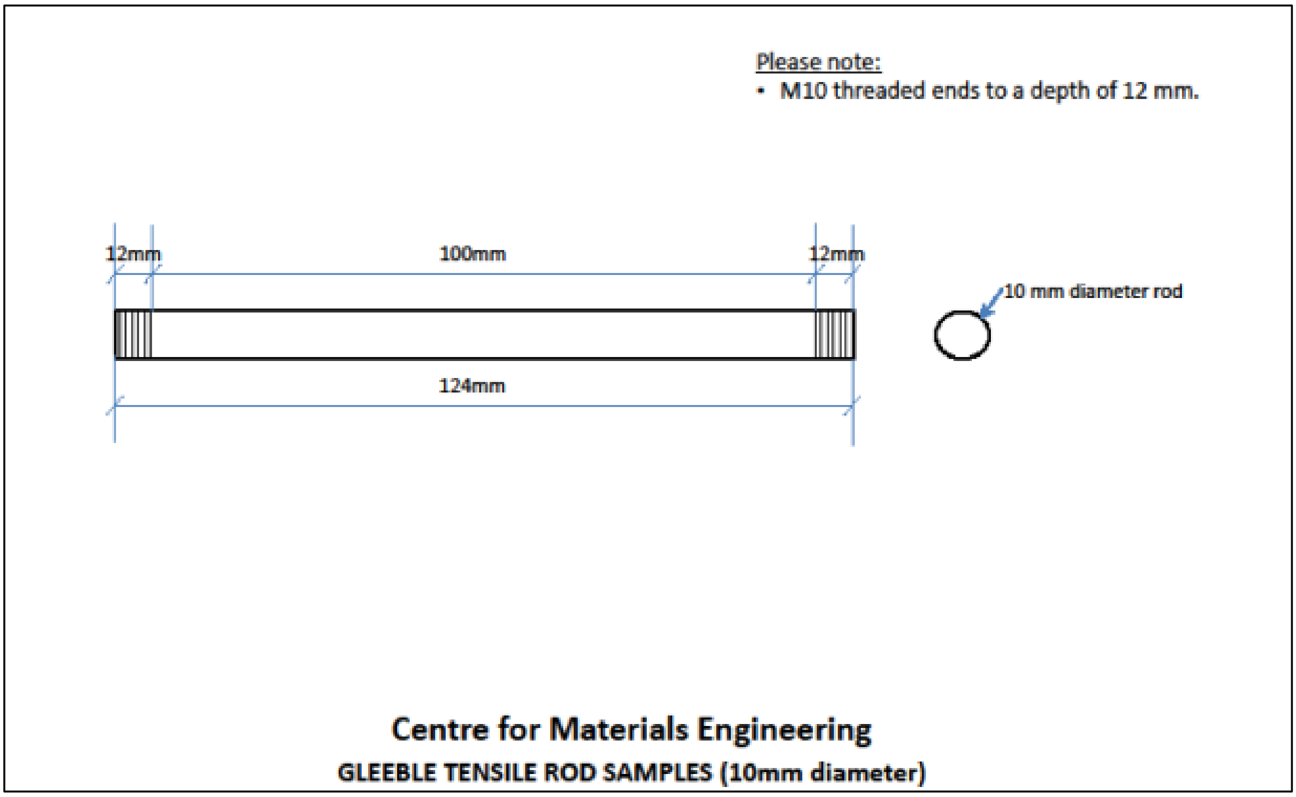

Figure 4.15 Manufacturing drawing for the material samples to be studied (EPPEI Specialization Centre of Materials Management at UCT)

A used piece of tube (approximately 200 000 hours) as well as a piece of virgin tube was tested, determining the yield strength of an old vs new tube. The temperatures that the materials were tested at ran from 30^{o}C to 1000^{o}C. The lab results are given in Table 4-10 and graphed in Figure 4.16.

Table 4-10 Lab test results for yield strength of old and new tube at elevated temperatures (provided by the EPPEI Specialization Centre for Materials Science at UCT)

Temperature [^{o}C]	Yield strength [Mpa]	
	Old Tube	**New Tube**
30	204	374
500	140	276
600	126	247
700	82.4	139
750	68	82.1
800	56	67.1
850	52	56.5
900	50	51.3
950	45	42.9
1000	42	37

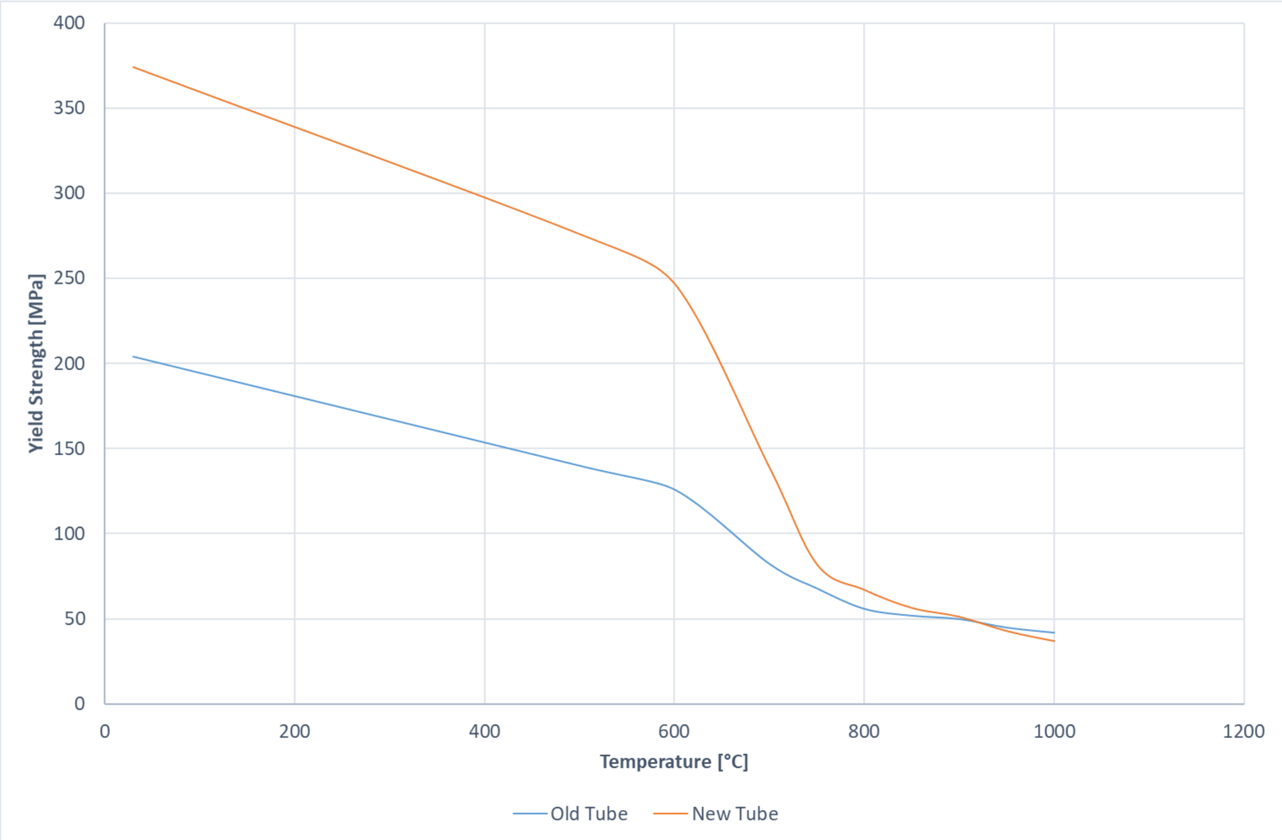

Figure 4.16 Lab test results graph for yield strength of old and new tube at elevated temperatures (provided by the EPPEI Specialization Centre for Materials Management at UCT)

4.8 Thermal stress model validation

SolidWorks® is a computer-aided design tool intended to create solid parts and assemblies. This software contains an add-in which can be used to perform finite element method analyses for such parts. In order to gain confidence in the thermal stress equation described in section 3.4, stress calculations were performed using SolidWorks®.

A short segment of a tube was modelled, and constrained such that it could expand in all directions, except its bottom face. The tube was modelled with the actual wall thickness of the superheater tube studied throughout this dissertation. The material was selected as carbon steel with known and constant properties.

Two load cases were applied to the tube – inner tube temperature and an outer tube temperature. These temperatures will differ for each boiler load scenario. Figure 4.17 shows the temperature distribution over the tube wall.

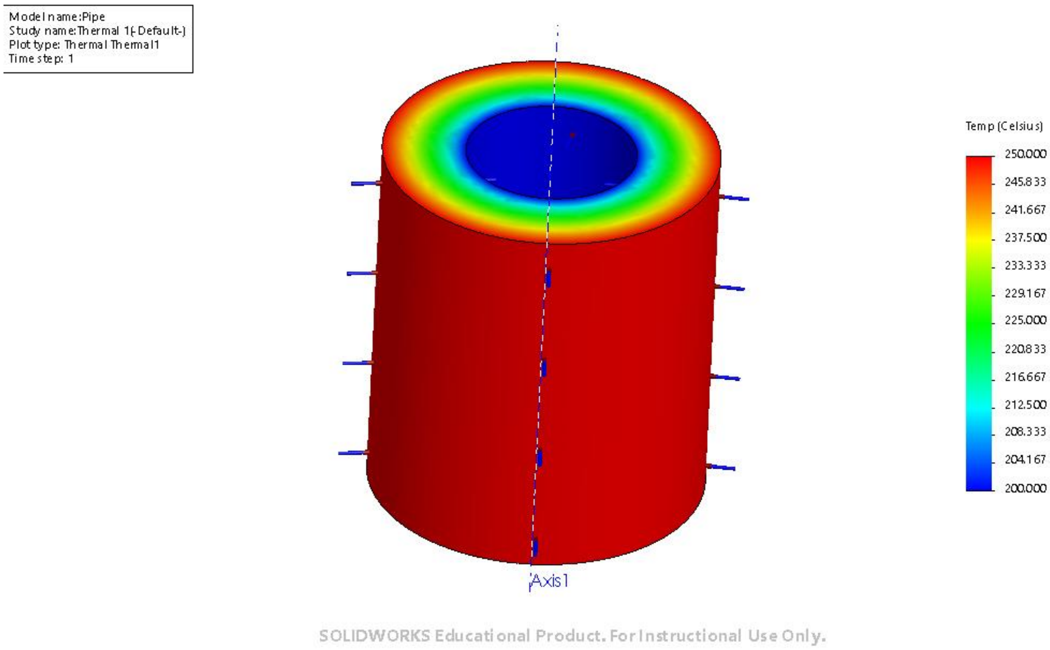

Figure 4.17 SolidWorks® FEM – temperature distribution over tube wall

The meshing for the tube is automatically created by the SolidWorks® software in order to determine the temperature distribution by means of conduction calculations. The mesh chosen is the finest mesh available in SolidWorks® and is made up of second-order tetrahedral elements. This type of element is generally considered to be good choice for solid geometry. The mesh is illustrated in Figure 4.18.

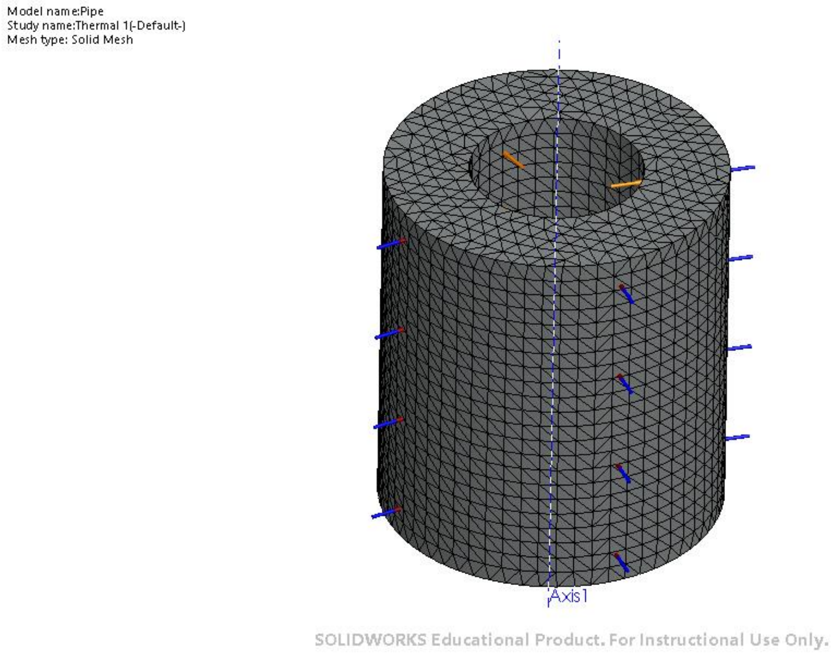

Figure 4.18 SolidWorks® FEM – quadratic mesh

After the temperature distribution had been determined, a thermal stress study is done on the tube. The temperature results for each element is automatically transferred to the stress analysis elements.

The results from the SolidWorks® FEM were compared to the circumferential and Von Mises stresses that were calculated in section 3.4. The circumferential stress is analytically calculated using eq. (3-35) and the relevant carbon steel property materials. The results corresponding to the temperature distribution shown in Figure 4.17 for the circumferential and Von Mises stresses are given in Figure 4.19 and Figure 4.20, respectively.

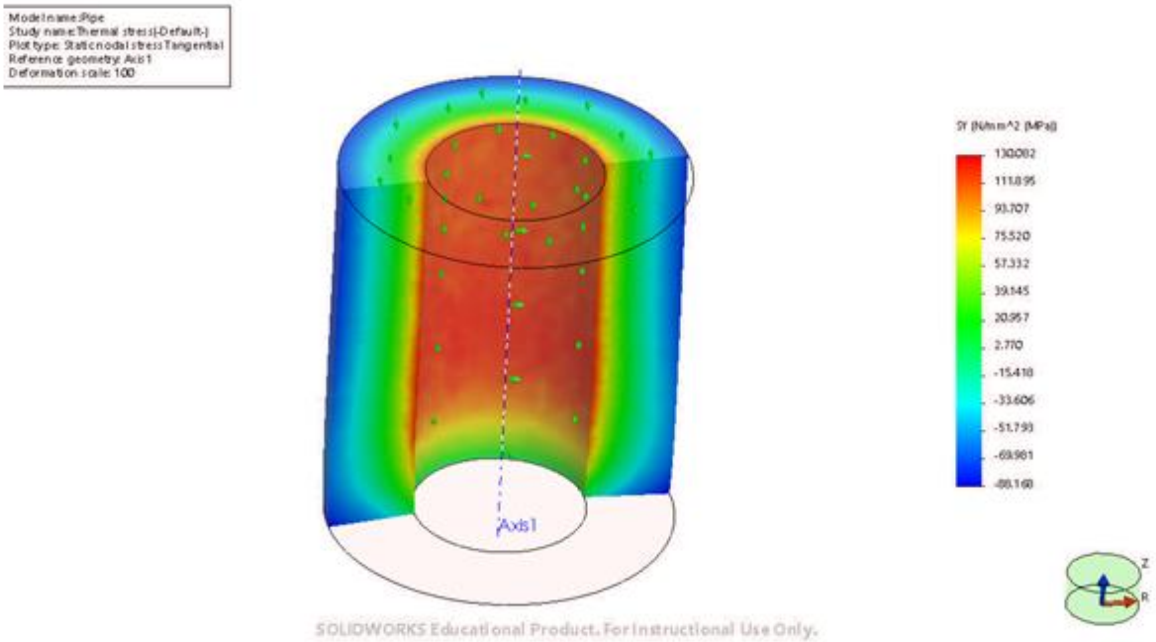

Figure 4.19 SolidWorks® FEM – example of circumferential stress analysis (sectional view)[3]

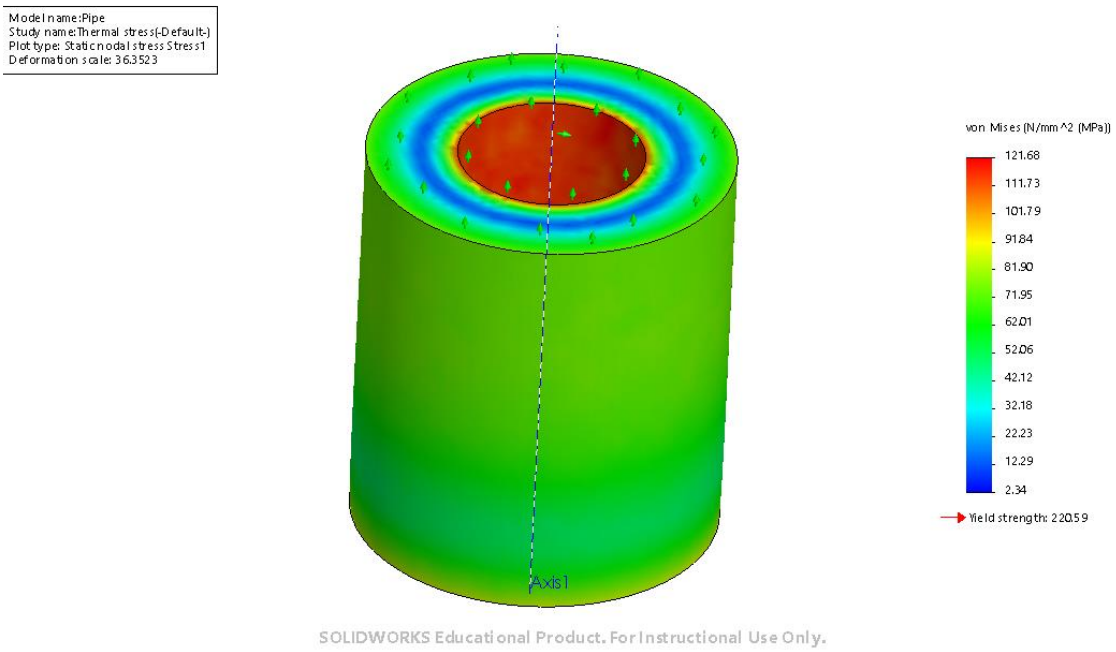

Figure 4.20 SolidWorks® FEM – example of Von Mises stress analysis

Figure 4.19 gives a sectional view of the FEM analysis, showing that the greatest stress is experienced on the inside of the tube. This indicates that the tube is being compressed from the outside and stretched from the inside. This corresponds with the normal expansion of a tube.

[3] The stress gradient at the bottom of the tube is due to the tube being fixed in place

The circumferential stress results of the FEM were compared to the results calculated using thick-walled cylinder stress. This was done to validate the use of eq. (3-34) in section 3.4. Temperature differences between 10°C and 50°C were applied to ensure that the equation is relevant for smaller and greater temperature distributions. The comparison is given in Table 4-11 and shown in Figure 4.21.

Table 4-11 Circumferential result comparison of SolidWorks® FEM and thick-walled cylinder calculations

Inner tube temperature [°C]	Outer tube temperature [°C]	ΔT [K]	Analytical thermal stress [MPa]	FEM thermal stress [MPa]
200	200	0	0.00	0.00
200	210	10	37.92	26.02
200	220	20	75.83	52.04
200	230	30	113.75	78.05
200	240	40	151.67	104.07
200	250	50	189.58	130.08

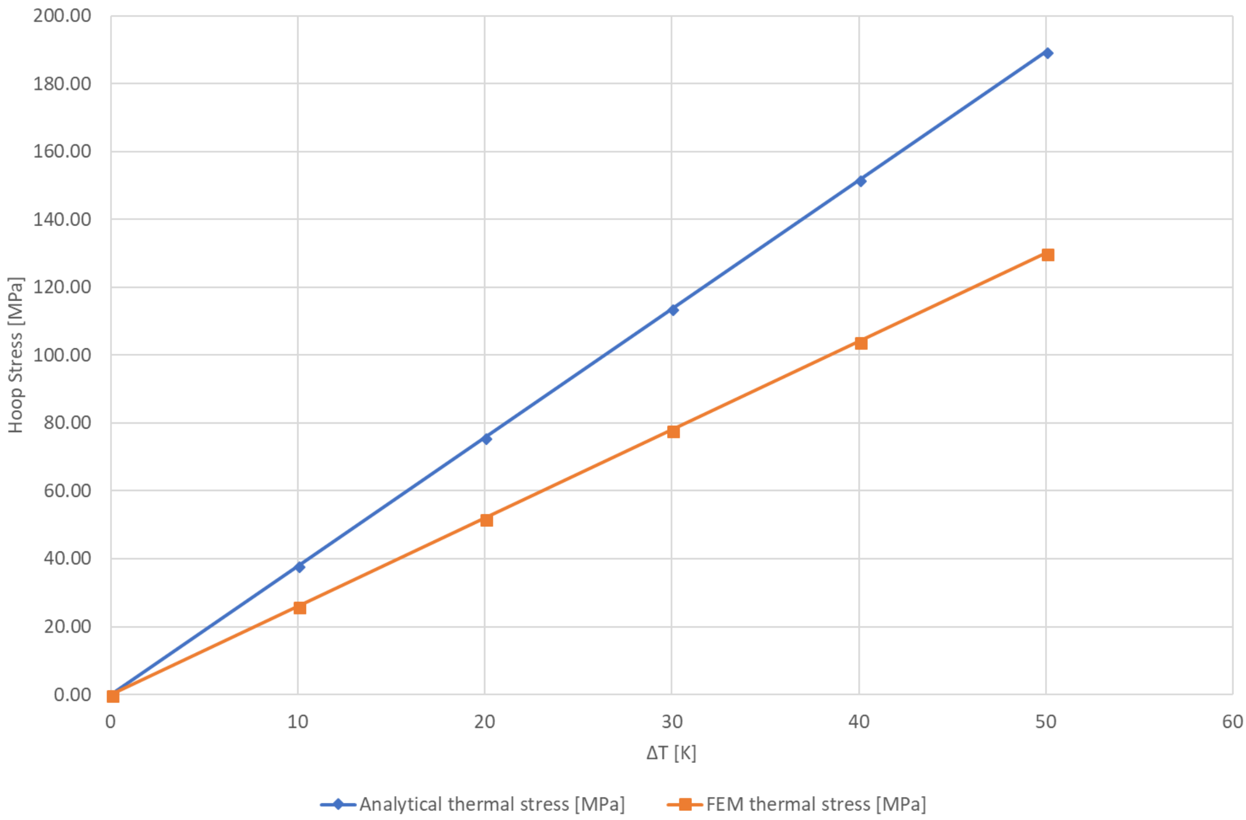

Figure 4.21 Circumferential stress graph of SolidWorks® FEM and thick-walled cylinder calculations

Analysing the results, it can be seen that they differ in value. However, as seen in Figure 4.21, the profiles of the results are similar. Both graphs are linear, intersecting at 0, but there is a slope difference between the two graphs. If the analytical calculation is calibrated with an adjustment factor of 0.69 (essentially setting the “stress concentration factor” to 0.69 instead of 1.0), the two graphs will align. This calibrated results graph is shown in Figure 4.22.

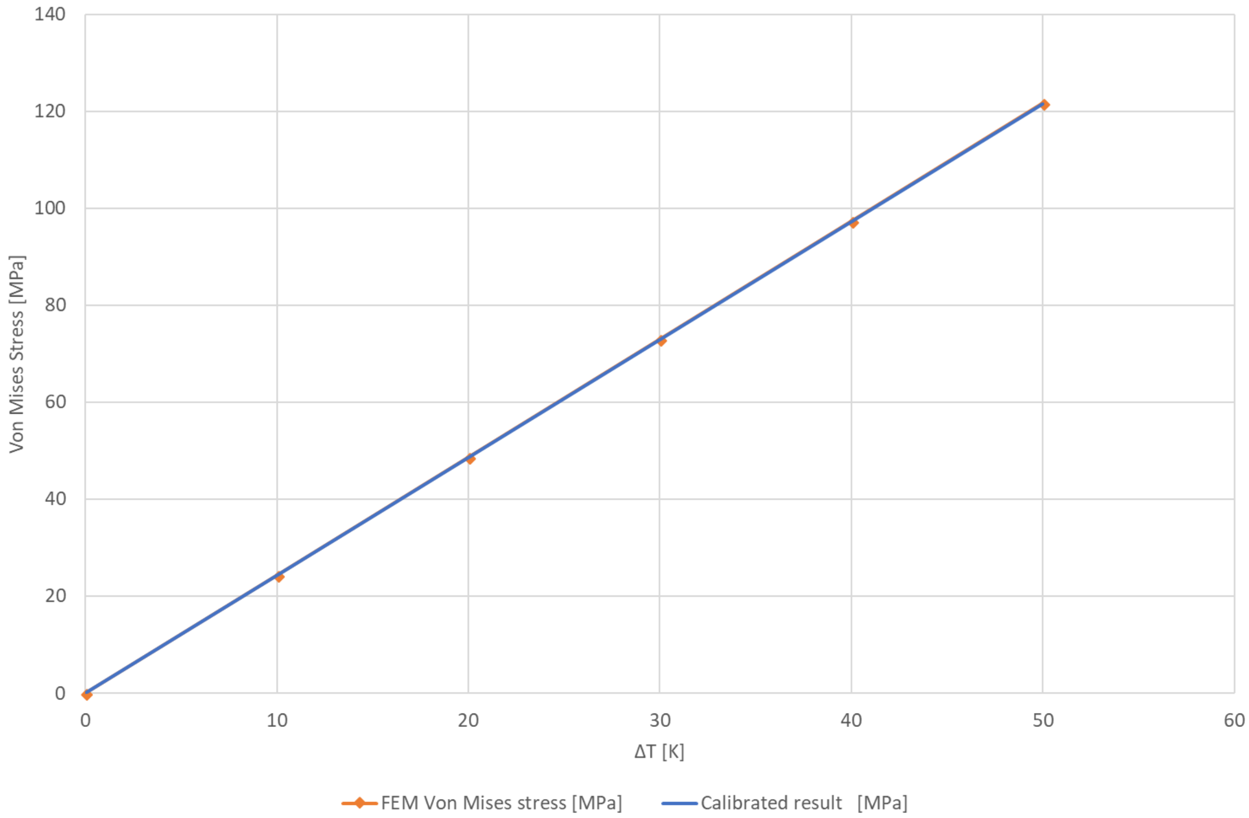

Figure 4.22 Circumferential stress graph of SolidWorks® FEM and calibrated calculation

From the analysis above, it is not completely clear how eq. (3-34) was derived or where it came from. However, the FEM analyses performed confirms the credibility the results acquired from eq. (3-34) with the use of an adjustment factor.

Applying this thermal stress calibration factor to some of the study scenarios, the Von Mises stress can also be verified. The Von Mises stress, as calculated in section 3.4, was compared to the FEM’s Von Mises stress result after applying the thermal stress calibration factor. The results are as given in Table 4-12.

Table 4-12 Von Mises result comparison

Scenario	Inner tube temperature [°C]	Outer tube temperature [°C]	Calculated thermal stress [MPa]	Calibrated thermal stress [MPa]	Analytical Von Mises stress [MPa]	FEM Von Mises stress [MPa]	Error [%]
4% BL 0% OF	561.51	561.33	0.61	0.42	40.39	41.01	1.54%
12% BL 0% OF	580.21	580.72	1.71	1.18	41.05	41.67	1.51%
20% BL 0% OF	607.61	608.54	3.05	2.10	41.86	41.51	0.84%
32% BL 0% OF	538.46	544.16	19.41	13.39	52.05	52.69	1.23%
32% BL 50% OF	551.06	559.65	29.09	17.45	55.82	59.08	5.84%

From the above table, the results show that the Von Mises stress calculations are compatible to the FEM as simulated in SolidWorks®. The errors calculated between the results are minimal (less than 10%) and it can therefore be concluded that the Von Mises calculation is acceptable.

4.9 Results and discussion

For each scenario load (4%, 12%, 20% and 32% of full boiler load), the water length of the column that would exist in the pipe due to the differential pressure over the superheater tube was calculated as explained in section 3.3.2. Table 4-13 shows the results of these calculations for both the water column length and the exposed length of tube at the outlet. These were the values used in the Flownex® model to finally determine the superheater tube wall temperatures.

Table 4-13 Water column lengths for various boiler loads

Boiler Load	Water column length [mm]	Exposed length at outlet [mm]
4%	238	16086
12%	1918	14406
20%	4039	12285
32%	8617	7707

The tube wall temperatures modelled in Flownex®, along with the internal tube pressure, are those that were used to determine the stresses over the tube wall. The values for these stresses for each scenario are given in Figure 4.23.

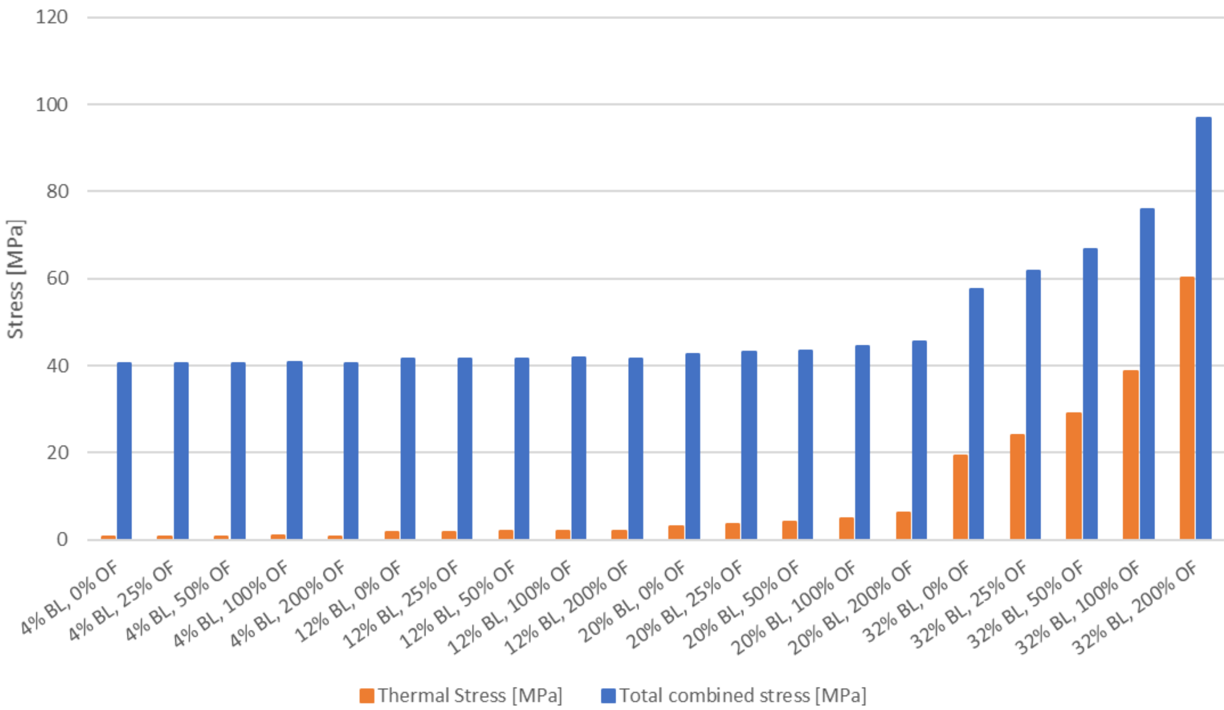

Figure 4.23 Stress values of outlet tube as simulated in Flownex®

An example of how these temperatures change over the ten-minute time period as calculated from the transient model is shown in Figure 4.24.

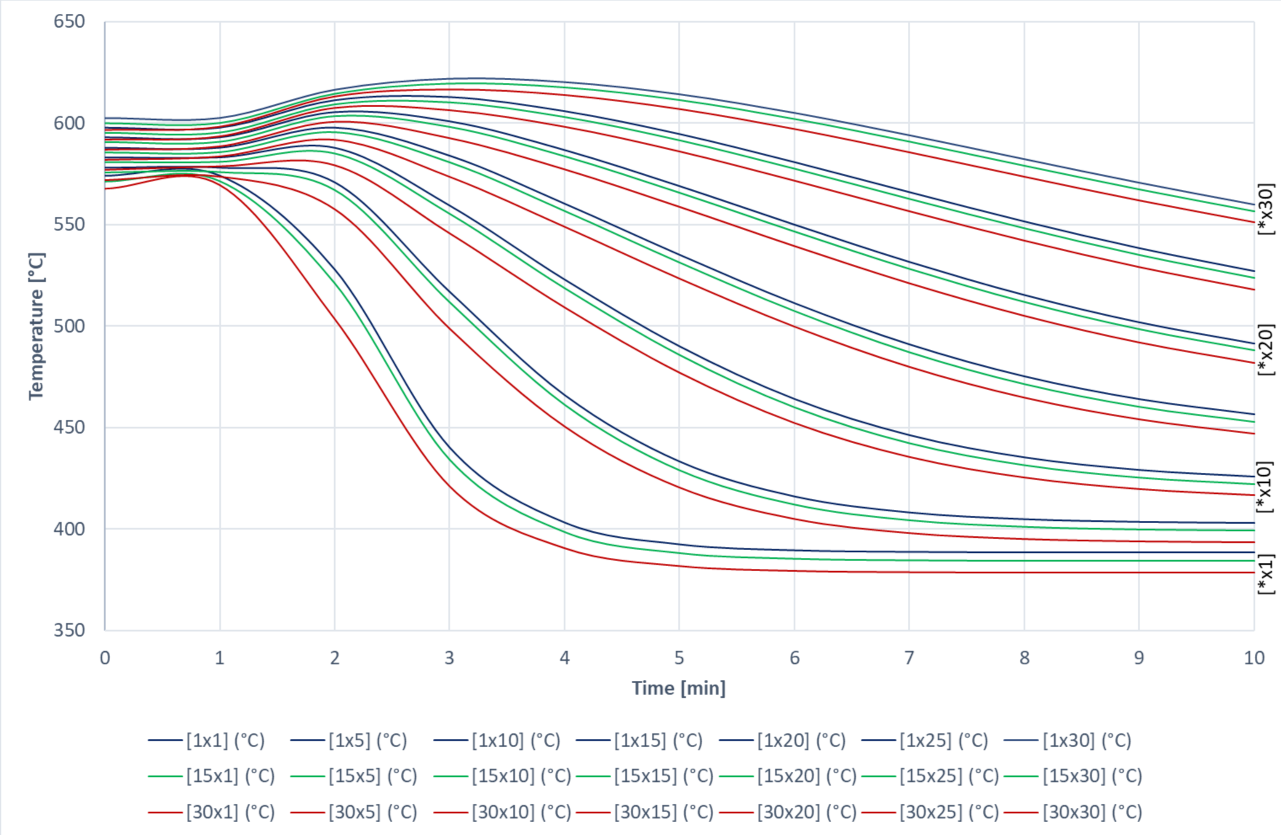

Figure 4.24 Scenario 32% BL, 50% OF tube wall temperatures over time

To better understand what is illustrated in Figure 4.24, refer back to Figure 4.8, which shows how the superheater tube was discretised. As explained in section 4.5, the simulation is run under normal boiler load conditions before the water wedge is introduced. From the graph above, it shows that the tube gradually starts heating up (especially in the lower region) in transient state as the water wedge becomes present. The lower part of the tube then suddenly starts cooling down. The water wedge starts to evaporate and the lower part of the tube continues to cool down. However, from the graph it can be seen that the top part is not yet receiving the evaporated steam for cooling and gradually increases in temperature. Once the top part of the tube makes contact with the evaporated steam, it gradually starts cooling down as well.

The graph shows that the differences between the inner wall temperatures and outer wall temperature do differ by a few degrees. This temperature distribution over the wall thickness is what contributes to the hoop stresses in the form of thermal stress.

There is a clear difference in temperature between the lower part of the outlet leg (closest to the water-wedge) and the top part of the outlet leg. This is an indication of how the top part of the tube becomes susceptible to short term overheating, since it is starved of steam for a longer period of time. However, for this specific scenario, STO will not occur, regardless of the time, because of the cooling from the saturated steam which brings the temperature back to even below normal operating conditions.

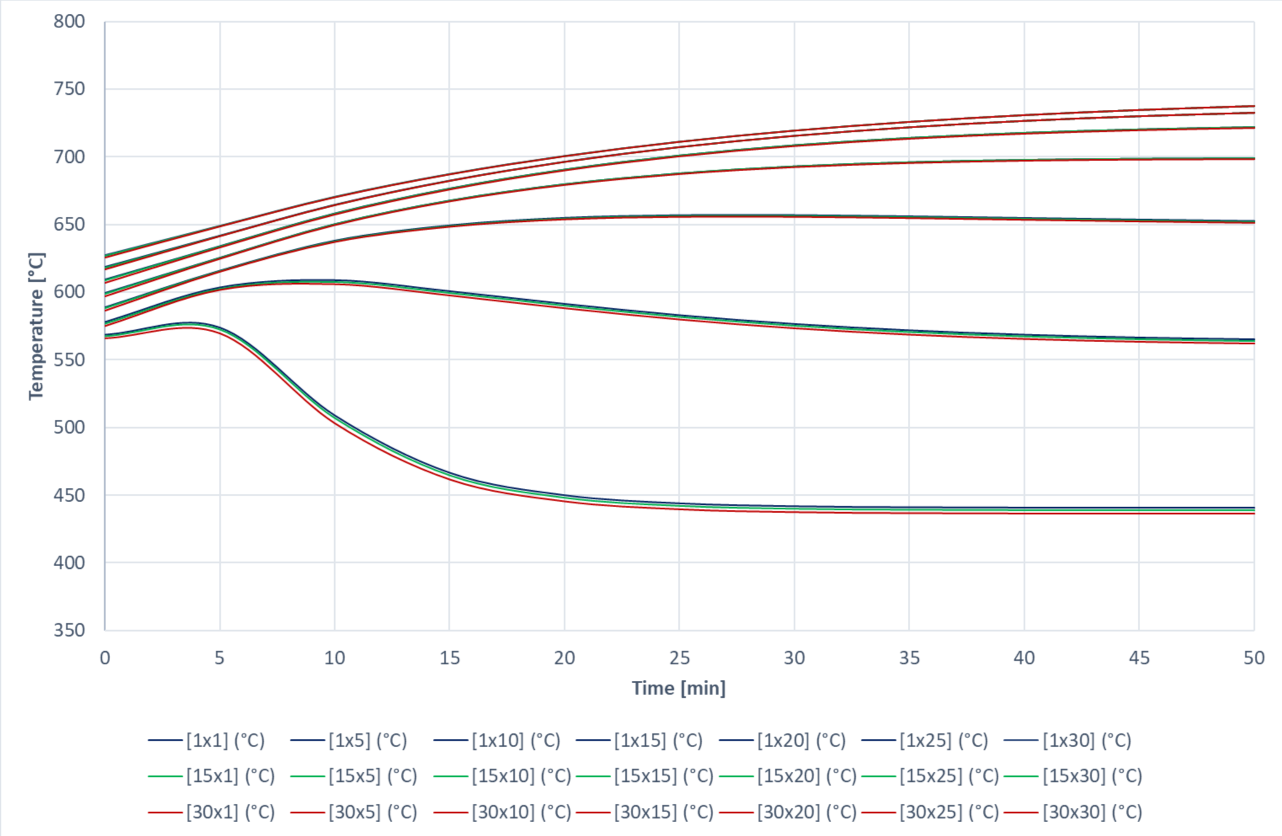

Figure 4.25 Scenario with smaller cooling effect over 50 minute period

Figure 4.25 shows a transient graph of a boiler scenario where the cooling effect is small, and the temperatures are still rising even after the 10 minutes. If no load change happens, and the water column can in fact remain for longer than 10 minutes, STO might occur.

With the material elasticity modulus and thermal expansion coefficient properties known along with the information extracted from the transient results, the possibility of short term overheating can be examined. The thick wall cylinder calculations determined the axial, circumferential, radial, thermal and finally the combined stresses over the tube wall for the various scenarios. The results for the thermal and Von Mises stresses are given in Figure 4.26, showing how the combined stress clearly increases as overfiring in the furnace takes place.

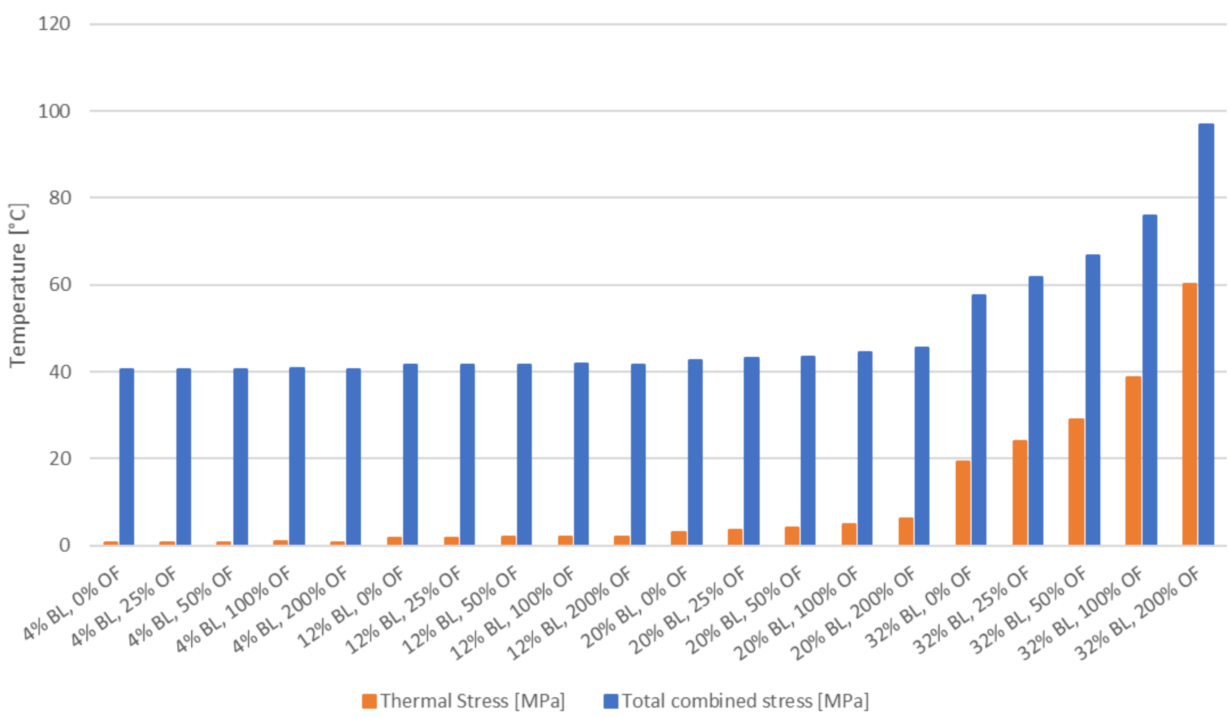

Figure 4.26 Thick wall cylinder stress results

Utilising the stress results and the tested lab results of old and new tube materials, a tube failure prediction can be made. The corresponding yield strength for the average wall temperature was determined from the graph as provided by the lab test results (both for the old and new tube). Finally, the calculated combined stress results for each scenario were considered.

If the yield strength of the tube material (either for the old or for the new tube samples) at the hottest tube temperature was less than the combined tube stress, it could be established that a tube failure might occur. These results are given in Figure 4.27.

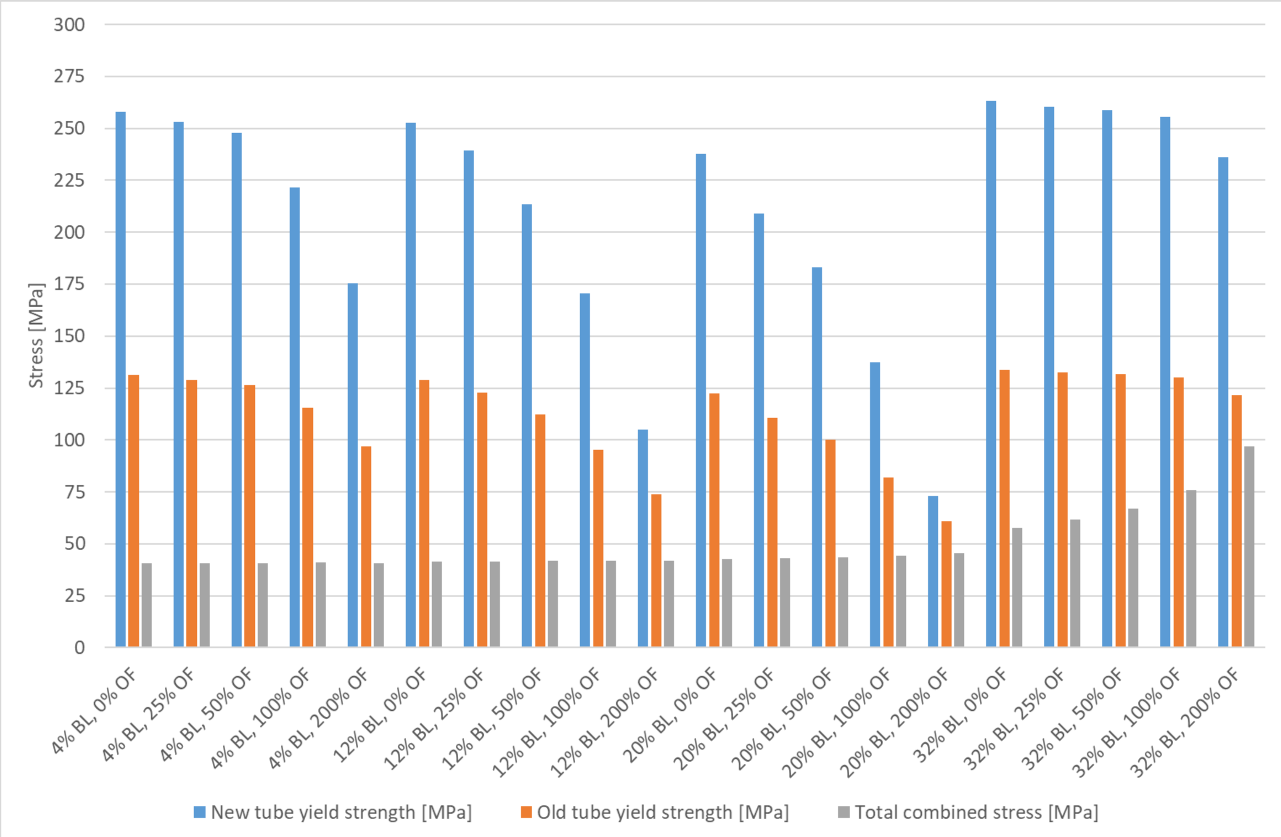

Figure 4.27 Graph indicating boiler failure

From Figure 4.27, it can be seen that the combined stress in the tube increases as the exposed outlet length of the pipe increases. An immediate observation that can be made from Figure 4.27 is that it appears that no boiler failure would occur due to water-wedging for any scenario under the specific circumstances, which is:

- A single primary tube failure;
- A complete water blockage occurrence, which evaporates due to heat from the furnace;
- A failure occurring on the outlet side of the tube;
- A failure that is not influenced by its surrounding tubes or elements;
- A sudden onset event (less than 10 minutes) of short term overheating due to water-wedging;
- Up to 200% of overfiring.

Under these conditions, it appears that no failure will occur, whether it is on a piece of virgin tube recently installed, or on a tube that has been in service for several hundred thousand hours. The results do, however, indicate that an occurrence is more likely to occur on an old tube. The yield strength of the old tube material is approximately half of that of the virgin tube material for every temperature indicated.

Taking the scenario indicating that the tube is close to failure (for this project it would be scenario 20% BL, 200% OF) a failure might occur if the outlet leg of the superheater tube is lengthened enough to further restrict the cooling capabilities of the evaporating water-wedge. This can be simulated by lengthening the outlet tube in the Flownex® model, which showed that, for the specific scenario mentioned, the tube needs to be lengthened by approximately 80 m and combined with unlikely overfiring conditions before it should fail after ten minutes. Alternatively the event needs to remain for longer than 11 hours.

This proves that, under these specific conditions as explained throughout the project, it is unlikely that a boiler failure would occur during boiler start-up or low load due to poor operation, and water-wedging as a result alone.

5. Conclusion and recommendations

5.1 Conclusion

This study aimed to determine if short term overheating can occur in a coal fired boiler due to water-wedging, which is caused by over-attemperation. The study was conducted on the outlet leg of a pendant boiler tube. The scenarios considered were at low boiler loads, since the pressure difference over the boiler tube under such conditions may be small enough to allow for a still-standing water column.

A transient simulation model was created for the various scenarios. A water column was introduced into the boiler tube and allowed to evaporate over a time-period of ten minutes while constantly being replenished by attemperation water. The stresses at the outlet leg was then determined. This was done for cases where there was also a substantial amount of overfiring in the furnace.

The results showed that short term overheating is unlikely to occur, even at low loads or during boiler start-up, at superheater outlet tubes due to water blockages alone. The stresses exerted in the tube wall and throughout the tube length is not enough to overcome the yield strength at elevated temperatures of the superheater tube material, even for aged material.

It may be possible for overheating to occur under the conditions studied if the exposed tube length was much longer. However, the superheater geometry becomes unrealistic and is not a practical approach to what authentically occurs in an Eskom boiler. Alternatively, the duration must be substantially more than 10 minutes, but it is unlikely that a standing water column as postulated in this study could remain for a prolonged duration.

Thus, the claim of over-attemperation as the root cause of a short term overheating failure is void, and other explanations for the failure must be observed, especially after a tube replacement during a boiler outage. Even though it is possible for water-wedging to occur, the phenomenon alone is unlikely the root cause for the occurrence of short term overheating.

It is however possible for the tube material to experience a thermal excursion which greatly exceeds its design limits. If this even occurs repeatedly, a form of thermal fatigue or accelerated creep can result.

5.2 Recommendations

The following recommendations are made for future study regarding the contents of the project discussed in this document:

- Studying a single tube in relation to the effects generated by the rest of the tube bundle (surrounding tubes).
- Studying a detailed start-up scenario, whereby a transient model is run, increasing the boiler load from 0 MW and accounting for the introduction of oil burners and pressure ramping etc.
- Studying the effects under the same conditions as explained in this document together with a varying scale component.
- Studying the possibility that a solid blockage (occurring due to poor care taken during maintenance activities) could more likely be the cause of short term overheating during a unit start-up, rather than a water blockage.
- Studying a scenario where there is already condensate in the superheater at start-up, which needs to heated up and boil out first.
- Studying the occurrence of short term overheating as a result of accelerated creep due to repetitive high-temperature events.

6. Bibliography

[1] Eskom, *Boiler Module 6: Boiler Steam System,* 2006.

[2] *Boiler Tube Failures in Eskom Coal Fired Power Stations.* [Film]. South Africa: Hooligan Picture Creations, 2012.

[3] R. Tarr, Interviewee, *Boiler information.* [Interview]. 3 June 2015.

[4] *Confidential: Special Permission Obtained from Eskom Holdings Ltd.*

[5] M. Rahman, J. Purbolaksono and J. Ahmad, "Root cause failure analysis of a division wall superheater tube of a coal-fired power station," *Elsevier,* pp. 1490-1494, 2010.

[6] Babcock & Wilcox, "Boiler Tube Analysis: Reduce Future Boiler Tube Failures".

[7] J. Ahmad, J. Purbolaksono and L. Beng, "Tube failures due to cooling process problem and foreign materials in power plants," *Elsevier,* p. 1882–1886, 2010.

[8] S. Chaudhuri, "Some aspects of metallurgical assessment of boiler tubes—Basic principles and case studies," *Elsevier,* pp. 90-99, 2006.

[9] J. Perdomo and T. Spry, "An Overheat Boiler Tube Failure," *ASM International,* no. 2, pp. 25-28, 2005.

[10] J. Purbolaksono, J. Ahmad, L. Beng, A. Rashid, A. Khinani and A. Ali, "Failure analysis on a primary superheater tube of a power plant," *Elsevier,* pp. 158-167, 2009.

[11] ASME Standards Technology, LLC, *Design Guidelines for the Effects of Corrosion, Erosion and Oxidation for Boiler Tube Components,* New York, 2011.

[12] D. DeWitt-Dick, S. McIntyre and J. Hofilena, "Boiler Failure Mechanisms," Ashland Specialty Chemical Company, Maryland.

[13] S. Jafar, "Failure Characteristics Of Boiler Pipes In Al-Emsaeb Electric Power Plants," *Journal of Babylon University,* vol. 20, no. 1, pp. 87-99, 2012.

[14] S. Bamrotwar and V. Deshpande, "Root Cause Analysis and Economic Implication of Boiler Tube Failures in 210 MW Thermal Power Plant," *Journal of Mechanical and Civil*

Engineering, pp. 6-10, 2012.

[15] *Confidential: Special permission Obtained from Eskom Holdings Ltd.*

[16] Eskom, *GPSS Data,* 2016.

[17] *Confidential: Special Permission Obtained from Eskom Holdings Ltd.*

[18] K. Coleman, "Short Term Overheating in Waterwall or Evaporator Tubing," in *Boiler and Heat Recovery Steam Generator Tube Failures: Theory and Practice Volume 2: Water-Touched Tubes*, California, Electric Power Research Institute, 2011, pp. 361-367.

[19] N. Mertens, F. Alobaid, R. Starkloff, B. Epple and H. Kim, "Comparative investigation of drum-type and once-through heat recovery steam generator during start-up," *Elsevier,* vol. 144, pp. 250-260, 2015.

[20] B. Munson, D. Younf, T. Okiishi and W. Huebsch, Fundamentals of Fluid Dynamics, Asia: John Wiley & Sons, 2010.

[21] Vinidex, "Hydraulic Design for PE Pippes," Vinidex (Pty) Ltd, 2016. [Online]. Available: http://www.vinidex.com.au/technical/pe-pressure-pipe/hydraulic-design-for-pe-pipes/. [Accessed 12 November 2016].

[22] F. Incropera, D. Dewitt, T. Bergman and L. A. , Principles of Heat and Mass Transfer, Singapore: John Wiley & Sons, 2013.

[23] A. Rossouw, "Boiler system modelling using Flownex®," University of Cape Town, Cape Town, 2015.

[24] C. MacGregor and N. Grossman, "Effects of Cyclic Loading on Mechanical Behavior of 24S-T4 and 75S-T6 Aluminum Alloys and SAE 4130 Steel," NACA TN 2812, Washington, 1952.

[25] Eskom, *C-schedules Confidential: Special Permission Obtained from Eskom Holdings Ltd..*

[26] D. Gandy, The Grade 22 Low Alloy Steel Handbook, California: EPRI, 2005.

[27] K. Hara and T. Rettig, "TubeMod technology for reduction of tube failures," 1995.

[28] Wolverine Tube, Inc., "Two-Phase Pressure Drops," in *Engineering Data Book III*, 2006, pp. 13-1-13-34.

[29] MTech Industrial, *Flownex Library Theory Manual,* 2014.

[30] R. Hibbeler, Mechanics of Materials, Singapore: Prentice Hall, 2011.

[31] Y. Zhu, *MAE 316 – Strength of Mechanical Components: Thick-Walled Cylinders (Notes,3.14),* North Carolina: North Carolina State University Department of Mechanical & Aerospace Engineering.

Appendix A. Boiler properties at various loads

The graphs below show various boiler properties (regarding flue gas, steam and spraywater) according to various load conditions completed in Mathcad. These values were extracted from the Eskom C-schedules for the specific power station that was used in this project [25]. Linear interpolation was utilized to determine the properties at other boiler load conditions as required.

Boiler load:

$$\mathrm{Load} := \begin{pmatrix} 424 \\ 599 \\ 618 \end{pmatrix} \mathrm{MW}$$

Flue gas (A):

$$T_{Ai} := \begin{pmatrix} 931 \\ 1022 \\ 1032 \end{pmatrix} {}^{\circ}\mathrm{C} \qquad T_{Ao} := \begin{pmatrix} 854 \\ 939 \\ 949 \end{pmatrix} {}^{\circ}\mathrm{C} \qquad m_A := \begin{pmatrix} 524.48 \\ 685.11 \\ 704.88 \end{pmatrix} \frac{\mathrm{kg}}{\mathrm{s}}$$

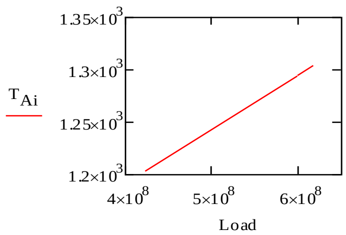

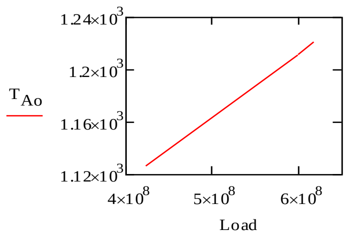

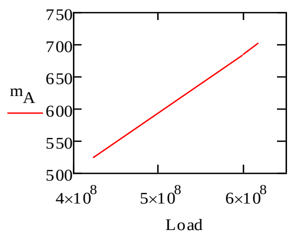

Steam (B):

$$T_{Bi} := \begin{pmatrix} 466 \\ 466 \\ 466 \end{pmatrix} {}^{\circ}\mathrm{C} \qquad T_{Bo} := \begin{pmatrix} 540 \\ 540 \\ 540 \end{pmatrix} {}^{\circ}\mathrm{C} \qquad m_B := \left(\frac{509.8\frac{\mathrm{kg}}{\mathrm{s}}}{618\mathrm{MW}} \right) \cdot \mathrm{Load} = \begin{pmatrix} 349.766 \\ 494.127 \\ 509.8 \end{pmatrix} \frac{\mathrm{kg}}{\mathrm{s}}$$

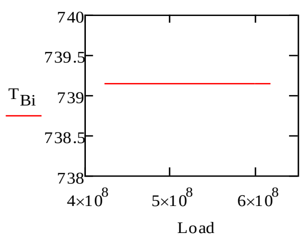

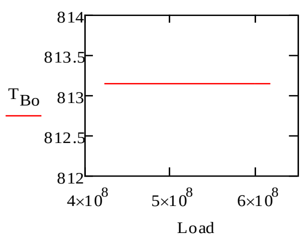

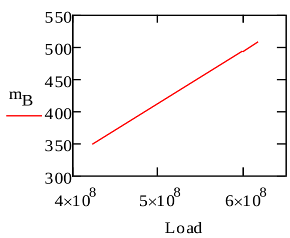

$$\Delta p_B := \begin{pmatrix} 0.27 \\ 0.51 \\ 0.53 \end{pmatrix} \mathrm{MPa} \qquad p_{Bo} := \begin{pmatrix} 17 \\ 17 \\ 17 \end{pmatrix} \mathrm{MPa}$$

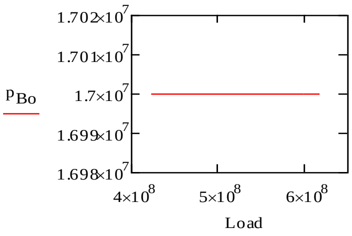

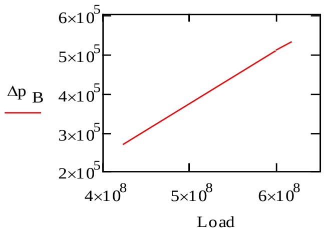

Spraywater (S):

$$p_S := \begin{pmatrix} 16.84 \\ 17.52 \\ 17.88 \end{pmatrix} \text{MPa} \qquad m_S := \begin{pmatrix} 3.5 \\ 4.95 \\ 5.1 \end{pmatrix} \frac{\text{kg}}{\text{s}} \qquad T_S := \begin{pmatrix} 230 \\ 247 \\ 249 \end{pmatrix} °\text{C}$$

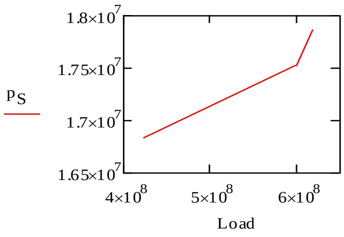

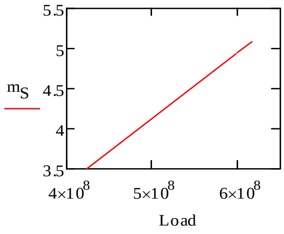

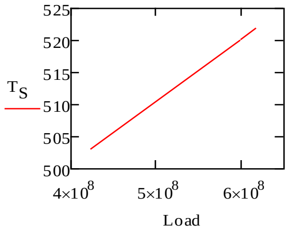

Appendix B. Analytical model

The following Mathcad model shows how the pressure drop over the final superheater tube, evaporation rate, evaporation time and tube length were calculated according to the calculations discussed in section 3 of this document.

Color code key

Desired results | Flownex use | From Flownex | Design values - constant | Design values - differs with load

Water column in pendant-type superheater calculations

The following data is based on the design of the final superheater tube A at Lethabo Power Station at a load given as:

$L_B := 75MW$

$L_{OF} := 155MW$

Tube geometry:

$D_o := 44.5mm$

$t_{t1} := 6.3mm$

$t_{t2} := 8.8mm$

$t_{t3} := 11mm$

$D_{i1} := D_o - 2t_{t1} = 31.9 \cdot mm$

$D_{i2} := D_o - 2t_{t2} = 26.9 \cdot mm$

$D_{i3} := D_o - 2t_{t3} = 22.5 \cdot mm$

$L_{t1} := 7761mm$

$L_{t2} := 16626mm$

$L_{t3} := 8261mm$

$L_t := L_{t1} + L_{t2} + L_{t3} = 32.648m$

$A_{ci.3} := \frac{\pi}{4} D_{i3}^{\,2} = 397.608mm^2$

$A_{ct} := \frac{\pi}{4}\left(D_o - D_{i3}\right)^2 = 380.133mm^2$

$k_t := 35\frac{W}{m \cdot K}$

$A_i := \pi\, D_{i1} \cdot L_{t1} + \pi\, D_{i2} \cdot L_{t2} + \pi \cdot D_{i3} \cdot L_{t3} = 2.767m^2$

$A_o := \pi\, D_o \cdot L_t = 4.564m^2$

$\varepsilon_t := 60\mu m$

Boiler properties dependant on load: (Boiler load)

Flue gas properties:

$T_{fgi} := \text{linterp}\left(Load, T_{Ai}, L_{OF}\right) = 791.12°C$ overfiring load)

$T_{fgo} := \text{linterp}\left(Load, T_{Ao}, L_{OF}\right) = 723.343°C$

$T_{fg} := \frac{\left(T_{fgi} + T_{fgo}\right)}{2} = 757.231°C$

$cp_{fg} := 1.006\frac{kJ}{kg \cdot K}$

$m_{fg} := \text{linterp}\left(Load, m_A, L_{OF}\right) = 277.569\frac{kg}{s}$

$\Delta p_{fg} := \text{linterp}\left(Load, \Delta p_A, L_{OF}\right) = 0.04MPa$

Boundary conditions:

$T_i := \text{linterp}\left(Load, T_{Bi}, L_B\right) = 466 \cdot °C$

$T_o := 540°C$

$\Delta T := T_o - T_i = 74K$

$T_{avg} := \frac{\left(T_i + T_o\right)}{2} = 503 \cdot °C$

$p_o := \text{linterp}\left(Load, p_{Bo}, L_B\right) = 17 \cdot MPa$

$\Delta p := \text{linterp}\left(Load, \Delta p_B, L_B\right) =$ [redacted] $\cdot MPa$

$m_{ftot} := \text{linterp}\left(Load, m_B, L_B\right) = 61.869\frac{kg}{s}$

$m_f := \frac{m_{ftot}}{4 \cdot 7 \cdot 34} = 0.065\frac{kg}{s}$

$$cp_f := Cp_{steam}(p_o, T_o, "" , "" , "" , "") = 2.84\,\frac{kJ}{kg}$$

$$\rho_f := \rho_{steam}(p_o, T_o, "" , "" , "") = 51.095\,\frac{kg}{m^3}$$

$$v_f := \frac{m_f}{\rho_f \cdot A_{ci.3}} = 3.199\,\frac{m}{s}$$

$$\mu_f := \mu_{steam}(p_o, T_o, "" , "" , "" , "") = 3.125\times 10^{-5}\,\frac{kg}{m\cdot s}$$

$$Pr_f := Pr_{steam}(p_o, T_o, "") = 1.02$$

$$k_f := \lambda_{steam}(p_o, T_o, "" , "" , "" , "") = 0.087\,\frac{W}{m\cdot K}$$

Calculation of pressure drop through each superheater section:

$$Re_{f1} := \frac{4m_f}{\pi\, D_{i1}\cdot \mu_f} = 8.301\times 10^4$$

$$Re_{f2} := \frac{4m_f}{\pi\, D_{i2}\cdot \mu_f} = 9.844\times 10^4$$

$$Re_{f3} := \frac{4m_f}{\pi\, D_{i3}\cdot \mu_f} = 1.177\times 10^5$$

$$f_{f1} := 0.25\left[\log\left[0.27\cdot\left(\frac{\varepsilon_t}{D_{i1}}\right) + \frac{5.74}{Re_{f1}^{\,0.9}}\right]\right]^{-2} = 0.025$$

$$f_{f2} := 0.25\left[\log\left[0.27\cdot\left(\frac{\varepsilon_t}{D_{i2}}\right) + \frac{5.74}{Re_{f2}^{\,0.9}}\right]\right]^{-2} = 0.026$$

$$f_{f3} := 0.25\left[\log\left[0.27\cdot\left(\frac{\varepsilon_t}{D_{i2}}\right) + \frac{5.74}{Re_{f3}^{\,0.9}}\right]\right]^{-2} = 0.026$$

$$ratio_1 := \frac{D_{i2}}{D_{i1}} = 0.843$$

$$ratio_2 := \frac{D_{i3}}{D_{i2}} = 0.836$$

$$\Sigma K_1 := 0.05 + 0.03 = 0.08$$

$$\Sigma K_2 := 0.267 + 0.367 + 0.267 + 0.03 = 0.931$$

$$\Sigma K_3 := 1 = 1$$

View Secondary Frictional Losses

$$\Delta p_1 := \left[\frac{(f_{f1}\cdot L_{t1})}{D_{i1}} + \Sigma K_1\right]\cdot\frac{\rho_f\cdot v_f^2}{2} = 1.632\times 10^{-3}\cdot MPa$$

$$\Delta p_2 := \left[\frac{(f_{f2}\cdot L_{t2})}{D_{i2}} + \Sigma K_2\right]\cdot\frac{\rho_f\cdot v_f^2}{2} = 4.435\times 10^{-3}\cdot MPa$$

$$\Delta p_3 := \left[\frac{(f_{f3}\cdot L_{t3})}{D_{i3}} + \Sigma K_3\right]\cdot\frac{\rho_f\cdot v_f^2}{2} = 2.727\times 10^{-3}\cdot MPa$$

$$\Delta p := \Delta p_1 + \Delta p_2 + \Delta p_3 = 8.794\times 10^{-3}\cdot MPa$$

$$p_i := p_o + \Delta p = 17.009\,MPa$$

$$p_{avg} := \frac{(p_i + p_o)}{2} = 17.004\,MPa$$

$$\mu_{avg} := \mu_{steam}(p_{avg}, T_{avg}, "" , "" , "" , "") = 2.972\times 10^{-5}\,\frac{kg}{m\cdot s}$$

$$Re_{avg} := \frac{4m_f}{\pi\, D_{i3}\cdot \mu_{avg}} = 1.238\times 10^5$$

Attemperating 2nd stage spraywater properties:

$$m_{att.total} := linterp(Load, m_S, L_B) = 0.608\,\frac{kg}{s}$$

$$f_{avg} := 0.25\left[\log\left[0.27\cdot\left(\frac{\varepsilon_t}{D_{i2}}\right) + \frac{5.74}{Re_{avg}^{\,0.9}}\right]\right]^{-2} = 0.026$$

$$m_{att} := \frac{m_{att.total}}{7\cdot 34} = 2.556\times 10^{-3}\,\frac{kg}{s}$$

$$p_{att} := linterp(Load, p_S, L_B) = 15.484\,MPa$$

$$T_{att} := linterp(Load, T_S, L_B) = 196.097\,°C$$

$$h_{att} := h_{steam}(p_{att}, T_{att}, "" , "" , "") = 841.117\,\frac{kJ}{kg}$$

Heat transfer calculations:

$$\begin{pmatrix} L_{raw} \\ h_{raw} \end{pmatrix} :=$$

Overfiring Load [MW]	Heat transfer coefficient [W/m2.K]
25	6.359
125	30.568
155	35.949
200	42.904
309	55.77
464	68.174
618	76.434

$$h_o := \mathrm{linterp}(L_d, h_d, L_{OF}) = 35.949\,\frac{W}{m^2K}$$

If plugged:

$$T_{sat} := T_{steam}(p_{avg}, "", "", "") = 352.315\,°C$$

$$\rho_w := \rho_{steam}("", T_{sat}, 0, "", "") = 565.092\,\frac{kg}{m^3}$$

Outlet leg steam properties:

$$p_{st} := p_o = 17\cdot MPa$$

$$\rho_{st} := \rho_{steam}(p_{st}, "", 1, "", "") = 119.485\,\frac{kg}{m^3}$$

$$cp_{st} := Cp_{steam}(p_{st}, "", "", 1, "", "") = 18.31\cdot\frac{k}{kg}$$

Water column calculations:

$$h_{top} := 71305\,mm$$

$$h_{bot} := 56000\,mm$$

$$h_t := h_{top} - h_{bot} = 15.305\,m$$

$$\Delta h := \frac{\Delta p}{(\rho_w - \rho_{st})\cdot g} = 2.012\,m$$

$$h_{st} := \begin{vmatrix} h_t - \Delta h & \text{if } (h_t - \Delta h) > 0 \\ h_t & \text{if } (h_t - \Delta h) \le 0 \end{vmatrix}$$

$$h_{st} = 13.293\,m$$

$$p_{wl} := \rho_{st}\cdot g\cdot h_t + p_o = 17.018\,MPa$$

$$T_{wl} := T_{steam}(p_{wl}, "", "", "") = 352.38\,°C$$

$$L_{wc} := \begin{vmatrix} 1.744\Delta h & \text{if } \Delta h < 1371\,mm \\ \Delta h + 1019\,mm & \text{if } \Delta h \ge 1371\,mm \end{vmatrix}$$

$$L_w := \begin{vmatrix} L_{wc} & \text{if } L_{wc} \le 30610\,mm \\ 0 & \text{if } L_{wc} > 30610\,mm \end{vmatrix}$$

$$L_w = 3.031\,m$$

$$A_{wo} := \pi\, D_o\cdot L_w + \pi\, D_o^2 = 0.43\,m^2$$

$$V_w := \pi\left(\frac{D_{i3}}{2}\right)^2\cdot L_w = 1.205\,L$$

$$m_w := V_w\cdot\rho_w = 0.681\,kg$$

If plugged (cont):

$$L_{new} := \begin{vmatrix} L_w & \text{if } L_w > 0 \\ h_{st} & \text{if } L_w = 0 \end{vmatrix}$$

$$R_{new} := \left(\frac{1}{h_o\cdot A_{wo}}\right) + \frac{\ln\left(\frac{D_o}{D_{i3}}\right)}{2\pi\, k_t\cdot L_{new}} = 0.066\,\frac{K}{W}$$

$$Q_p := \frac{T_{fg} - T_{sat}}{R_{new}} = 6.162\,kW$$

$$h_{fe} := h_{steam}(p_{wl}, "", "", 0, "") = 1.691\times 10^3\cdot\frac{kJ}{kg}$$

$$h_{ge} := h_{steam}(p_{wl}, "", "", 1, "") = 2.547\times 10^3\cdot\frac{kJ}{kg}$$

$$h_{fge} := h_{ge} - h_{fe} = 856.005\,\frac{kJ}{kg}$$

$$m_e := \frac{Q_p}{h_{fge}} = 7.199\times 10^{-3}\,\frac{kg}{s}$$

$$\Delta h_e := h_{ge} - h_{att} = 1.706\times 10^3\cdot\frac{kJ}{kg}$$

$$t_e := \frac{m_w\cdot\Delta h_e}{Q_p} = 188.534\,s$$

Appendix C. Heat transfer analysis

The Mathcad calculations below shows how the heat transfer coefficient from the flue gas in the furnace was calculated as explained in section 3.2.2 of this document. These results were used to create a table in order to utilise the correct heat transfer coefficient in the model of Appendix B due to overfiring conditions.

$$h_{fi} := h_{steam}\left(p_i, T_i, \text{""}, \text{""}, \text{""}\right) = 3.176\times 10^{3}\cdot\frac{kJ}{kg}$$

$$h_{fo} := h_{steam}\left(p_o, T_o, \text{""}, \text{""}, \text{""}\right) = 3.401\times 10^{3}\cdot\frac{k}{k}$$

$$Q_f := m_f\cdot h_{fo} - \left(m_f - m_{att}\right)\cdot h_{fi} - m_{att}\cdot h_{att} = 20.6$$

$$n := 0.4$$

$$Nu_f := \begin{cases} 3.66 & \text{if } Re_{f3} \le 2300 \\ 0.023 Re_{f3}^{\frac{4}{5}}\, Pr_f^{\,n} & \text{if } Re_{f3} > 2300 \end{cases}$$

$$Nu_f = 264.095$$

$$h_i := \frac{Nu_f\cdot k_f}{D_{i3}} = 1.021\times 10^{3}\cdot\frac{W}{m^2 K}$$

$$R_i := \frac{1}{h_i\cdot A_i} = 3.539\times 10^{-4}\cdot\frac{K}{W}$$

$$R_t := \frac{\ln\left(\frac{D_o}{D_{i3}}\right)}{2\pi\, k_t\cdot L_t} = 9.499\times 10^{-5}\cdot\frac{K}{W}$$

$$T_{to} := Q_f\cdot\left(R_i + R_t\right) + T_{avg} = 512.251\,°C$$

$$L_d := L_{raw}\cdot MW$$

$$R_{tot} := \frac{\left(T_{fg} - T_{avg}\right)}{Q_f} = 0.012\frac{K}{W}$$

$$h_d := h_{raw}\cdot\frac{W}{m^2 K}$$

$$R_o := R_{tot} - R_i - R_t = 0.012\frac{K}{W}$$

$$h_o := \frac{1}{R_o\cdot A_o} = 18.428\frac{W}{m^2\cdot K}$$

Appendix D. Thick wall cylinder stresses

The Mathcad calculations below shows how the material stresses were calculated as explained in section 3.4 of this document.

Thick-walled cylinder stress calculations:

$$r_i := \frac{D_{i3}}{2} = 0.011\,\mathrm{m}$$

$$r_o := \frac{D_o}{2} = 0.022\,\mathrm{m}$$

$$p_1 := 17.003\,\mathrm{MPa}$$

$$p_2 := 100\,\mathrm{kPa}$$

$$t_t := t_{t3} = 0.011\,\mathrm{m}$$

$$r_m := \frac{(r_i + r_o)}{2}$$

$$\mathrm{ratio} := \frac{r_m}{t_t} = 1.523$$

Axial stress:

$$\sigma_a := \frac{\left(p_1 \cdot r_i^2 - p_2 \cdot r_o^2\right)}{r_o^2 - r_i^2} = 5.705\,\mathrm{MPa}$$

Circumferential stress (hoop):

$$\sigma_c := \frac{p_1 \cdot r_i^2 - p_2 \cdot r_o^2}{r_o^2 - r_i^2} - r_i^2 \cdot r_o^2 \cdot \frac{(p_2 - p_1)}{r_i^2 \cdot \left(r_o^2 - r_i^2\right)} = 2$$

$$\sigma_h := p_1 \cdot \frac{\left(r_i + \frac{t_t}{2}\right)}{t_t} = 25.891\,\mathrm{MPa}$$

Radial stress:

$$\sigma_{ro} := \frac{p_1 \cdot r_i^2 - p_2 \cdot r_o^2}{r_o^2 - r_i^2} + r_i^2 \cdot r_o^2 \cdot \frac{(p_2 - p_1)}{r_o^2 \cdot \left(r_o^2 - r_i^2\right)} = -0.1 \cdot \mathrm{M}$$

$$\sigma_{ri} := \frac{p_1 \cdot r_i^2 - p_2 \cdot r_o^2}{r_o^2 - r_i^2} + r_i^2 \cdot r_o^2 \cdot \frac{(p_2 - p_1)}{r_i^2 \cdot \left(r_o^2 - r_i^2\right)} = -17.003\mathrm{M}$$

$$\sigma_r := \begin{vmatrix} \sigma_{ro} \text{ if } |\sigma_{ro}| > |\sigma_{ri}| \\ \sigma_{ri} \text{ if } |\sigma_{ri}| > |\sigma_{ro}| \end{vmatrix} = -17.003\,\mathrm{MPa}$$

Thermal stresses (Mechanics of Materials, Hibbeler):

$$T_{wi} := 807.71\,°\mathrm{C}$$

$$\begin{pmatrix} T_{raw} \\ E_{raw} \\ \alpha_{raw} \end{pmatrix} :=$$

Temperature [K]	Elastic modulus [MPa]	Thermal expansion [µm/m/K
283.15	211898.87	11.55
310.93	209600.62	11.70
338.71	207532.19	11.70
366.48	205463.77	11.88
394.26	204084.82	12.24
422.04	202705.86	12.42
449.82	200637.44	12.57
477.59	198569.01	12.73
505.37	196845.32	12.87
533.15	195121.63	13.01
560.93	193053.20	13.15
588.71	190984.78	13.28
616.48	188916.35	13.39
644.26	186847.92	13.50
672.04	183400.54	13.61
699.82	181332.12	13.72
727.59	178574.21	13.82
755.37	176505.79	13.91
783.15	173058.41	14.00
810.93	169611.03	14.08
838.71	166853.13	14.15
866.48	163405.75	14.22
894.26	159268.89	14.29
922.04	155132.04	14.35
949.82	150995.18	14.40
977.59	146858.33	14.45
1005.37	142721.48	14.51
1033.15	138584.62	14.56
1060.93	134447.77	14.62
1088.71	130310.91	14.67

$$T_d := T_{raw} \cdot \mathrm{K}$$

$$T_{wo} := 813.16\,°\mathrm{C}$$

$$E_d := E_{raw} \cdot \mathrm{MPa}$$

$$T_{wavg} := \frac{(T_{wi} + T_{wo})}{2} = 1.084 \times 10^3 \cdot \mathrm{K}$$

$$\alpha_d := \alpha_{raw} \cdot \frac{\frac{\mu\mathrm{m}}{\mathrm{m}}}{\mathrm{K}}$$

$$\Delta T_w := T_{wo} - T_{wi} = 5.45\,\mathrm{K}$$

$$E_w := \mathrm{linterp}(T_d, E_d, T_{wavg}) = 1.311 \times 10^{-4} \cdot \mathrm{GPa}$$

$$\alpha_w := \text{linterp}(T_d, \alpha_d, T_{wavg}) = 14.66\frac{1}{K}$$

$$\nu_w := 0.3$$

$$\sigma_{th} := \frac{(\alpha_w \cdot E_w)}{1-\nu_w} \cdot \Delta T_w = 14.961\text{MPa}$$

Combined stress (Von Mises):

$$\sigma_x := \sigma_a = 5.705\text{MPa}$$

$$\sigma_y := \sigma_c + \sigma_{th} = 43.374\text{MPa}$$

$$\sigma_z := \sigma_r = -17.003\text{MPa}$$

$$A_v := \sigma_x + \sigma_y + \sigma_z = 32.077\text{MPa}$$

$$B_v := \sigma_x \cdot \sigma_y + \sigma_y \cdot \sigma_z + \sigma_x \cdot \sigma_z = -587.035\text{MPa}^2$$

$$C_v := \sigma_x \cdot \sigma_y \cdot \sigma_z = -4.208 \times 10^3 \cdot \text{MPa}^3$$

$$\sigma_1 := \max(\sigma_x, \sigma_y, \sigma_z) = 43.374\text{MPa}$$

$$\sigma_2 := A_v - \sigma_y - \sigma_z = 5.705\text{MPa}$$

$$\sigma_3 := \min(\sigma_x, \sigma_y, \sigma_z) = -17.003\text{MPa}$$

$$\sigma_{vm} := \sqrt{\frac{(\sigma_1-\sigma_2)^2 + (\sigma_2-\sigma_3)^2 + (\sigma_3-\sigma_1)^2}{2}} = 52.821\text{MPa}$$

Appendix E. Calculated evaporation rates

Table 6-1 below illustrates the calculated results of the evaporation rate and the time to reach this evaporation rate for each scenario simulated in the Flownex® transient model using eq. (3-22) and eq. (3-29) of section 3.3.2, respectively.

Table 6-1 Rate of evaporations for scenarios

Scenario	Time [s]	m_e [kg/s]
4% BL, 0% OF	847	0.0001
4% BL, 25% OF	711	0.0002
4% BL, 50% OF	596	0.0002
4% BL, 100% OF	465	0.0002
4% BL, 200% OF	315	0.0003
12% BL, 0% OF	365	0.0024
12% BL, 25% OF	289	0.0030
12% BL, 50% OF	240	0.0036
12% BL, 100% OF	182	0.0047
12% BL, 200% OF	129	0.0067
20% BL, 0% OF	213	0.0084
20% BL, 25% OF	174	0.0102
20% BL, 50% OF	149	0.0120
20% BL, 100% OF	118	0.0152
20% BL, 200% OF	84	0.0214
32% BL, 0% OF	139	0.0269
32% BL, 25% OF	116	0.0322
32% BL, 50% OF	99	0.0378
32% BL, 100% OF	78	0.0478
32% BL, 200% OF	55	0.0674

Appendix F. Sensitivity Analysis

The analysis below is a summary of the data extracted from the Flownex® model under steady state conditions (32% BL, 100% OF) to determine the amount of increments required for both the tube wall and the length. The final recommendation was a 30x30 grid.

Temperatures in °C

Sensitivity analysis of temperatures through tube wall to determine number of wall thickness elements

	1X10		5X10		10X10		20X10		30X10		40X10		50X10	
	E1	E10	E1	E10	E1	E10	E1	E10	E1	E10	E1	E10	E1	E10
WT1	367.26	371.92	369.41	374.05	369.61	373.22	369.7	374.23	369.73	374.37	369.74	374.28	369.75	374.29
WT5			365.53	370.12										
WT10					365.23	369.82								
WT20							365.07	369.66						
WT30									365.01	369.6				
WT40											364.99	369.68		
WT50													364.97	369.66

Sensitivity analysis over tube length to determine number of tube length elements

	30X5		30X10		30X20		30X30		30X40		30X50		30X60	
	E1	E5	E1	E20	E1	E20	E1	E30	E1	E40	E1	E50	E1	E60
WT1	369.97	374.12	369.73	374.37	369.64	374.36	369.62	374.49	369.61	374.39	369.61	374.5	369.6	374.5
WT30	365.25	369.36	365.01	369.6	364.92	369.81	364.89	369.73	364.88	369.84	364.87	369.74	364.87	369.74

Wall thickness increment roughness analysis (A)

X	[1x1]	[nx1]	[1x10]	[nx10]
1x10	367.26	367.26	371.92	371.92
5x10	369.41	365.53	373.22	370.12
10x10	369.61	365.23	374.23	369.82
20x10	369.7	365.07	374.37	369.66
30x10	369.73	365.01	374.28	369.6
40x10	369.74	364.99	374.29	369.68
50x10	369.75	364.97	374.29	369.66

Tube length increment roughness analysis (B)

X	[1x1]	[1xn]	[30x1]	[30xn]
30x5	369.97	374.12	365.25	369.36
30x10	369.73	374.37	365.01	369.6
30x20	369.64	374.36	364.92	369.81
30x30	369.62	374.49	364.89	369.73
30x40	369.61	374.39	364.88	369.84
30x50	369.61	374.5	364.87	369.74
30x60	369.6	374.5	364.87	369.74

AxB where A = wall thickness element
B = tube length element

Conditions: 200 MW
Action setup: 100% load conditions

Figure 6.1 Sensitivity analysis performed to determine number of increments through tube length and wall for Flownex® model

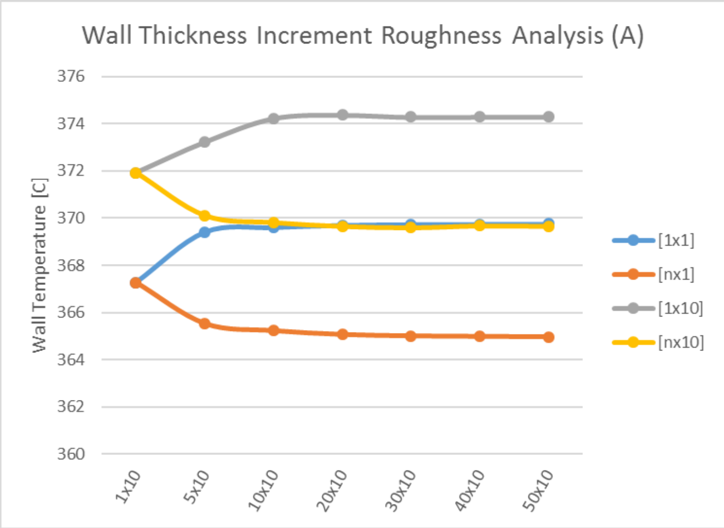

Figure 6.2 Wall thickness increment roughness graph

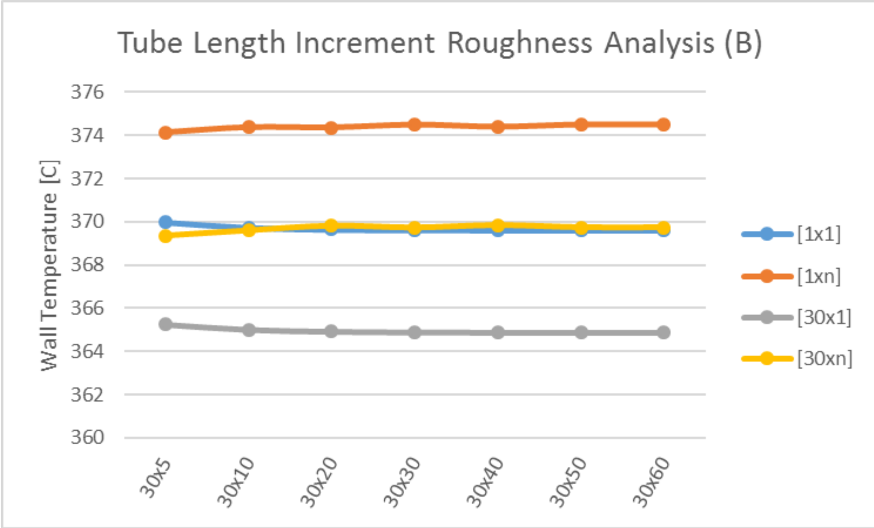

Figure 6.3 Tube length increment roughness analysis graph

Appendix G. Geometry specifications

The following figures explain what geometry specifications was used for each boiler load condition. The water column illustrated is not necessarily a true representation – refer to section length values to determine where the water wedge would end (explained in section 4.4). Each condition also applies for its associated overfiring scenarios

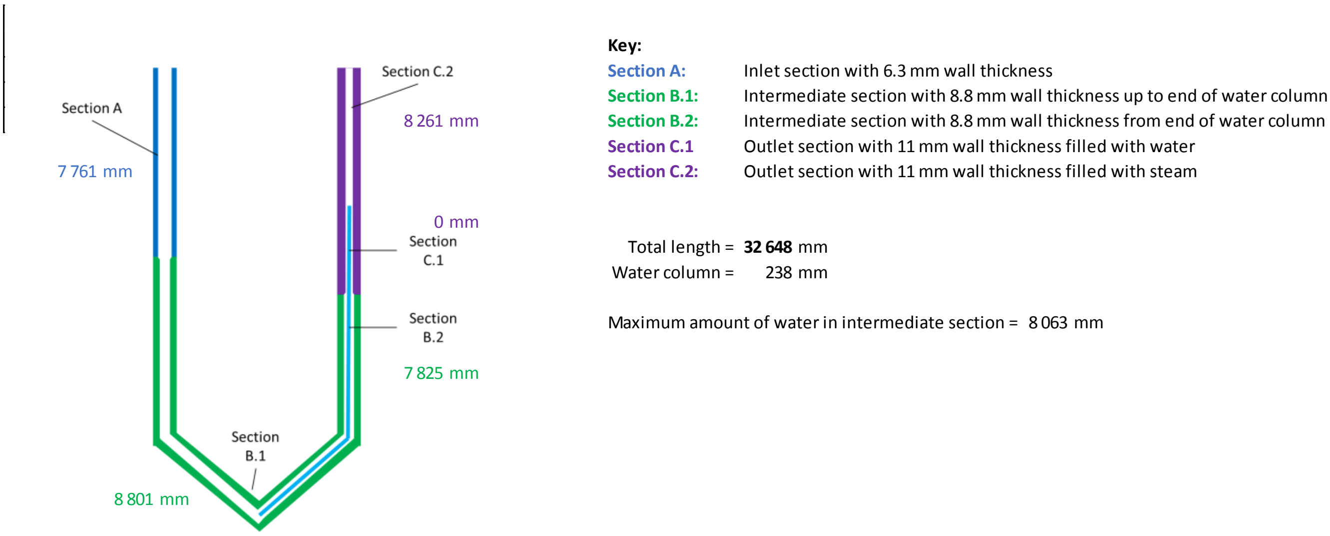

Figure 6.4 Scenario of blocked superheater tube at 4% boiler load

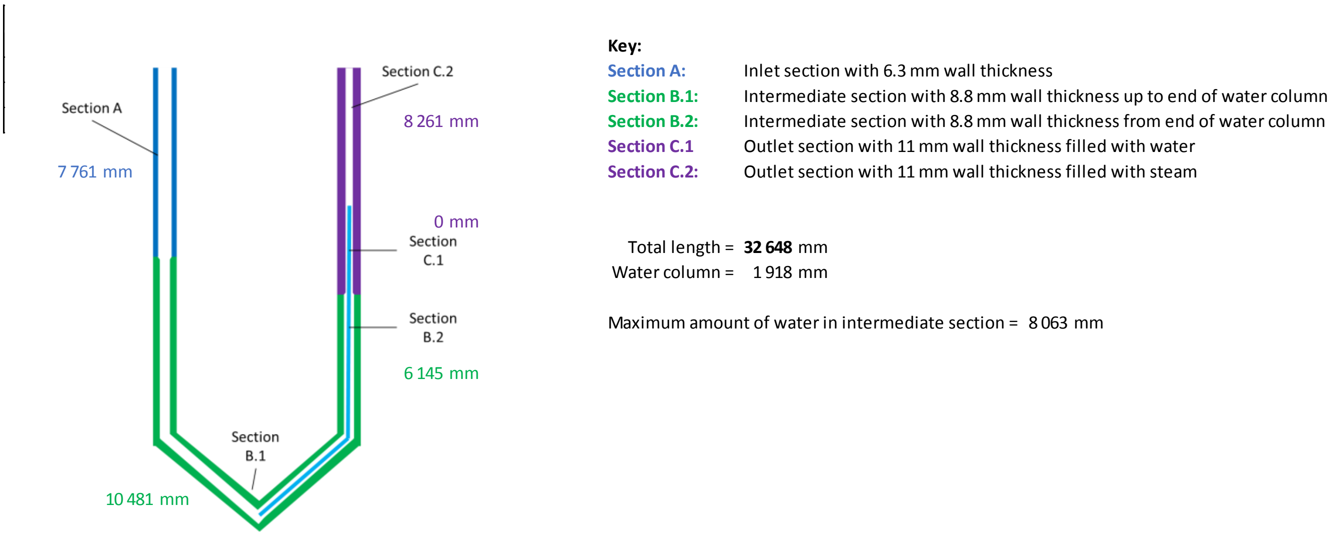

Figure 6.5 Scenario of blocked superheater tube at 12% boiler load

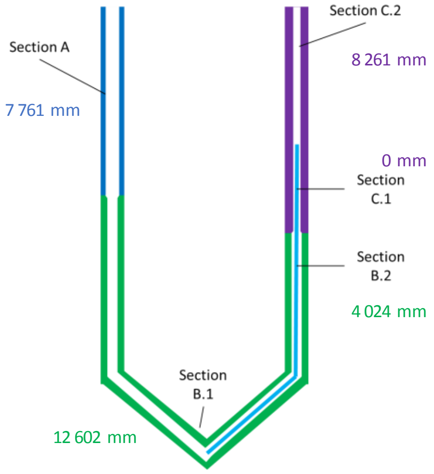

Key:

Section A:	Inlet section with 6.3 mm wall thickness
Section B.1:	Intermediate section with 8.8 mm wall thickness up to end of water column
Section B.2:	Intermediate section with 8.8 mm wall thickness from end of water column
Section C.1	Outlet section with 11 mm wall thickness filled with water
Section C.2:	Outlet section with 11 mm wall thickness filled with steam

Total length = **32 648** mm
Water column = 4 039 mm

Maximum amount of water in intermediate section = 8 063 mm

Figure 6.6 Scenario of blocked superheater tube at 20% boiler load

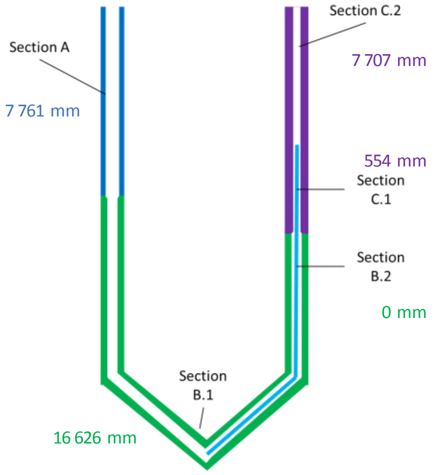

Key:

Section A:	Inlet section with 6.3 mm wall thickness
Section B.1:	Intermediate section with 8.8 mm wall thickness up to end of water column
Section B.2:	Intermediate section with 8.8 mm wall thickness from end of water column
Section C.1	Outlet section with 11 mm wall thickness filled with water
Section C.2:	Outlet section with 11 mm wall thickness filled with steam

Total length = **32 648** mm
Water column = 8 617 mm

Maximum amount of water in intermediate section = 8 063 mm

Figure 6.7 Scenario of blocked superheater tube at 32% boiler load

Appendix H. Complete results

Figure 6.8 gives the complete results from the study discussed in this dissertation. The table includes all of the scenarios examined, input properties, calculation results and all results acquired from the Flownex® model.

Scenario	4% BL, 0% OF	4% BL, 25% OF	4% BL, 50% OF	4% BL, 100% OF	4% BL, 200% OF	12% BL, 0% OF	12% BL, 25% OF	12% BL, 50% OF	12% BL, 100% OF	12% BL, 200% OF	20% BL, 0% OF	20% BL, 25% OF	20% BL, 50% OF	20% BL, 100% OF	20% BL, 200% OF	32% BL, 0% OF	32% BL, 25% OF	32% BL, 50% OF	32% BL, 100% OF	32% BL, 200% OF
Full boiler load %	**4%**	**4%**	**4%**	**4%**	**4%**	**12%**	**12%**	**12%**	**12%**	**12%**	**20%**	**20%**	**20%**	**20%**	**20%**	**32%**	**32%**	**32%**	**32%**	**32%**
Overfiring % on running boiler load	**0%**	**25%**	**50%**	**100%**	**200%**	**0%**	**25%**	**50%**	**100%**	**200%**	**0%**	**25%**	**50%**	**100%**	**200%**	**0%**	**25%**	**50%**	**100%**	**200%**
FG temperature [°C]	691.86	694.88	698.40	704.43	717.00	716.50	726.05	735.11	753.71	790.92	741.64	757.23	772.82	804.00	866.35	778.85	804.00	828.64	878.42	977.99
FG mass flow rate [kg/s]	158.24	163.75	170.18	181.19	204.14	203.22	220.66	237.18	271.14	339.07	249.11	277.57	306.02	362.93	476.75	317.04	362.93	407.91	498.78	680.52
Heat transfer coefficient [W/m^2.K]	8.165	9.657	11.398	14.383	20.602	20.353	25.079	29.556	37.288	48.421	32.789	38.582	43.519	51.579	64.120	45.430	51.579	57.530	66.076	78.727
Fluid mass flow rate [kg/s]	0.0217	0.0217	0.0217	0.0217	0.0217	0.0641	0.0641	0.0641	0.0641	0.0641	0.1074	0.1074	0.1074	0.1074	0.1074	0.1716	0.1716	0.1716	0.1716	0.1716
Attemperating pressure [MPa]	15.29	15.29	15.29	15.29	15.29	15.48	15.48	15.48	15.48	15.48	15.67	15.67	15.67	15.67	15.67	15.96	15.96	15.96	15.96	15.96
Attemperating temperature [°C]	191.24	191.24	191.24	191.24	191.24	196.00	196.00	196.00	196.00	196.00	200.86	200.86	200.86	200.86	200.86	208.05	208.05	208.05	208.05	208.05
Attemperating mass flow rate [kg/s]	0.00082	0.00082	0.00082	0.00082	0.00082	0.00252	0.00252	0.00252	0.00252	0.00252	0.00426	0.00426	0.00426	0.00426	0.00426	0.00684	0.00684	0.00684	0.00684	0.00684
Differential pressure over SH [MPa]	0.0006	0.0006	0.0006	0.0006	0.0006	0.0048	0.0048	0.0048	0.0048	0.0048	0.0132	0.0132	0.0132	0.0132	0.0132	0.0332	0.0332	0.0332	0.0332	0.0332
Water column length [mm]	238	238	238	238	238	1918	1918	1918	1918	1918	4039	4039	4039	4039	4039	8617	8617	8617	8617	8617
Steam length at outlet [mm]	16086	16086	16086	16086	16086	14406	14406	14406	14406	14406	12285	12285	12285	12285	12285	7707	7707	7707	7707	7707
Evaporation rate [kg/s]	0.00013	0.0002	0.0002	0.0002	0.0003	0.0024	0.0030	0.0036	0.0047	0.0067	0.0084	0.0102	0.0120	0.0152	0.0214	0.0269	0.0322	0.0378	0.0478	0.0674
Evaporation time [s]	847	711	596	465	315	365	289	240	182	129	213	174	149	118	84	139	116	99	78	55
Internal pressure [MPa]	17.30	17.30	17.30	17.30	17.30	17.30	17.30	17.30	17.30	17.30	17.30	17.30	17.30	17.30	17.30	17.30	17.30	17.30	17.30	17.30
Outer wall T (1x30) [°C]	561.51	578.65	596.55	623.58	666.45	580.72	607.22	631.20	670.75	729.76	608.54	635.28	659.08	701.35	779.69	544.16	553.47	559.65	570.60	609.96
Inner wall T (30x30) [°C]	561.33	578.45	596.34	623.37	666.25	580.21	606.66	630.60	670.10	729.11	607.61	634.17	657.80	699.73	777.47	538.46	546.42	551.06	559.13	591.74
Axial stress [MPa]	5.81	5.81	5.81	5.81	5.81	5.81	5.81	5.81	5.81	5.81	5.81	5.81	5.81	5.81	5.81	5.81	5.81	5.81	5.81	5.81
Circumferential stress [MPa]	28.91	28.91	28.91	28.91	28.91	28.91	28.91	28.91	28.91	28.91	28.91	28.91	28.91	28.91	28.91	28.91	28.91	28.91	28.91	28.91
Radial stress [MPa]	-17.30	-17.30	-17.30	-17.30	-17.30	-17.30	-17.30	-17.30	-17.30	-17.30	-17.30	-17.30	-17.30	-17.30	-17.30	-17.30	-17.30	-17.30	-17.30	-17.30
Thermal Stress [MPa]	0.61	0.67	0.70	1.01	0.63	1.71	1.84	1.94	2.03	1.93	3.05	3.57	4.04	4.93	6.29	19.41	23.93	29.09	38.69	60.15
Total combined stress [MPa]	40.55	40.60	40.63	40.90	40.57	41.51	41.63	41.71	41.79	41.70	42.70	43.15	43.57	44.36	45.58	57.66	61.91	66.82	76.03	96.90
New tube yield strength [MPa]	258.16	253.19	248.00	221.53	175.23	252.59	239.20	213.30	170.59	105.13	237.78	208.90	183.19	137.46	73.19	263.19	260.49	258.70	255.53	236.24
Will failure occur with new tube?	**NO**	**NO**	**NO**	**NO**	**NO**	**NO**	**NO**	**NO**	**NO**	**NO**	**NO**	**NO**	**NO**	**NO**	**NO**	**NO**	**NO**	**NO**	**NO**	**NO**
Old tube yield strength [MPa]	131.39	128.99	126.48	115.72	97.03	128.70	122.85	112.40	95.15	73.83	122.28	110.62	100.24	82.01	60.87	133.82	132.51	131.65	130.12	121.66
Will failure occur with old tube?	**NO**	**NO**	**NO**	**NO**	**NO**	**NO**	**NO**	**NO**	**NO**	**NO**	**NO**	**NO**	**NO**	**NO**	**NO**	**NO**	**NO**	**NO**	**NO**	**NO**

Figure 6.8 Complete results from study